Developments in the Built Environment 13 (2023) 100114

Contents lists available at ScienceDirect

Developments in the Built Environment

journal homepage: www.sciencedirect.com/journal/developments-in-the-built-environment

Nanomaterials in geopolymer composites: A review

R. Samuvel Raj [a], G. Prince Arulraj [a], N. Anand [a,**], Balamurali Kanagaraj [a], Eva Lubloy [b,*], M.Z. Naser [c]

[a] Department of Civil Engineering, Karunya Institute of Technology and Sciences, Coimbatore, India
[b] Department of Construction Materials and Technologies, Faculty of Civil Engineering, Budapest University of Technology and Economics, Budapest, 1521, Hungary
[c] AI Research Institute for Science and Engineering (AIRISE), Clemson University, Clemson, SC, 29634, USA

ARTICLE INFO

Keywords:
Geopolymer composites
Nano materials
Nanotechnology
Fresh properties
Mechanical properties
Durability properties
Micro-structure

ABSTRACT

Nanomaterials (NMs) are being used to enhance the properties of construction materials. This review focuses on the use of NMs to improve the characteristics of fresh and hardened Geopolymer Composites (GC). Over 335 research publications are reviewed to detail the benefits and drawbacks of the integration of NMs in GC. More specifically, this review outlines the effects of numerous NMs such as Nano Silica (NS), Nano Alumina (NA), Nano Titanium dioxide (NT), Carbon Nano Tubes (CNT), Multiwall Carbon Nano Tubes (MCNT), Nano Calcium Carbonate (NCC), Nano Zinc oxide (NZ), Graphene Oxide (GO), Nano Metakaolin (NMK), Nano Fly Ash (NFA), Nano Glass Powder (NGP) and Nano-clay(NC) on Geo-polymer Paste (GPP), Geo-polymer Mortar (GPM) and Geo-polymer Concrete (GPC). The presence of NMs was found to enhance the geo-polymerization reaction and result in a denser matrix. The presence of NMs also enhances the durability of GC by preventing micro-pores inter-connectivity. In hindsight, our review indicates that the addition of NMs is directly tied to producing high-performance GC, which the construction industry can effectively readily adopt. Additional insights, challenges, and future research directions are identified and discussed toward the end of this review.

1. Introduction

The production of Portland cement is often considered as the world's most significant source of greenhouse gas emissions. It contributes approximately 5–8 percent of the total CO_2 emissions (He et al., 2019; Gartner, 2004). In addition, Portland Cement manufacturing is responsible for at least 70% of greenhouse gas emissions globally (Belaïd, 2022; Korczak et al., 2022). For example, one tonne of Portland cement requires roughly 2.8 tonnes of raw materials. Each year, the concrete industry requires approximately trillion liters of water (Edser, 2005) and 110 to 120 kWh of electricity (dutta joydev assessment of soil, 2007). At the same time, beyond aluminium and steel production, Portland cement manufacturing is the most energy-consuming area. Simply, this is a resource-intensive process that also requires a lot of natural resources like shale and limestone to make Portland Cement clinkers (Guo et al., 2010). The recent research works are mainly focussing on reducing the generation of CO_2 emissions in construction materials (Yildirim et al., 2015).

For economic development, efficient use of renewable and non-renewable raw materials is required (Shalini and Gurunarayanan, 2016). Portland Cement-based concrete remains the most widely utilized primary material in the construction sector. The development of novel materials to replace PC has become a critical area of research owing to the rise in environmental issues (Suwan and Fan, 2014; Mathews et al., 2020). At the same time, due to the high expense and health risks associated with disposing of industrial and agricultural waste by-products such as Fly Ash (FA), Ground Granulated Blast Furnace Slag (GGBFS), and Rice husk Ash (RA). Recycling and reusing these by-product materials have become a growing concern in recent years (Charitha et al., 2021; de Azevedo et al., 2022; Junaid et al., 2022; Chinnu et al., 2021).

The geopolymer technology was first invented by Davidovits in France in 1970 (Abdel-Gawwad and Abo-El-Enein, 2016) and is a convenient and acceptable replacement for traditional concrete. Traditional concrete is still a widely accepted building material for infrastructure development due to its excellent characteristics. However,

* Corresponding author.
** Corresponding author.
E-mail addresses: samuvelraj1004@gmail.com (R. Samuvel Raj), princearulraj@karunya.edu (G. Prince Arulraj), nanand@karunya.edu (N. Anand), balakmurali31@gmail.com (B. Kanagaraj), lubloy.eva@epito.bme.hu (E. Lubloy), mznaser@clemson.edu (M.Z. Naser).

https://doi.org/10.1016/j.dibe.2022.100114
Received 11 October 2022; Received in revised form 26 November 2022; Accepted 21 December 2022
Available online 28 December 2022

considering the construction industry's sustainability aspects, novel sustainable cement-based materials are being developed. In geopolymer concrete, the eco-efficiency, i.e., carbon emission, mainly depends on the concentration of NaOH solution. When the concentration of NaOH exceeds its optimal limit, the carbon emission also increases especially in the case of high-strength and high-performance geopolymer concrete. Alsalman and Kanagaraj replaced fly ash with GGBFS in the preparation of self-compacting geopolymer concrete. It was reported that comparatively lower carbon emissions were observed from the geopolymer concrete than from Portland cement concrete (Alsalman et al., 2021; Kanagaraj et al., 2022a). FA, GGBFS, Metakaolin (MK), Palm oil Fuel Ash (PFA), and RA are examples of inorganic Alumina Silicate (AS) polymers used to produce geopolymer. Alkaline silicates and alkaline hydroxide are the most frequent Alkaline Activated Solutions used for the development of geopolymers. The alkali activators act as an activator, and the oxides of AS-rich materials react with the alkali activators to produce polymeric Si–O–Al linkages resulting in alkali-activated cementitious materials. A structural network of silicon-oxo-aluminate (sialate) is generated in the polymerization reaction, in which aluminate (AlO_4) and silicate (SiO_4) have joined tetrahedrally by sharing an oxygen atom (Ng et al., 2018).

In the first stage, the dissolving of the binder's silicate and aluminium components in a high-alkalinity water solution leads to the creation of silicon and aluminium oxide ions. In the second stage, a mixture of silicate, aluminate, and AS species is generated, which causes the development of an amorphous gel via a contemporaneous polycondensation-gelation process (Duxson et al., 2007). The end product of the polymerization reaction is affected by the combination of chemical compounds of the origin binder material and alkali activators. At greater temperatures, this polymerization is typically accelerated (Diaz et al., 2010; Yip et al., 2008). Therefore, geopolymer represents the third generation of cementing ingredients after lime and Portland Cement (Sumesh et al., 2017).

Geopolymer is an environment-friendly material that produces around 70% lesser carbon emissions than Portland Cement concrete (as it makes extensive use of waste materials in mixtures) (Weil et al., 2009; Kanagaraj et al., 2022b). The AS origin binder, coarse and fine aggregates, alkali activators, and water comprise the GC combined proportions. These chemicals produce solid concrete that is substantially equivalent to normal concrete due to polymerization (Omer et al., 2015). The geopolymer technology can be used in additive manufacturing, GPC, ceramics, and 3D concrete printing (Panda et al., 2017). The concentration of Sodium Hydroxide (SH) (Parveen et al., 2018; Patankar et al., 2014), the ratio of Sodium Silicates (SS) to SH (Ghafoor et al., 2021; Pavithra et al., 2016a; Aliabdo et al., 2016), the silicate modulus (Mijarsh et al., 2015), the curing method and curing period (Xie and Ozbakkaloglu, 2015; Hassan et al., 2019; Vijai et al., 2010; Nath et al., 2015), the water to solids ratio (Yahya et al., 2015), the alkali activators to binder ratio (Fang et al., 2018; Pavithra et al., 2016b), the combination of chemical elements, type of origin binder (Yip et al., 2008; Kanagaraj et al., 2022c), the ratio of Silicon to Aluminium in the geopolymer matrix (Thokchom et al., 2012; Khale and Chaudhary, 2007), resting time, mixing period (Hardjito et al., 2004), the consequences of Na_2O to H_2O ratio (Khale and Chaudhary, 2007), superplasticizer quantity and additional H_2O content (PATANKAR et al., 2012), Coarse Aggregate (CA), Fine Aggregate (FA) content (Joseph and Mathew, 2012; Mermerdaş et al., 2017; Sreenivasulu et al., Kumar) are the main elements which influence the performance of the GC.

Greater Compressive Strength, superior resistance to fire, minimal creep, low shrinkage, higher resistance to acidic environments, and durability are all characteristics of geopolymer materials (Chen et al., 2022; Asadi et al., 2022; Cong and Cheng, 2021). The majority of GC research has focused on adjusting the molarity of alkalis, exchanging curing methods, or altering the curing temperature to examine the strength variation and durability features of GC with FA, RA, and MK as base materials (Aliabdo et al., 2016; Chindaprasirt, 2007). Some researchers have undergone further in their research, looking into the relationship between different properties of GC (Gunasekera et al., 2014; Zhang and Zong, 2014; Isil Ozer, 2015). The compressive strength of GC cured at room temperature is low (Sonal et al., 2022; Sajjad et al., 2021; Ge et al., 2022). In geopolymer, heat curing methods are commonly used to speed up the polymerization process (Atis et al., 2017; Noushini et al., 2016; Görür et al., 2015; Carolina et al., 2017; Hussin et al., 2014). Because NMs have a higher surface area to volume ratio, they are more reactive and have an impact on reaction rates (Wiesner, 2007; Aggarwal et al., 2015). As a result, without using temperature curing, NMs have a microscopic level impact on the GC microstructure. This significantly improves the structural performance of both raw concrete and hardened concrete (Taylor et al., 2014). Several studies focused on improving the mechanical performance and durability of GC by integrating regular Portland Cement (Huo et al., 2021; Azeem et al., 2021), GGBFS (An et al., 2022; Yaswanth et al., 2022; Shi et al., 2022a), NS (Razi et al., 2022; Unis et al., 2022; Zhang et al., 2020a), and Alccofine (Parveen et al., 2018; Saxena et al., 2018) at room temperature curing.

Nanotechnology involves the manipulation of matter and materials on scales that are less than 100 nm (Wiesner, 2007; Wei et al., 2022). Owing to its novel science and cutting-edge applications, nanotechnology is a rapidly expanding field of research that has gained popularity in recent decades. Because NMs have distinctive chemical and physical performance. Due to the ultrafine type of NMs, building with nanocomposite materials is a goal for researchers. (Bhushan and Sharma, 2020). In recent years, there has been a surge in interest in using nanotechnology in GC (Kotop et al., 2021; Naskar and Kumar, 2016; Abdalla et al., 2022a).

1.1. Research significance

Over the last decade, extensive research has been conducted on the addition of various NMs to GC. Furthermore, earlier publications highlighted the influence of NMs on GC but did not provide the information in a detailed manner. This paper examines all previous and current studies on the effects of different NMs on the performance of various GC. As far as the author's knowledge, this is one of the complete review papers on this topic in recent years, with an organized study, discussion, and investigation to extend this frontier. We cover a variety of studies that tackled the impact of various NMs (NCC, NC, NMK, NGP, NS, NA, MCNT, NZ, NT, CNT, and GO) on the properties of GC. Even though various NMs have comparable effects on the behavior of GC, they are split into different categories, and the field's research needs and constraints are discussed in depth. In addition, a dedicated discussion on the efficiency of cost comparison between different NMs incorporated GC is also presented. This research provides a detailed analysis of the usage of NMs in GC in terms of their fresh, hardened, durability, and microstructural properties. All prior and current literature in this field was reviewed to determine the influence of various types of NMs on the different performances of GC. Finally, the field's research requirements and limitations are discussed.

2. Nanomaterials in geopolymer composites

Hardened properties, morphology, surface energy, electron conductivity, reactiveness of chemicals, and optical absorption of composites change dramatically when the size of the material changes from macroscale to nanoscale (Falikman and Gusev, 2015). A variety of studies have been conducted to investigate the properties of NMs in GC, including hardened properties and chemical resistance (Youssf et al., 2022; Dehkordi et al., 2022; Saloni et al., 2021a), structural properties (Hassan et al., 2020), raw and microstructure properties (Pawluczuk et al., 2021; Hamidi et al., 2022), physio-mechanical strength (Aziz et al., 2021), permeability (Arafa et al., 2021; Saloni et al., 2021b, 2021c), and protection against elevated temperatures (Tayeh et al.,

2021; Zhang et al., 2020b).

When NMs are introduced to cement granulations, free water becomes stationary because NMs fill pores and spaces between Portland cement particles, which is known as the filler effect. Furthermore, the NMs participate in the pozzolanic process, which results in novel calcium silicate hydrate (C–S–H) gel production, enhancing the strength of the bond between steel and concrete properties of the mix by strengthening the transitional interfacial region between aggregates and binding pastes (Al-Azzawi et al., 2018; Nuaklong et al., 2020). When cured under ambient curing conditions, GC has low compressive strength and gains strength slowly (Poloju and Srinivasu, 2020; Du et al., 2022), but they have high compressive strength when cured by temperature, which limits the usage of GC in in-situ applications (Mohammed et al., 2021; Zhang et al., 2020c; Han et al., 2017). To achieve an ambient curing GPC with suitable strength, one option for tackling researchers could employ NMs to speed up the reaction between the chemicals within GC. This is carried out atomically by altering the microstructure of GPC, which significantly enhances the material's hardened and raw state properties (Hussin et al., 2014; Du et al., 2022).

Over the past fifteen years, data were collected in the research on GC with different NMs and which is represented graphically in Fig. 1. This graph clearly shows that every year the research progress graph in the area of GC with NMs has increased rapidly. So this means that there is lots of scope in the area of GC with NMs in the future era.

The literature survey reveals that the usage of NS (Saini and Vattipalli, 2020), NA (Alomayri, 2019), NT (Sastry et al., 2021), CNT (Rovnaník et al., 2016), MCNT (Li et al., 2021), NCC (Assaedi, 2021), NZ (Zidi et al., 2020), GO (Bellum et al., 2020), NMK (Kaur et al., 2018), NFA (Rajendran and Akasi, 2020), NGP (Hamzah et al., 2020) and NC (Ravitheja and Kiran Kumar, 2019) on GC. In this study, the term "composites" is used to refer to Geo Polymer Paste (GPP), mortar, and concrete.

2.1. Carbon Nano Tubes (CNT) and Multiwall Carbon Nano Tubes (MCNT)

Cylindrical Nano diameter molecules with pipe-like bonds CNT are hollow strings made of carbon-carbon that were discovered by Sumio Ijima (Ashby et al., 2009; Su et al., 2020; Ding et al., 2022) (Manzur et al., 2016). By rolling up Graphite sheets, CNT can be produced as single-walled, double-walled, or multi-walled, and their length may vary from micro to millimeter range (Ferro et al., 2011). Single-walled CNT is cheaper than multi-walled CNT. CNT is mainly used for the production

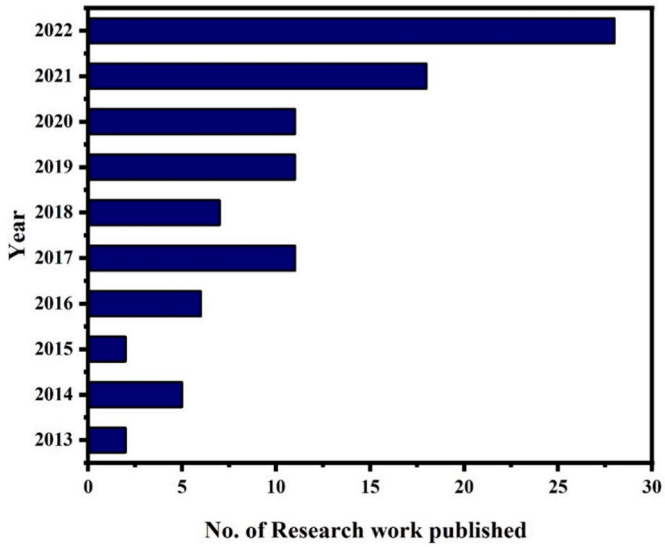

Fig. 1. Work progress in geopolymer concrete with nanomaterials.

of fiber-reinforced concrete due to its high mechanical strength, high thermal conductivity, high modulus of elasticity, and high tensile strength (Sekkal and Zaoui, 2022; Maho et al., 2021). Due to their good material properties, CNT gives concrete better mechanical strength and durability properties (Azeem et al., 2021; Zhu et al., 2021). In the past few years, numerous studies have been conducted to examine the results of CNT addition on the mechanical and microstructural properties of GPP, GPM, and GPC (Carriço et al., 2018; Abbasi et al., 2016).

Due to the MCNT surface area to volume ratio, Vander wall forces between the molecules are strong, which retard the dispersion of the MCNT within the composites. But the alkali activators used in the preparation of GC have a major role in the dispersion of MCNT and GC due to their capacity to enhance the interaction between them (Khater and Abd El Gawaad, 2016). MCNT creates more sites for the geo-polymerization process between the composites by increasing the amount of C–S–H gel. Therefore, an adequate amount of CNT enhances the microstructural properties by reducing the Nano cracks through the complete geo-polymerization process (Rovnaník et al., 2016; Kim et al., 2019; da Luz et al., 2019).

2.2. Nano-alumina (NA)

Commercially available NA is in powder form, and it is produced through several techniques such as ball milling, pyrolysis, hydrothermal, laser ablation, sputtering and sol-gel. NA can be used to produce concrete with better mechanical properties due to its higher stability, hardness, insulation, and transparency. The mechanical properties of concrete can be enhanced by filling the pores in the composites (Anil Kumar Reddy, 2022; Li et al., 2006, 2017a). The durability properties of NA-filled concrete can be enhanced by reducing the effect of chloride attack and water absorption (Mohseni et al., 2019; Ahmed et al., 2021). The mechanical and microstructural properties of GPC can be improved by the addition of NA by densifying the whole system (Alomayri, 2019; Behfarnia and Salemi, 2013; Nazari and Sanjayan, 2015; Shekari and Razzaghi, 2011). The surface area of the geopolymer material can be increased by reducing Si/Al ratio, which is significant for the absorption process. Geo-polymerization in GC can be improved by the use of crystalline Al_2O_3, which results in reducing the Si/Al ratio in the alkali activators (Alomayri, 2019; Duxson et al., 2005; Huang and Han, 2011). NA does not have any influence on the geo-polymerization process, and it may be added as Nano-fillers (Phoo-ngernkham et al., 2014; Riahi and Nazari, 2012). But, Hajimohammadi et al. investigated that the NA was used as a major ingredient and acted as a catalyst for the geopolymer gel formation. By enabling the geopolymer gel, NA reacts significantly, causing the polymer gel to accumulate (Zidi et al., 2019; Nazari and Riahi, 2013). NA can be used as a filler material and an accelerating agent for geo-polymerization in FA-based GC. Therefore, it can be accepted as good NMs by producing denser composites due to its proper inter-bonding between each particle (Shahrajabian and Behfarnia, 2018; Chindaprasirt et al., 2012). Due to their high aluminium content, these NMs can be used to produce GPC with low aluminium base materials such as RA (Mohseni et al., 2019).

2.3. Nano silica (NS)

The crystalline and amorphous form of NS is widely used to improve the properties of Portland Cement composites due to more reactive as well as the pore-filling effect (El-Feky et al., 2022; Abhilash et al., 2021). Commonly, NS, in its amorphous form, can be used to produce nano concrete (Yang et al., 2021; Zhang et al., 2012; Okoye et al., 2017). NS has a specific surface area of 15–25 m^2/g, and spherical particles with 150 nm diameter can be produced by vaporizing silica in an electric arc furnace with a temperature between 1500 and 2000 °C. Due to the smaller particle size of NS, concrete made with NS provides better mechanical and durability properties. Commonly, NS can be used as a slurry form to avoid health issues due to the inhaling of NMs (Bai et al.,

2022; Huang et al., 2022).

Due to the above-mentioned advantage of NS in the properties of cement composites, several researchers carried out investigations on GC with NS. NS with MK-based GC shows several unsaturated bonds and different hydroxyl bonding. But, the geo-polymerization process will enhance when the NS surface is in an active state due to its high free energy(Gao et al., 2014; Matalkah et al., 2022). Diluted silica increases the geo-polymerization in GPM by the formation of silicate oligomers in the GC. Also, it is reported that the geo-polymerization process is increased in MK-based GC by increasing the concentration of SH solution as well as the higher specific surface area of NS (Deb et al., 2015, 2016). Due to the amorphous nature of NS, larger surface area and Si–Al and Si dissolution rates are significant factors in enhancing the geo-polymerization process in FA-based GC (Adak et al., 2017; Kumar, 2022). NS promotes the formation of C–S–H and N-A-S-H, thus strengthening the polymerization process in natural pozzolana-based GC (Alvee et al., 2022; Ibrahim et al., 2018). Therefore, from the above literature, it is clear that NS can improve the geo-polymerization process by increasing the amount of geopolymer gel and increasing the dissolution rate of silica and alumina. Also, provide good microstructural properties due to its higher specific surface area.

2.4. Nano-titanium dioxide (NT)

Natural minerals like anatase, rutile, and brookite are the natural sources of TiO_2. The major applications of TiO_2 in drugs, cosmetics, and paints are due to its low toxicity, low industrial cost, availability, semiconductivity, and high chemical stability. NT was produced by a deposition method, microwave-assisted method, hydro solvo thermal, sol-gel, sono chemical, and oxidation (Taylor et al., 2014; Abdalla et al., 2022a; Weir et al., 2012). NT enhances the mechanical strength and electrical properties by filling the pore structure, reducing the drying shrinkage, and fastening the setting time (Li et al., 2017b; Jiang et al., 2018). Also, it protects the concrete from pollution (Wang et al., 2022a; Elia, 2018). Due to its better photo-catalytic effect and more reactive nature, it is normally used for surface coating, which results in excellent durability properties (Noorvand et al., 2013; Maury-Ramirez et al., 2012). The above-mentioned literature clearly shows that there is a scope for the area in mechanical properties of GC with the addition of NT.

2.5. Nano-clay (NC)

NC is the Nano filling material with fine-grained and sheet-like structures. It is also hydrous silicate amorphous, and it is produced by heating high-purity kaolin at a temperature of 800 °C (Amiri et al., 2022; Niu et al., 2021; Hakamy et al., 2015). It is the cheapest and most easily available filling material having a particle size of 50–100 nm. Due to its surface area, interlayer bonding, and particle size, it can have several applications in the civil engineering field (Nazir et al., 2016). NC increases the mechanical strength of GPC by reducing the porosity and improving the microstructural properties (Hakamy et al., 2015; Gadkar and Subramaniam, 2021; Basiri et al., 2022; Wei and Meyer, 2014; Hosseini et al., 2017). The addition of NC in a small proportion leads to the enhancement of mechanical properties in GGBFS-based GPC under a water-cooled process. Still, the addition of a larger proportion leads to the reduction of the mechanical strength of GPC by more desiccating and crack formation in the composite (Assaedi et al., 2016a, 2016b). The addition of NC in the GPP increases the gel formation and which leads to the creation of micro dispersion (Chindaprasirt, 2007; Basiri et al., 2022). Also reported by Assaedi et al. (Ravitheja and Kiran Kumar, 2019; Gadkar and Subramaniam, 2021), the addition of NC in FA-based GPC increases geo-polymerization by enhancing the silica content and very fine particles resulting in a denser GC. They also concluded that amorphous materials play an important role in the formation of gel in the polymeric medium.

2.6. Nano-Calcium Carbonate (NCC)

Nano-Calcium Carbonate is commonly employed in cementitious composites due to the benefits it provides as filler and nucleation. Because of its excellent efficacy and low cost, NCC is widely used as an enhancement added to the plastic sector. However, aggregation of NCC can greatly limit its effects (Assaedi, 2021). According to research, incorporating NCC in cementitious composites is not damaging to their mechanical properties. Camiletti et al. (Assaedi et al., 2020; Cao et al., 2019) found that it has a good synergic influence on early-age strength, the hydration process, and the durability of cementitious composites. Therefore, substantial research has been conducted to ascertain the impact of $CaCO_3$ on cement composites and GC. The $CaCO_3$ was created in an experimental setup by reacting calcium oxide with carbon dioxide. NCC particles were produced and incorporated into cementitious composites in various percentages depending on the binder weight (Khalaf et al., 2021; Chu et al., 2021). According to the findings, increasing NCC content improves the flexural strength and compressive strength of OPC composites after 7 days of curing, even though the best additional percentage was found as 2%. In contrast to sample specimens, after 28 days of curing, specimens with the addition of NCC had worse mechanical characteristics than sample specimens (Yang et al., 2020; Camiletti et al., 2013). Because NCC functions as a seed for this reaction, this means that the hydration process was hastened. On the other hand, a larger quantity of NCC particles may have reduced the filling effect of the particles due to aggregation effects. If NCC has a positive impact on concrete qualities, it could be a viable and promising option for nano-modified concrete applications. However, NCC may be difficult to disperse in Portland Cement paste and may be harmful to Portland Cement hydration, especially at late ages, because many additives, such as coupling agents, were used in the manufacturing process of NCC powder to achieve compatible performance between NCC and organic-based materials (Ali et al., 2021; Fu et al., 2022). As a result, even if some interesting results about the effect of pure NCC powder on the hydration process of Portland Cement have been reported (Feng et al., 2021; McDonald et al., 2022), it may be improper to utilize NCC powder directly in concrete (Qian et al., 2019). The amount of NCC in a combination depends on its composition, water-to-cementitious ratio, and flowability.

2.7. Nano Fly Ash (NFA)

FA fillers are obtained from thermal power plants at a cheap rate and come in micron sizes. Using a planetary ball mill, this micron-sized FA was reduced to nano size. The micro-level fillers were subjected to significant plastic deformation in this ball milling procedure due to the repetitive compressive pressures coming from the impacts between the balls and the fillers. Finally, it created fillers with Nano meter-scale crystallite sizes. The greater particles of fly ash are converted into smaller Nanoparticles using a ball mill. Impact and attrition is the working principle behind this cylindrical apparatus. The ball mill uses 50 tungsten carbide balls of weight 8 g each to grind fly ash of quantity 40 g for 240 min. This ball mill setup utilizes fly ash to ball ratio of 1:10. The raw fly ash having a higher particle size range of up to 827 nm is obtained from a thermal power plant. The particle sizes are reduced to 73 nm with the help of a locally available ball mill. The purpose of a ball mill is to make finer particles rather than coarser raw materials. The compressive strength of geopolymer specimens is higher than that of control specimens. The Nano fly ash added geopolymer mortar compressive strength is higher among all the panels. This higher strength achievement is due to the ability of pore filling leads to dense microstructure with good bonding nature through its glassy, inert, and smooth surface of Nano fly ash. The Nano fly ash-based specimen results in lower water absorption since the Nano fly ash enhances the strength and durability of the specimen by its pore-filling nature. The Nano fly ash-based geopolymer panels have a higher amount of energy

absorption among all panels. This may attribute to higher ductility and less susceptibility to brittleness (Mudgal et al., 2020; Satheesh Raja and Manisekar, 2016).

2.8. Nano metakaolin (NMK)

NMK is a derivative of kaolin ($Al_2O_3{\cdot}2SiO_2{\cdot}2H_2O$). After the dehydroxylation at temperatures between 600 °C and 800 °C, most of the octahedral alumina is converted into more active tetra-coordinated and penta-coordinated units. When the crystal structure is completely or partially broken, or the bonds between kaolinite layers are broken, metakaolin with phase variation is formed. Finally, NMK is obtained by mechanical grinding. The dehydroxylation process of kaolin and the structure variation of NMK are very sensitive to the heating temperature rate, and the exothermic dehydroxylation reaction. The diffraction peaks of NMK are diffuse and show a transition phase between the crystalline and amorphous and disordered structure of NMK particles. NMK exhibited a large thickness aspect ratio. The flake thickness of the NMK particle was much less than 100 nm, making it a nano-scale material (Xie et al., 2020; min Zhan et al., 2020). The shape and surface texture of NMK is similar to MK. MK has a plate structure, and during the high-temperature calcination, the tetrahedron and layering of flakes are diluted to cause the fact surface of NMK to become smoother, and the higher specific surface area and filling efficiency are obtained. The calcination temperature of NMK has a great effect on the pozzolanic activity. Fly ash-based geopolymer mortar incorporated with nano metakaolin gained about 70–80% of its 28 days compressive strength after 3 days of ambient curing. The reason for the increase in compressive strength of fly ash-based geopolymer mortar with different percentage levels of NMK may be attributed to the contribution of silica and alumina oxide of NMK in the geopolymerization reaction. It is observed that there is a significant increase in compressive strength at the optimal percentage of NMK due to the homogeneous dispersion of nano-metakaolin leading to the formation of nucleation material for geopolymerization reaction. This geopolymer reaction results in a more compact structure(Muhd Norhasri et al., 2016; Hassaan et al., 2015).

2.8.1. Nano-zinc oxide (NZ)

Photocatalytic-based organic pollutants degradation, radiation-insulating dyes, steel bar corrosion prevention, etc., are some of the applications of NZ (Mohamed et al., 2019). The remarkable physico-chemical features of NZ, including as strong photosensitivity, electron mobility, and chemical stability, have piqued researchers' curiosity. Increases in NZ content above a threshold limit of 1.5 percent may have negative consequences for mechanical characteristics (Zidi et al., 2020). The nano-ZnO as an additive is related to its capacity to produce well-compacted geopolymers. The cost is low, and it has a wide range of applications. It is effective in improving the properties of many polymers. The characteristics that are beneficial for ceramic applications are the high heat capacity, low thermal expansion, and high melting temperature of ZnO. The synthesis of ZnO nanoparticles by the sol-gel technique was performed by dissolving 2 g of zinc acetate dehydrate in 14 ml of methanol under magnetic stirring at room temperature until a homogenous solution was obtained. The solution was dried rapidly in an autoclave under supercritical conditions at a heating rate of 50 °C/h. It has spherical morphology; average particle diameter of 20 nm; specific surface $\geq$40 m^2/g; density of 5.6 (20 °C), and pH of 6.5–7.5. Increasing the percentage of nano-ZnO in the mixes by up to 0.5% increased the density of the geopolymers. A reverse negative result is reported at 0.7% of nano-ZnO. This may be attributable to the agglomeration of nanoparticles, which may result in micro-cracks development. Geopolymers with nano-ZnO had higher mechanical strength than normal geopolymers. The compressive strength of composites increased with the increase in the concentration of nano-ZnO up to 0.5% and then decreased(Arefi and Rezaei-Zarchi, 2012).

2.9. Graphene Oxide (GO)

A novel material known as GO, a one-atom-thick planar sheet made of an SP-2 bonded carbon structure, has emerged as a rapidly emerging star in material research. GO exhibits extraordinarily excellent crystal and electrical quality (Zaid et al., 2022). GO possesses several unique features, including a large surface area, surface functionalization, and superior aqueous solvent dispersibility (Jamnam et al., 2022; Konios et al., 2014). On their basal planes, GO sheets have diverse oxygen-containing groups, primarily epoxides and hydroxyls, and carboxyls on their edges, which can help GO disperse in water (Lin et al., 2016). As a result, GO has been regarded as an effective agent for improving fiber-matrix interfacial characteristics (Chen et al., 2016). It has been found that a tiny amount of GO (0.01–0.06 percent) can significantly improve the mechanical strength of concrete (Lin et al., 2016; Lv et al., 2013; Shi et al., 2022b). GO is a layered NMs made up of hydrophilic oxygenated graphene sheets with hydroxyl and epoxide functional groups on the basal planes and carbonyl and carboxyl groups at the sheet edges (Zhu and Zhang, 2021). The surface area of GO is vast, and it has good mechanical properties (Ng et al., 2018; Akarsh et al., 2021). As a result, when compared to CNT-reinforced concrete, GO displays a higher gain in compressive strength at a lower concentration (Basquiroto de Souza et al., 2022; Mowlaei et al., 2021; Sheng et al., 2021; Chintalapudi and Pannem, 2020). The interaction of the GO sheets with the alkaline solution used to process the geopolymeric composites yielded highly reduced and cross-linked GO sheets. The addition of these GO sheets into geopolymers at very low contents simultaneously improved the mechanical properties and reduced the overall porosity of geopolymers. The malleable GO sheets and the small scraps of GO sheets that were moved by the fly ash particles filled the voids and hollow spaces in the matrix. The incorporation of GO sheets improved the mechanical properties of the geopolymeric composites as a result of their 2-dimensional structure and good chemical bonding with the matrix. (Shi et al., 2022b; Liu et al., 2022a). However, because of the huge specific surface area of GO, adding it to Portland Cement paste and concrete can significantly increase viscosity and reduce workability performance, restricting its use. It is a stumbling block in enhancing the fluidity and workability of GO-cement slurry (Devi and Khan, 2020a, 2020b; Yu and Wu, 2020; Habibnejad Korayem et al., 2020; Sui et al., 2021). The GO–geopolymeric composites can be an environmentally friendly and economical alternative to Portland Cement due to their low greenhouse gas emissions and improved mechanical properties. The in-situ reduction of GO makes geopolymers ideal candidates for high-performance and (potentially) self-sensing structural materials for various applications such as bridges, roadways, and smart structures with inherent increased durability due to their near pore-free morphology (Devi and Khan, 2020a, 2020b; Yu and Wu, 2020; Habibnejad Korayem et al., 2020; Sui et al., 2021).

2.10. Nano water glass (NGP)

Glasses are substantial waste materials that might be utilized in the manufacturing of concrete, which would be an environmentally favorable technique. Every year, millions of tonnes of glass bottles are dumped all around the world (Moukannaa et al., 2022; Lin et al., 2012; Xiao et al., 2022). Huseien et al. prepared nano glass powder by cleaning the glass bottles using normal tap water to remove the contaminants and crushing them with a crusher machine. The crushed glass was sieved through 600 mm to separate large glass particles. Subsequently, they used Los Angeles Abrasion Machine with a 25 kg capacity was utilized to grind the sieved glass for 3 h to get a medium particle size of 25 mm using 16 diameters of 40 mm stainless balls. The resultant powder was heated in an oven at 110 °C ($\pm$5) for 60 min and was grinded for 7 h using a ball mill machine to achieve optimum distribution of nano-particles. The specific surface area of ternary binder was widened with the increase in Nano glass powder content in alkaline activated mortars

matrix as GGBFS replacement. It was concluded that the high specific area could enhance the water demand and thus lead to reduced workability. The workability of alkaline-activated mortar dropped as the NGP content increased. The flow diameter decreased from 15.5 cm to 15.3, 14.7, 14.2, and 13.5 cm with increasing Nano glass powder content from 0 to 5, 10, 15, and 20%, respectively. The initial setting time and final setting time increased from 34 min to 51 min and from 52 min to 76 min with the rise in NGP content from 0% to 20% as GGBFS replacement, respectively. The compressive strength increased monotonically with the increase in NGP content from 0 to 5%. The compressive strength increased from 56.2 MPa to 65.5 MPa with the increase in NGP content in alkaline activated mortar matrix from 0 to 5%, respectively. However, the strength reduced to 42.1 MPa when the NGP content increased beyond 5% and reached 20%. The water absorption decreased with increasing NGP up to 10%. The water absorption property of alkaline-activated mortars was greatly influenced by the ratio of NGP replacing GGBFS (Xiao et al., 2022; Rashad, 2014). It has been established that bottle-derived shredded glass scraps, or NGPNGP, may include significant levels of aluminum and silicon in non-crystalline form. Glass trash has these qualities, making it a potential pozzolanic or cement-like substance (Zhang and Yue, 2018). It is important to note that its utilization may alter the features of the completed items. Before crushing, discarded bottles made of glass were cleaned with normal water to eliminate contaminants (Harrison et al., 2020; Hamada et al., 2022; Bagheri and Moukannaa, 2021). The crushed glass was then filtered through a 600 μm sieve to remove large glass particles. The sieved glass was grounded for 3 h in a Los Angeles Abrasion Machine with 16 stainless balls to obtain 25 μm particles (diameter: 40 mm). To ensure that the nanoparticles were dispersed effectively, the powder was preheated in an oven for an hour at a temperature of 110 °C ((±5) and then grounded for 7 h in the ball mill machine. The method for obtaining nano-powder or NGP from glass bottles was employed for the production of concrete (Sun et al., 2022; Bohn et al., 2021).

A survey of the research found that extensive studies had been made on the impact of different NMs being added or replaced on the characteristics of cementitious material, which prompted investigators to look into the impact of NMs on the characteristics of geopolymer goods. Fig. 2 shows that 46.3% of the research is devoted to studying the effects of NS, while 7.2 percent and 4.7 percent are devoted to NA and CNT, respectively. NT and NC were utilized up to 11.4% and 8.5% in different research works. The remaining NMs receive less than 5% of the reviewed research. It is worth noting that there's very little literature on the effects of NM, NZ, NGP, NCC, NFA, and GO on the properties of geopolymer products, indicating that there's a lot more research to be done. Fig. 3 shows the SEM images of different NMs have been used in the GC, and Table 1 lists the characteristics of NMs used in the previous literature.

3. Effects of nanomaterials on geopolymer composite properties

3.1. Characteristics of fresh concrete

The main fresh concrete properties are workability and setting time. Some parameters affecting fresh concrete's properties are source materials, alkali activators, the molar concentration of NaOH solution, and the dispersion of particle sizes for the binding and filler materials (Shahrajabian and Behfarnia, 2018; Abdalla et al., 2022b). The addition of NMs also can have a greater influence on the fresh concrete properties due to its finer size. The workability and setting times of geopolymer products are essential factors that indicate their fresh-state features. It's worth noting that, unlike Portland cement, the geopolymer binder lacks the tri-calcium aluminate, and tri-calcium silicate chemicals can cause the heat of hydration, resulting in a lack of research on the heat of the hydration process.

3.1.1. Nano silica (NS)

To improve the qualities of fresh GPP, NS-based activators may be utilized. Findings revealed that it reduces the viscosity and improves the workability of concrete (Alvee et al., 2022). It is reported that the workability of the FA-based GPM increases with an increase in the percentage of NS (Saini and Vattipalli, 2020; Ahmed et al., 2022a; Mustakim et al., 2020; Gülşan et al., 2019). Increasing the NS significantly is tied to negatively affecting the slump value of the GGBFS-FA based GC due to its fine particle size, which increases the water demand. Therefore, a suitable water-reducing agent should be utilized to get to achieve the needed slump value of the GPC carrying NS (Adak et al., 2017; Isfahani et al., 2016). In the case of MK-based GPC with a determined solid-to-liquid ratio, NS reduces the setting time by activating the polymerization process (Zidi et al., 2021). An increase in the content of SS makes GC more sticky, which is attributed to an increase in the initial as well as the final setting time of MK-based GC containing NS content with the increase of SiO_2/Na_2O (Gao et al., 2014). Suitable retarders can reduce the rate of the polymerization process without affecting the strength of the composite. The addition of the mixture of NS and alumina can reduce the setting time of Class C FA-based GC by activating the polymerization process. This is because of free calcium ions present in class C FA; as a result formation of C–S–H gel accelerates

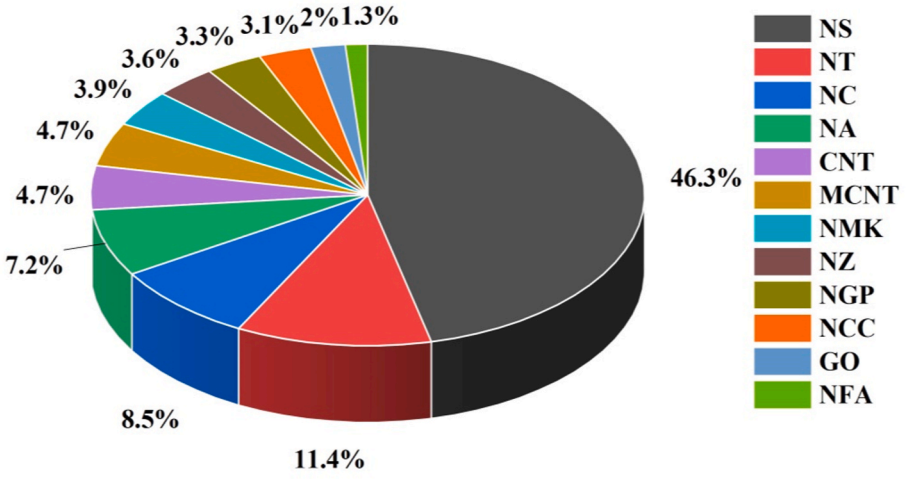

Fig. 2. Contribution of various NM's to GC preparation.
[Note: NS-Nano Silica; NT-Nano Titania; NC-Nano Clay; NA-Nano Alumina; CNT-Carbon Nano Tube; MCNT- MultiWalled Carbon Nano Tube; NMK-Nano Metakaolin; NZ-Nano Zinc oxide; NGP-Nano Water Glass; NCC-Nano Calcium Carbonate; GO-Graphene Oxide; NFA-Nano Fly ash].

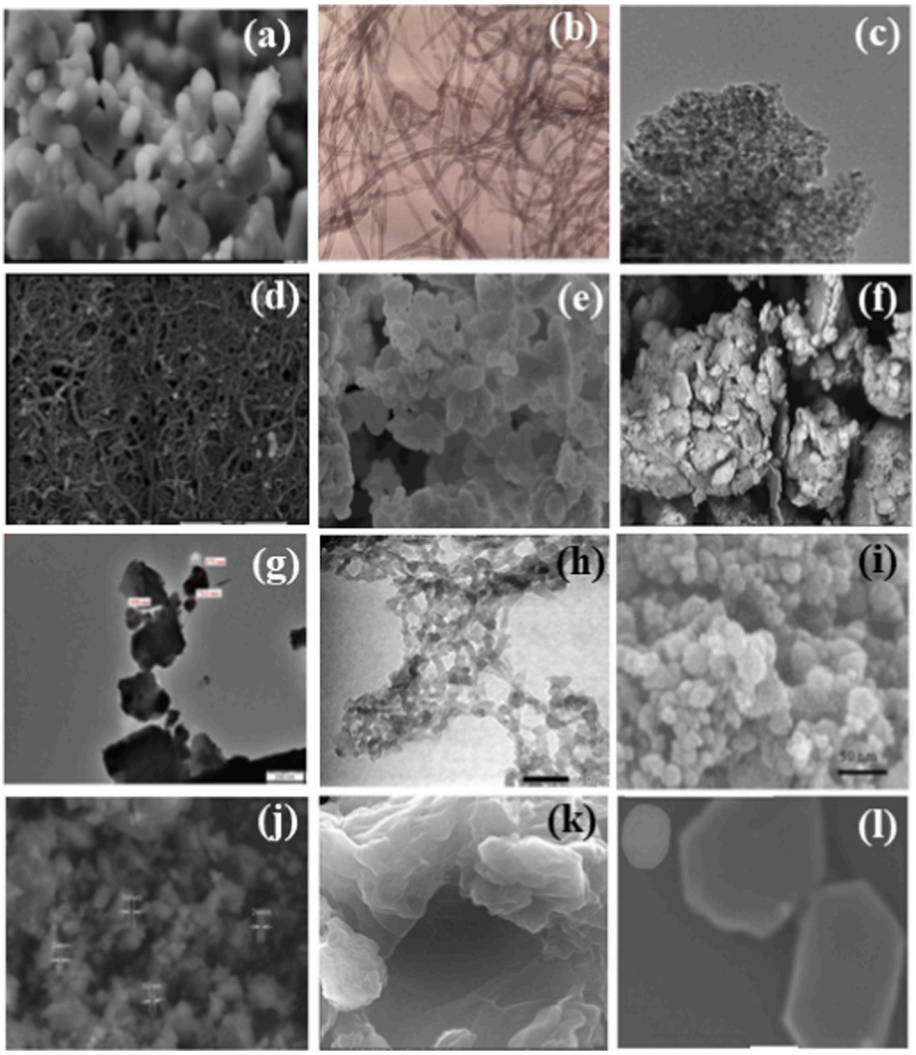

Fig. 3. SEM image of the Nanomaterials (a) Nano Alumina (Mohammed et al., 2021); (b) Multiwalled Carbon Nano Tube (Hamzah et al., 2020); (c) Nano Titania (Ahmed et al., 2022a); (d) Carbon Nano Tube (Unis et al., 2022); (e) Nano Calcium Carbonate (Saxena et al., 2018); (f) Nano Clay (Saxena et al., 2018); (g) Nano Glass Powder (Shaikh and Supit, 2015); (h) Nano Silica (Taylor et al., 2014); (i) Nano Zink Oxide (Xie et al., 2020); (j) Nano Fly Ash (Assaedi, 2021); (k) Graphene Oxide (McDonald et al., 2022); (l) Nano Metakaolin (McDonald et al., 2022).

the initial and final setting process of the composite (Phoo-ngernkham et al., 2014; Zidi et al., 2021). Therefore, it can be concluded that the initial, as well as the final setting time of the GC, is directly dependent on the source material, solid-to-liquid ratio, and then added NMs.

3.1.2. Nano-alumina (NA)

A few researchers examined the impact of NA on the development of class F FA-based GC due to its slow setting rate. When compared with NS, NA has less reduction in the setting time of GC (Zidi et al., 2019). When the content of NA exceeds 7% by weight of the binder, initial as well as the final setting times are greatly reduced in the case of high calcium FA-based GC (Li et al., 2017a). The use of NA does not accelerate the polymerization process of GC. Nano Alumina (NA) does influence the setting time of geopolymer composite. Therefore, NA does not have any effect on the polymerization process, but it has a direct effect on the setting time of geopolymer composites (Phoo-ngernkham et al., 2014; Chindaprasirt et al., 2012; Pardal et al., 2009; Yip et al., 2005; Garcia-Lodeiro et al., 2011). Therefore, increases in the percentage of NMs are directly proportional to the setting of high calcium FA GC.

3.1.3. Nano titanium dioxide (NT)

The addition of NT decreases the workability of GC without consideration of base materials. Duan et al. stated that the workability of FA-based GC decreases with increasing the percentage of NT (Duan et al., 2016). They also examined that the incorporation of NT by 3% and 5% to the GPP reduces workability by 21.86% and 31.12%. Similarly, the addition of NT to the MK-based GC decreases the setting time of the matrix also, which may be attributed to accelerating the polymerization process (Sastry et al., 2021; Guzmán-Aponte et al., 2017). Therefore, the addition of NT accelerates the setting of the composite. Still, on the other hand, it affects the workability of the whole system, which requires a high range of water reducer.

3.1.4. Nano-clay (NC)

In a similar way to reducing the workability of the addition of NMs, the addition of NC also reduces the fresh properties of GC. When compared with other NMs like NS and NA, NC exhibits less reactivity with alkali activators and water (Ravitheja and Kiran Kumar, 2019). In the limited availability of investigation on geopolymer with NC, it may be concluded that the addition of NMs reduces the initial and final setting times of GC in a broad sense.

In the case of GPP and GPC, NMs addition reduces the workability, whereas the workability of GPM increases with the increasing proportion of NMs. NMs addition reduces the setting time of the GC, especially if the percentage of adding NA exceeds 7%, a great reduction in the initial as well as the final setting time of GC. There are few research works that evaluated the different fresh concrete properties of CNT, MCNT, NCC, NFA, NM, NZ, GO, and NGP added in GC. However, there is currently an unavailability of details on these NMs' impacts on the fresh

Table 1
Characteristics of nanomaterials.

Composite type	NMs and percentage	Particle size	Surface area	Purity (%)	Density	Other Properties	Ref.
GPC	CNT (0.01 and 0.02); MCNT (0.01, 0.03, 0.05, 0.07, and 0.09%)	Length = 10–100 mm, inner diameter = 1.5–15 nm, outer diameter = 50 nm; Length (μm) = 1–5, Inner diameter(nm) = 20–30	Surface area (m^2/g)>300	97		Aspect ratio(%) = 120, Amorphous carbon (%) = 0, Ash(%) = 3,	Sekkal and Zaoui (2022)
GPC	CNT (2, 5, and 10)	Diameter of 20–120 nm					Gao et al. (2015)
GPP	MCNT (0.5 and 1)	Length (μm) = 10, Inner diameter (nm) = 10-20	Surface area (m^2/g) = 250–280,	>95,		Amorphous carbon% = 3, Ash % = 0.2,	Manzur et al. (2016)
GPM	MCNT (0.1, 0.2, 0.3, and 0.4%)	Outer diameter (nm) 20–30 Inner diameter (nm) 4, Length (mm) 1–5		97		Ash (%) 3 Amorphous (%) 0, Field (%) 800	Zhu et al. (2021)
GPC	NA (1.0, 2.0, and 3.0%); NS (2.0, 4.0, 6.0, and 8.0%); NC (2.5, 5.0, and 7.0%)	Particle size (nm) = 20; particle size = 10 nm		99.7		, Blaine (m^2/gr) = 100,; SiO_2 = 61.24, Al_2O_3 = 20.89	Huang and Han (2011)
GPP	NA (1.0, 2.0, and 3.0%)	Average size = 50 nm		99.9%	Density = 0.4–0.5 g/cm^3,		Mohammed et al. (2021)
GPP	NA (1.0, 2.0, and 3.0%)	Particle size = 80 nm,	Specific surface>10 m^2/g	99.9%	density = 1.6 g/cm^3	Appearance- White powder	Li et al. (2017a)
GPC	NS (6)	Particle size = 4–16 nm,	BET specific area = 50 m^2/g,	99.8	density (g/cm^3) = 2.37,	Viscosity (Pa.S) = 8.5, pH = 9.0–9.6, Solid content (% Wt.) = 31	Huang et al. (2022)
GPC	NS (1.0, 2.5, 5.0, and 7.5%)	Particle size = 35 nm,; particle size = 50–70 nm	Specific surface area = 80 m^2/g,		Bulk density = 1.4 g/cm^3	pH = 9.5, 99.8% SiO_2; Solid content = 50%,	Wang et al. (2019)
GPC	NS (0.5, 1.0, and 1.5%)	Particle size = 12 nm	Surface area = 200 ± 25 m^2/g	99.8,	Bulk density = 1.4 g/cm^3	PH in 4%, dispersion = 3.4–4.7	Li et al. (2012)
GPC	NS (1.0, 2.0, and 3.0%)	Average size = 12 nm	Surface area (m^2/g) = 200	99.8,	Bulk density = 1.4 g/cm^3,	pH = 9.5 Viscosity (cps) = 15	Wang et al. (2022b)
GPP	NS (0.5, 1.0, and 2.0%)	Particle size = 10 nm	, surface area = 670 m^2/g	99.9%,	Compacted density = 0.14 g/cm^3	phase = non-crystal, Appearance- white powder	Azeem et al. (2021)
GPC	NT (1.0, 2.0, 3.0, 4.0, and 5.0%)	Grain size (20-10 μm)				titanium and 40.55% oxygen	Weir et al. (2012)
GPP	NT (0.5 and 1.0%)	Particle size = 21 nm				Anatase/Rutile = 80:20	Ahmed et al. (2022a)
GPC	NFA (10%)					Through the ball milling process	Assaedi (2021)
GPC	NM (2.0, 4.0, 6.0, and 8.0%)	Particle size = 88.7 nm	Surface area (m^2/g) = 140.792				Li et al. (2021)
GPC	NZ (0.3, 0.5, and 0.7%)					Through sol-gel techniques	Sastry et al. (2021)
GPC	GO (0.0, 0.1, 0.35 and 0.5%)	Hydrophilic and oxygenated 1.1 nm, thick pristine GO sheets,0.5–5 μm.		>90%			Rovnaník et al. (2016)
GPC	NCC (1, 2 and 3%)	Particle size-15–40(nm),		>97.5	Bulk Density (g/ml) 0.68	pH 8.0–9.0, Moisture Content (w%) 0.5, Morphology: Cubic	Alomayri (2019)
GPM	NGP (5,10,15 and 20%)	The particle size of 25 μm.				Los Angeles Abrasion Machine method	Bayiha et al. (2019)

qualities of geopolymer materials in the literature. As a result, there is a large gap in the study on the impact of CNT, MCNT, NCC, NFA, NM, NZ, GO, and NGP on the fresh concrete composite properties of geopolymer-based products. Fig. 4 shows the fresh concrete properties of NMs-embedded GC mixes.

3.2. Mechanical properties of hardened concrete

The mechanical performance of concrete is related to the packing density and microstructure. In the previous part, it is explained that the addition of different NMs notably affects the microstructure of the matrix. This section reveals the influence of different NMs on the hardened performance of GC is explained. The packing density and microstructure of the mix are the key factors that influence mechanical properties such as compressive strength, tensile strength, flexural strength, and modulus of elasticity (Mathews et al., 2021; Thanaraj et al., 2020).

3.2.1. Nano-silica (NS)

The addition of NS in high calcium FA GPP shows some improvement in compressive strength and flexural strength under ambient curing conditions (Deb et al., 2015; Wang et al., 2019; Kiran Kumar and Gopala Krishna Sastry, 2017). The authors explained that the impact of the incorporation of 2% NS in the GC at the age of 90 days exhibits 51.8 MPa and 5.98 MPa of compressive strength and flexural strength, respectively, which is 32% and 38% more than those of the specimen without NS. This is because of the generation of polymer gel due to the reaction of calcium with NS. They further reported that the excessive NMs dispersed the ingredients, which resulted in a less dense structure (Prakasam et al., 2020). Therefore, the mechanical strength gets reduced when the proportion of the NS is increased by 3% (Gülşan et al., 2019). Deb et al. (2015) published a similar study on FA GPM with NS. They also reported similar results. Due to the unreacted particles, 2% gives better results than 3% of NS in the GC. A similar pattern was shown in the case of Portland cement, and GGBFS blended GC with NS. Gao et al. (2013) examined the impact of the incorporation of 1% of NS with different solid-to-liquid ratios in the MK-based GC. The study indicated an increase in mechanical strength and bulk density. When the proportion of NS exceeds 1%, strength gets starts to reduce due to the

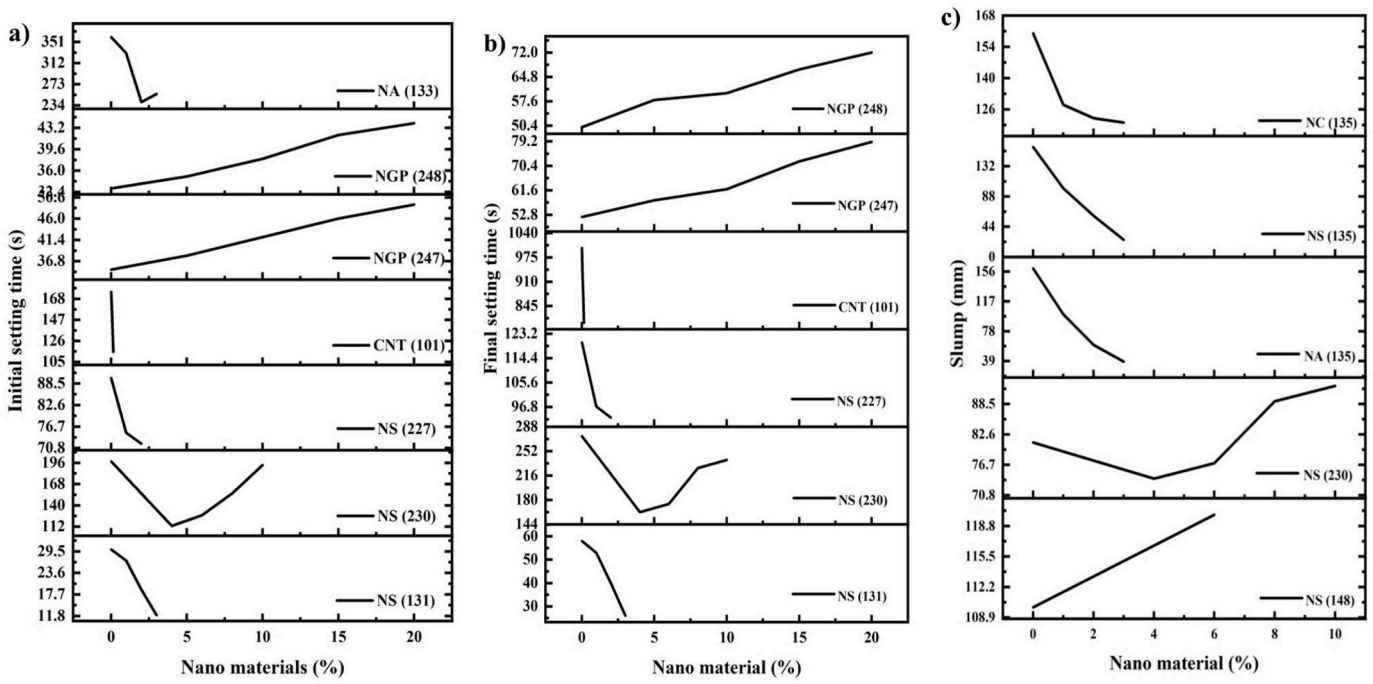

Fig. 4. (a) Initial setting time of geopolymer composite; (b) Final setting time of geopolymer composite; (c) Slump of geopolymer composite.

leaching of excess NMs. But, according to Gao et al., the addition of 2% NS to alkali activators GGBFS-FA concrete was found to be the optimum content (Gao et al., 2015).

Concrete that contains 2% of NS has higher strength than the specimens with other percentages of NMs due to its pore-filling effect. Adak et al. (2014) studied the impact of colloidal NS on the structural properties of FA-GPC, and they reported that the addition of 6% colloidal NS made the mix homogeneous by increasing the Si/Al ratio. As a result, the formation of a substantial improvement in the bond and flexural strength by the powerful transition zone between geopolymer mixtures and aggregates. Wang et al. (2019) examined the effect of NS (0.5–3%) in GGBFS-GPP, and they concluded that the NS content beyond 2% does not provide any strength to the matrix, but it decreases the strength. Therefore, it can be concluded that most of the researchers found the optimal percentage of 2% of NS to provide better strength than the other percentages. This may be due to the performance of NS for the accelerated geo-polymerization and its pore-filling capacity(Mustakim et al., 2020; Revathi et al., 2018; Rodríguez et al., 2013; Çevik et al., 2018; Ekinci et al., 2019); (Mustakim et al., 2020; Revathi et al., 2018; Rodríguez et al., 2013; Çevik et al., 2018; Ekinci et al., 2019).

3.2.2. Nano-alumina (NA)

The combination of NA and NS improves the strength of class F-based GC (Phoo-ngernkham et al., 2014). The main reason for the higher strength is due to the formation of the extra amount of C-A-S-H and N-A-S-H gels in the GC. Shahrajabian and Behfarnia (Chindaprasirt et al., 2012) studied the effect of NA on the GGBFS-based GC, and they reported that the maximum compressive strength was attained with 2% of NA with different curing periods due to the denser geopolymer gel formation and micro dispersion. Also, it was reported that the strength gets reduced with an increase in the percentage of NA content by 3% due to the mass deposition of NMs, which leads to the matrix becoming heterogeneous. The mechanical strength of GPP containing NA was studied by Thamer Alomayri (2019), and he reported that the maximum strength was obtained at a percentage of 2% of NMs, which is due to the acceleration of polymerization reaction by the NA. Beyond this percentage, a reduction in strength was noticed due to the unreacted NMs. NS and NA also exhibited a similar pattern with an optimal percentage of 2%, and the extra percentage of NMs was found to affect the strength due to the agglomeration effect.

3.2.3. Nano titanium dioxide (NT)

Duan et al. (2016) studied the fluidized bed FA-based GC with the addition of NT 1%, 3%, and 5%. An increase in the percentage of NT accelerated the polymerization process and increased the compressive strength at an early age as well as at a later age. Yang et al. (2015) studied the mechanical properties of GGBFS-based GPP with 0.5% of NT. The compressive strength was found to increase by 10%, 15%, and 9%, while flexural strength was increased by 25%, 25%, and 38% at corresponding curing periods of 3, 7, and 28 days.

3.2.4. Carbon nanotubes (CNT)

As explained in the fresh concrete properties of GC incorporated with CNT, Abbasi et al. (2016) reported that adding 0.5% MCNT in the MK-based GC increases mechanical strength. Rather, 1% of MCNT addition leads to an agglomeration effect which reduces the strength of GGBFS-based GC (Li et al., 2021; Su et al., 2020). Rovnanik et al. (Rovnaník et al., 2016) reported that a 0.15% percentage of MCNT was optimal in the case of FA-based GC. However, it has been explained that CNTs in limited amounts (up to 0.5%) can be utilized to enhance the hardened performance of GC. At the same time, greater concentrations of CNT might cause agglomeration, which can be detrimental (Naskar and Kumar, 2016; Abbasi et al., 2016; Khater and Abd El Gawaad, 2016; Jittabut and Horpibulsuk, 2019; Saafi et al., 2013). Luz et al. (da Luz et al., 2019) investigated the mechanical, rheological, and microstructural properties of MK-based GPP with pristine and functionalized CNT. When 0.1 percent CNT was introduced to the GPP when relative to the standard GPP, the density of macropores was decreased by 19%, which could describe the improved hardened properties. The drop in compressive strength and flexural strength with 0.2 percent CNT addition, on the other hand, can be interpreted as an increase in total porosity (+13%) because of a possible improvement in CNT group development.

3.2.5. Nanoclay (NC)

Assaedi et al. (2016a) investigated FA-based GC with NC, and they

reported that the optimal amount to be added to obtain maximum mechanical properties is 2%. Shahrajabian and Behfarnia (2018) studied the effects of the addition of NC with a different percentage in GGBFS-based alkali-activated concrete. The results showed that a concrete mix containing 1% NC diminishes compressive strength at 7 and 28 days, but the strength was higher at later ages. However, the addition of 2 and 3 percent NC increased compressive strength at each curing period, with the addition of 2% NC being shown to be the optimal percent. Based on the available literature, it can be concluded that using a small amount of NC to improve the mechanical performance of GC may be beneficial (Kotop et al., 2021; Ravitheja and Kiran Kumar, 2019; Assaedi et al., 2016b; Joshi et al., 2015). However, various waste materials that are high content of AS could be used to determine the best dose of NC to use with diverse materials.

3.2.6. Nano Calcium Carbonate (NCC)

Assaedi (2021) investigated the compressive strength and flexural strength of GC with NCC particles at 1, 2, and 3%. These findings show that adding NCC particles to materials does not considerably improve their compressive strength. The compressive strength of GC consisting of 1 and 3% NCC is 33% greater than that of the standard geopolymer, which contains no NMs. But, as compared to the control geopolymer, the sample containing 2.0 wt percent NMs had a compressive strength increase of roughly 14 percent; this was lower than the GC consisting of 1.0 and 3.0 wt percent. A less compact microstructure or an uneven distribution of fibers across the mixture may be to blame for this. Comparing this specimen to those with 1 and 3 wt percent NMs, non-uniformity may lead to poor distribution and clustering, lowering the packing effect and pozzolanic reaction of the NMs. The increment could be attributable to the NCC components' packing effect, which helps to consolidate and increase the density of the GC matrix. Furthermore, when exposed to alkali activators, the NCC particles may partially react, generating a C–S–H gel in addition to the main geopolymer binder (sodium silicate aluminium hydrate, N-A-S-H) within the matrix. A similar trend was seen by Shaikh and Supit (2015) and Bayiha et al. (2019), who found that introducing varying amounts of calcium compounds boosted the enlarging strength of thermal halloysite clay and FA geopolymer. When the NCC component was increased from 1.0 to 2.0 percent, the flexural strength of GC increased dramatically, with a less proportionate rise when 3.0 percent was added. The flexural strength of the pure geopolymer, are those including 1.0, 2.0, and 3.0 wt percent NCC particles and which consisting of 1.0, 2.0, and 3.0 wt percent NCC particles were 2.59, 4.76, 9.08, and 7.96 MPa, respectively. The sample containing 2.0 percent NCC particles showed the greatest improvement in strength (9.08 MPa). Better adhesion or contact between the NCC nanoparticles and the fibers may have contributed to the higher flexural strength by providing more density. However, the combined action of fibers and NMs is responsible for this improvement; employing both provided better workability, lesser micro gaps or micro-cracks, and a homogenous dissipation in the geopolymer mixture (Abdalla et al., 2022a). In summary, both additives contributed to the sample's composition being densified and strengthened. The researchers discovered that the lack of flowability or non-uniformity of the fibers inside the material, which would permit trapped air to be trapped in the mixture and poor strength, was the cause of the poor strength in specimens with more than 2.0 wt percent of NCC.

3.2.7. Nano Fly ash (NF)

Rajendran and Akasi (2020) studied the performance of Crumb Rubber and NFA Based Ferro-geopolymer panels under impact load. In comparison to control specimens, GP specimens had a higher compressive strength. GGBFS-based GPM has a higher compressive strength than FA-based GPM, which is 17 percent higher. The presence of CaO, a more compacted structure from N-A-S-H and C–S–H gel formation, and the 3D AS structure from the polycondensation process are the key reasons for the increased strength. The addition of rubber to the mix reduces compressive strength by 5%, which is offset by the addition of NFA to the mix. The compressive strength of the NFA-infused GPM is 35 MPa, which is the highest of all the panels. This increased strength is due to NFA's capacity to fill pore spaces, resulting in a dense microstructure with good bonding properties due to its glassy, inert, and smooth surface (Mudgal et al., 2020; M and Bharathi, 2022).

3.2.8. Nano metakaolin (NMK)

M. Kaur et al. (2018) studied the microstructure and strength development of FA-based GPM with the addition of NMK. According to studies, a 4 percent replacement level of NMK in FA-based GPM resulted in a considerable increase in compressive strength. After 28 days of ambient curing, the percentage change in compressive strength for the mixes containing 2%, 4%, 6%, 8%, and 10% of NMK w 9.27, 22.66, 9.55, 4.32, and −1.27, respectively. After three days of ambient curing, an FA-based GPM incorporating NMK regained roughly 70–80% of its 28-day compressive strength. The involvement of silica and alumina oxide of NMK in the polymerization reaction may be the explanation for the improvement in compressive strength of FA-based GPM with varying percentage levels of NMK. Because of the homogenous dispersion of NMK, which leads to the development of nucleation material for the polymerization reaction, there is a considerable increase in compressive strength at 4 percent NMK. The result of this geopolymer reaction is a more compact structure (Hassaan et al., 2015).

3.2.9. Nano-zinc oxide (NZ)

Zidi et al. (2020) studied the impact of NZ on the hardened performance of concrete of GC. Compressive strength tests were conducted to investigate the mechanical properties of GPM with various NZ levels (0.3–0.7%). Pure geopolymer demonstrated lower mechanical strength than geopolymer with NZ added. The compressive strength of composites improves with increasing NZ concentrations and then declines. When the dosage of NZ was 0.5 percent, it attained the maximum compressive strength (38 MPa). This is due to the NZ particles' interfacial adherence to the geopolymer, which reduces the interfacial transition zone (ITZ) (Sarkar et al., 2018). An investigation found by Rustan et al. (Rustan and Irhamsyah, 2017) when the NZ dose was 0.7 percent, the compressive strength was reduced due to the agglomeration of NMs that weren't evenly distributed. In this research, the addition of 0.3% NZ provided an increase in compressive strength of about 16%. In the current investigation, the addition of 0.5 percent NZ boosted compressive strength by 26%.

3.2.10. Graphene Oxide (GO)

Bellum et al. (2020) examined the properties enhancement of FA-GGBFS based GO GPC. They added 1, 2, 3, and 4 percent of GO to the composite to enhance the properties of geopolymer. With the inclusion of GO, the strength of GPC is enhanced at both younger and older ages. The continual strength development of the GO-based mixtures was visible over time from the date of ambient curing. The physical and chemical connection of GO and geopolymer matrixes determines the compressive strength of GO-based GPC samples. Additionally, the addition of GO to GPC creates a denser structure that serves as a mechanical filler material, improving compressive strength at an initial stage (Saafi et al., 2015). The experimental findings showed that adding a small amount of GO to GPC boosted compressive strength significantly at all curing ages. A 3% increase in GO, on the other hand, has been demonstrated to outperform all previous levels. Because of the larger surfaces and irregular forms of GO nanosheets, higher strengths were achieved. Due to this shape, the connection technique inside the geopolymer matrices has been enhanced. In comparison to the 3 percent GO-based GPC mix series, the addition of 4 percent GO resulted in a drop in compressive strength values. Due to the substantial porous structure and hydrophilic nature of GO, aggregation of GO nanosheets in the GPC resulted in a decrease in compressive strength with increased GO content. With the rise in reaction time, it was found that GO's

extraordinarily large specific surface region, thicker morphology, and lesser amorphous degree play a crucial role in enhancing strength attainment(Li et al., 2022a). The addition of GO connective to the extra polymer gel generation is responsible for the increased strength. The addition of a small amount of GO, on the other hand, had a greater impact on the ME values of FA - GGBFS based GPC, with the best results achieved at a 3% GO addition(Krishna et al., 2021).

3.2.11. *Nano glass powder (NGP)*

The effects of NGP on the hardened and durability qualities of GGBFS GPM were examined in an experimental research study. They discovered that adding NGP to the GPM improves the tensile strength at a dose of 5%, and thereafter it was reduced. As an illustrative example, when such NGP percentage was raised from 0% to 5%, tensile strength was greatly improved (22.2%). The better hydration abilities of nanopowder, which is present in the morphology of the GPM, may be the cause of the rise in tensile strength. While the tensile strength of the GPM was modestly (5.55 percent) enhanced at 10% NGP for the standard specimens, increasing at 15 and 20 percent NGP concentrations caused a 19.4 percent and a 22.2 percent drop in the splitting tensile strength of the GPM (Hamzah et al., 2020). The addition of NGP to the GPM enhances the flexural strength at a 5% NGP dosage, but then the flexural strength declines. For example, as NGP concentration grew from 0% to 5%, flexural strength greatly improved (14%). The improvement in flexural strength could be attributed to the addition of nanopowder, which has better hydration properties, to the morphology. While the flexural strength of the GM was the same as the control samples at 10% NGP, increasing the NGP dose caused the flexural strength of the GPM to drop to 9.5 percent and 15.6 percent at 15 and 20 percent NGP contents (Samadi et al., 2020; Huseien et al., 2020). This can be a result of rising water requirements. Due to this, the hydration process was negatively affected.

Furthermore, laboratory experiments have demonstrated the impact of various NGP doses (0, 5, 10, 15, and 20 percent) on the hardened and microstructural features of GGBFS GPM. They found that the modulus of elasticity improved from 5% of NGP to 15.4 GPa, but then declined from 10% of NGP to 14.4 GPa, relative to the NGP standard specimen, which had a modulus of elasticity of 14.1 GPa. At 15–20 percent NGP, the

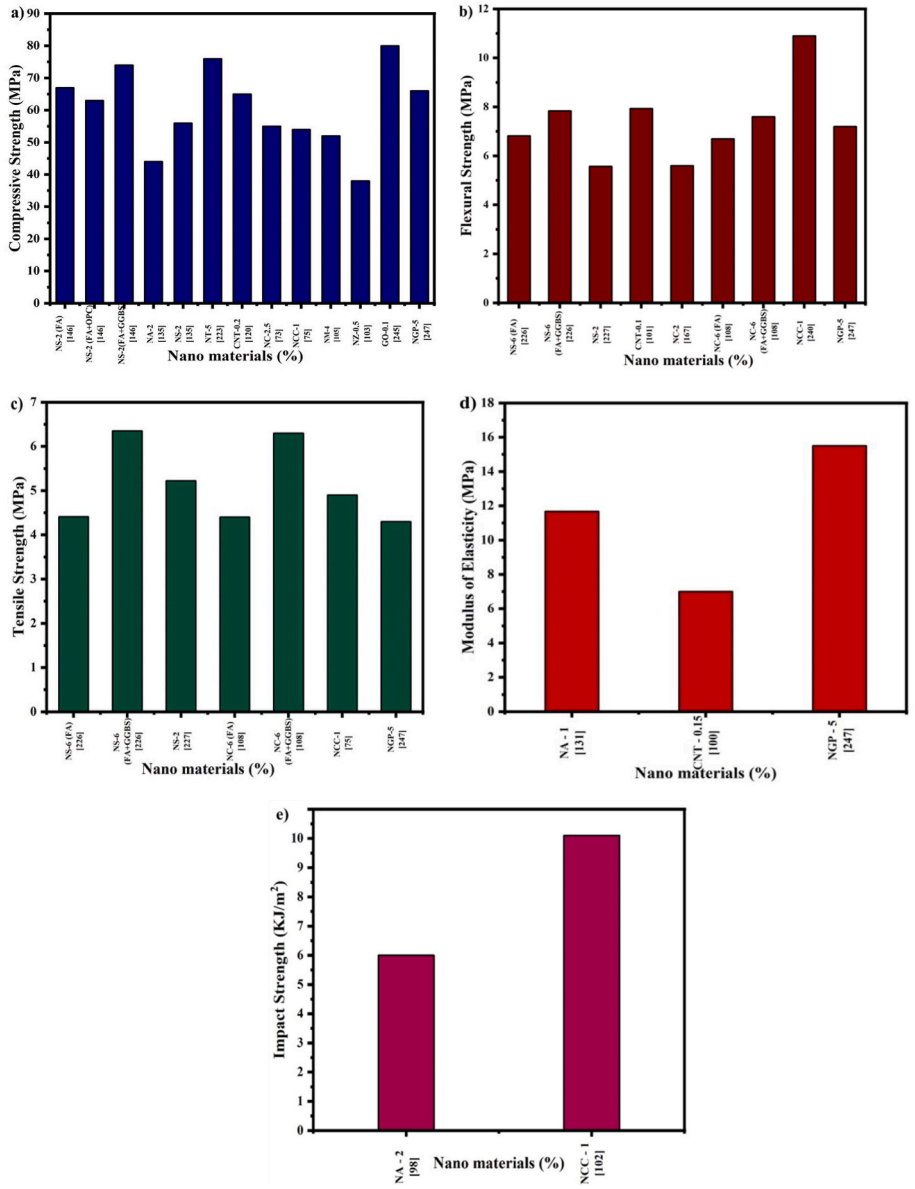

Fig. 5. Mechanical strength of Geopolymer concrete with nanomaterials. a) Compressive strength; b) Flexural strength; c) Tensile strength; d) Modulus of elasticity; e) Impact strength.

modulus of elasticity of the GGBFS-based GPM reduced from 13.8 to 13.6 GPa (Derinpinar et al., 2022). Huseien et al. (2020) reported similar results. The decreased calcium content of GGBFS-based GPM having less than 10% NGP was blamed for the lower modulus of elasticity. From Fig. 5, it is clear that the addition of NMs enhances the overall mechanical characteristics.

3.3. Durability properties

3.3.1. Nano-silica (NS)

According to Gao et al. (2015), adding NS in the 1 to 3 percent to GGBFS blended FA-based GPC decreases the porosity. When compared to the control mix, the porosity of the 2% NS mixture decreased by 26.4%. Porosity increased marginally with a larger NS content which is to the reduction in workability and, as a result, an increase in air molecule, which resulted in the previous. Deb et al. (2016) studied the resistance towards acid and sorptivity of GC with 0 and 2 percent of NS. According to the authors, a reduction in sorptivity was caused by two factors: first, the inclusion of NS densified the microstructure, and second, the production of extra AS gels as a result of the polymerization reaction. Furthermore, the addition of NS to GC boosted resistance to mass loss owing to sulfate assault(Çevik et al., 2018). Water absorption and Rapid chloride penetration tests were conducted with different NS content and different molar concentration. The results show that increase in the concentration of SH correspondingly, the charge passed through each GPM get decreased, and the addition of 6% NS showed the highest resistance to charge transmitted. The existence of more crystalline components in NS increased the durability properties(Ekinci et al., 2019).

The results of the water absorption test showed a similar pattern. Meanwhile, the scientists claim that the RCPT test, which measures moisture content, is not appropriate for geopolymer-based goods because it primarily assesses ionic activity through concrete samples subjected to a greater potential variation of 60 V. However, the situation of GPC specimens with a larger coefficient of diffusion at 60 V, due to GPC's higher conductivity than ordinary Portland cement concretes, RCPT experiments may provide inaccurate flow rate. The provided induced voltage heats the test cubes in RCPT, increasing the open crack fluid's conductivity and affecting the flow rate (Shi, 2004). But, as Noushini and Castel (2018) noted in their study, the RCPT test may be successfully done on GPC at a lower cell potential of 10 V. Based on the findings of the previous studies, As a result of the formation of additional AS gel and the filling of micro-pores during the polymerization process, it has been suggested that incorporating NS in a definite proportion can densify the morphology of geopolymer, which reduces sorptivity and improves durability.

3.3.2. Nano Titanium dioxide (NT)

Carbonation is an essential characteristic of concrete that determines its long-term durability. According to Duan et al. (2016), the addition of NT in GPC reduces carbonation depth. In comparison to the reference mix, geopolymer mixes including NT were shown to have decreased carbonation depth, especially mixes containing 5% NT. This was attributed to the microstructure densification caused by the addition of NT, which resulted in greater resistance to carbonation depth. According to Yang et al. (2015), adding 0.5 percent NT in GC lowered the porosity of pore size 1.25–25 nm, further enhancing the pore size dispersion. Based on the findings, it can be concluded that the addition of NT to the geopolymer matrix can plug nano-pores in the composite, resulting in higher resistance to carbonation attack and, as a result, improved geopolymer durability (Ambikakumari Sanalkumar and Yang, 2021).

3.3.3. Carbon nanotubes (CNT)

Khater and Gawaad (Khater and Abd El Gawaad, 2016) used MCNT in the proportions of 0.1%, 0.2%, 0.3%, and 0.4% to investigate the water absorption of GC at 7, 28, and 90 days. The findings showed that water retention for each GC substantially decreased with increasing curing period. The quantity of water retention was decreased as a result of the condensation of three-dimensional geopolymer complexes in the gaps of the mixture, which resulted in the microstructure's densification. Water absorption was lowest at 0.1 percent MCNT, but as the amount of MCNT added increased, the amount of water absorption also increased. When higher doses of MCNT were introduced, the geopolymer network system didn't form as quickly, which caused an increase in water absorption, resulting in agglomeration and an increase in void content. It has been concluded that adding MCNT to a product does not considerably improve its durability, but if used in higher amounts than 0.1 percent, it can cause agglomeration, which can increase micro-voids and compromise the product's longevity (Khater and El-Nagar, 2020). The authors reported that more research is needed to determine the optimal dose of MCNTs when using various types of AS source materials.

3.3.4. Nano clay (NC)

Assaedi et al. (2016a) investigated the impact of three different NC content levels (1%, 2%, and 3%) on the geopolymer nanocomposite's permeability and moisture absorption. For each percentage, NC addition improved the durability performance by reducing porosity and water absorption. Comparatively to a standard geopolymer mixture, the optimum proportion of NC was found to be 2%. GC, with the addition of 2% of NC, reduced porosity and water absorption by 7.1% and 17%, respectively. With the incorporation of the same variant of NC as noted in Shahrajabian and Behfarnia (2018) to determine how freezing-thawing cycles affect mass and compressive strength. They found that as the number of freezing and thawing cycles increased, the compressive strength of each combination decreased. The compressive strength loss was found to be the minimum in the mix containing 2% NC. The mixes containing NC that had been frozen and thawed, on the other hand, had higher compressive strength than the control concrete. Density in NC mixtures was observed to decrease associated with revealed freezing-thawing phases. The damage to the edges of the samples was determined to be the primary cause of mass loss in the concrete mixtures. In the case of mass loss and compressive strength, the 2% NC mix outperformed the other mixes in the freezing-thawing test (Gadkar and Subramaniam, 2021). It can be concluded from the aforementioned experiments that a small amount of NC (up to 2%) improves microstructure, reduces porosity, and reduces water absorption, therefore enhancing freezing and thawing resistance and hence improving durability.

3.3.5. Nano Fly ash (NF)

Rajendran and Akasi (2020) studied the addition of NFA to the durability properties of Ferro-geopolymer panels. Because NFA boosts the strength and durability of the specimen due to its pore-filling nature, the absorption of the NFA-based specimen is reduced.

3.3.6. Nano-zinc oxide (NZ)

As opposed to the aforementioned findings, Zidi et al. (2020) found that adding NZ to A lot of small gaps increased. In contrast, the percentage of bigger gaps decreased as a result of the varied ways that geopolymer slurry mixtures affected the geopolymer pores distribution. This outcome is the result of the nature of NMs moisture absorbing properties.

3.3.7. Graphene Oxide (GO)

The electrical conductivity of the GPC was measured over around 6 h during the experiment. It was discovered that GO incorporated FA GGBFS mixed GPC mixes have chloride ion penetration. Increasing the GO concentration in FA-based GGBFS GPC was discovered to provide the best resistance to chloride ion permeability. Permeability is poor in the mix with 3 percent GO, which could be ascribed to the higher GO content. On the other hand, the control mix falls into the high chloride ion-

permeable class, which, with a 3 percent rise in GO incorporation, enhanced resistance towards chloride ion penetration. However, the mix containing 30% GGBFS, 70% FA, and 3% GO had lower chloride ion penetration than the other mixes. This means that even a modest amount of GO has a greater impact on chloride ion permeability protection. It seems related to a skillful enhancement of GPC's microspores. The exceptional resistance of GO-modified GPC specimens to chloride ion permeability was discovered by a fast chloride permeability test. The chloride ion permeability was found to be much lower in GO-based mixtures (3%) than in the other mixes (Saafi et al., 2015).

3.3.8. Nano glass powder (NGP)

Huseien et al. (2020) and Samadi et al. (2020) investigated the effects of NGP on the mechanical and durability parameters of blended FA/GGBFS-based GPM in the laboratory experimentally. They discovered that up to 10% of NGP doses reduced water absorption, which then increased. In comparison to control GPM mixtures, the bulk density of GPM was decreased by 12.66 and 5.79 percent, respectively, at 5 and 10 percent NGP additions, even as it enhanced by 1.96 and 5 percent, in both, at 15 and 20 percent NGP inclusions, comparison with the control samples. It resulted from the polymer gel becoming denser up to 10% of NGP dosages, increasing strength while lowering moisture absorption. More pores were filled in the newly constructed C–S–H (Hamzah et al., 2020). More porosity is obtained in the GPM mixtures when NGP dosages are more than 10%.

The majority of research has focused on how NA is microstructurally structured and how it affects the hardened characteristics of paste and concrete. Only very few studies related to other NMs, like NS, NC, and NT, on the durability of GC are available in the literature. In the case of NA-added GC, there is a gap in the literature on investigations related to durability properties. Therefore, there is a significant gap in the area of durability properties of NA, NCC and NM-added GC. Fig. 6 shows the Percentage of research contribution to different durability studies.

3.3.8.1. Shrinkage of geopolymers with nanomaterials. Ugheoko et al. (UGHEOKE et al., 2006) studied the shrinkage of the geopolymer with MCNT. The drying shrinkage measurements were done on geopolymer mortar samples produced with different MCNT ratios which were cured for 28 and 90 days. Shrinkage decreased with longer hydration times and with MCNT up to 0.1%. A substantial drying shrinkage implies that the mixture might absorb much water, showing fine mixture particles. This indicates the plasticity of the mixture to some extent. Higher shrinkage values, particularly in the control mix, show that most total drying and autogenous shrinkage occur in the early ages. This is due to the lower degree of polymerization and formation of zeolite structures with higher water content, which is highlighted by XRD data. These zeolite structures absorb a lot of water content and raise shrinkage values. However, doping with MCNT reduces shrinkage significantly, down to 0.1%, and MCNTs achieve this by increasing the nucleation sites and the amount of C–S–H gel that is formed. This results in high hardness, improved pore structures, control over nanoscale cracks, and a decrease in autogenous shrinkage of the geopolymer composites (Han et al., 2011; Parveen et al., 2013). The acceleration effect of nanotubes causes the formation of more compact geopolymer structures with low shrinkage values; however, an increase in the MCNT content causes agglomeration and bundling despite sonicated dispersion, which can contribute to an increase in the shrinkage data but still leave a significant difference between control mix and geopolymer mixes containing MCNTs (Chen et al., 2011). After 28 days, the drying shrinkage values for composites produced with 0.1, 0.2, and 0.4% MCTs decreased to around 92, 88, and 74%, respectively (Al-Shether et al., 2016).

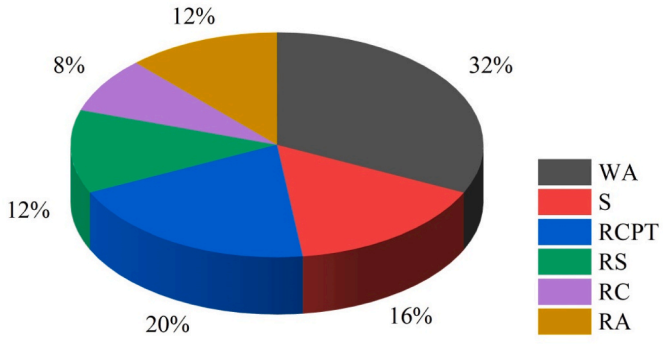

Fig. 6. Percentage of research contribution to different durability studies. [Note: WA-Water absorption; S-Sorptivity; RCPT- Rapid chloride penetration test; RS-Resistance to Sulfate; RC- Resistance to Chloride; RA-Resistance to Alkaline environments.].

There is a trend toward identical drying shrinkage of geopolymer paste specimens both before and after the inclusion of NT particles. It is clear that the reference specimen, particularly the specimen with 5% TiO_2 incorporation, has a larger shrinkage value than specimens containing NT particles. For 1% TiO_2 integrated specimens, the shrinkage-decreasing effect of TiO_2 addition can be seen clearly after 5 days. However, for 3% and 5% TiO_2 incorporated specimens, the effect can be noticed after 2 days. The drying shrinkage of cementitious materials may be caused by a bigger volume of mesopores, which increases the capillary stress caused by the water meniscus formed in the paste's capillary pores and generates a higher level of drying shrinkage (Triwulan et al., 2017).

As can be seen, the reference group and TiO_2 group shrank to around 1400 microstrain and 1650 microstrain, respectively, at 90 days after curing at a relative humidity of 90 ± 5%. The alkali-activated slag paste in both groups exhibited a considerable drying shrinkage from the beginning of curing until 90 days, when the relative humidity of curing was 55 ± 5%. At 90 days, the reference group and the TiO_2 group both experienced drying shrinkage that reached 6400 microstrains and 5080 microstrains, respectively. When TiO_2 was added to alkali-activated slag paste, it was found to reduce shrinkage under both curing conditions. When the curing relative humidity was chosen to be 90 ± 5% and 55 ± 5%, respectively, the reduction in shrinkage of the TiO_2 group at 90 days was measured to be 18% and 27%, in comparison to that of the reference group. When the curing relative humidity was 90 ± 5 percent, it was discovered that 83–84% of the shrinkage occurred within 7 days and 95–98% by 28 days.

The curves of both alkali-activated slag paste groups tend to level off after 28 days. Only 67–70% of the shrinkage occurred within 7 days and 89–93% during 28 days at a curing relative humidity of 55 ± 5%. No matter whether NT is used or not, it is clear that the drying process of alkali-activated slag paste at 55 ± 5% relative humidity lasts much longer than under 90 ± 5% relative humidity. These findings show that the addition of 0.5% NT increased the mechanical strength of alkali-activated slag paste and reduced shrinkage under 20 °C. According to literature data (Yang et al., 2015; Baghabra Al-Amoudi et al., 2009), the main variables influencing the shrinkage in Portland Cement and alkali-activated slag paste are the pore size distribution and features of hydration products.

4. Microstructure of geopolymer composites

As previously stated, microstructure enhancement is the fundamental mechanism for increasing the properties of geopolymer with various NMs. The incorporation of NMs in the polymerization process and nanofiller capacity significantly enhances the bonding interface and permeability of the material. Microscopic examination is commonly employed to study the evolution of microstructure in geopolymer. The density and porosity of the structure are directly proportional to the mechanical and durability performance of the composites, which are additionally impacted by the GC's morphology (Shilar et al., 2022; Fu et al., 2021).

Geopolymer materials with reduced porosity, increased density, and a condensed microstructure generally have greater strength qualities (Ahmed et al., 2022b; Li et al., 2022b). Researchers employed different equipment and procedures to examine distinct microstructural characteristics of GC such as Scanning Electron Microscope (SEM) (Akbari et al., 2022), Fourier Transform Infrared (FTIR) Spectroscopy (Kambham et al., 2019; Witkowski and Koniorczyk, 2018), X-ray Diffraction (XRD) (Arivumangai et al., 2020; Bahoria et al., 2018), Thermogravimetric Analyzer (TGA) (Aguirre-Guerrero and Mejía de Gutiérrez, 2018), Mercury Intrusion Porosimetry (MIP) (Han et al., 2022; Chen et al., 2021), X-ray fluorescence (XRF) (Wang et al., 2022b), Derivative Thermograms (DTG) (Charpentier et al., 2022), Transmission Electron Microscope (TEM) (Ghods et al., 2013), Field Emission Scan Electron Microscopy (FESEM) (Kambham et al., 2019), dispersive energy X-ray (EDX) (Quackatz et al., 2022; Wilson et al., 2017; Bazán et al., 2018) and Differential Scanning Calorimeter (DSC) (Li et al., 2017c). The voids and porosity percent inside the composites are intimately related to the base materials' physical, mechanical, and durability qualities. Generally, geopolymer specimens with lower porosity, higher density, and a dense microstructure have better strength (Kamseu et al., 2021; Nana et al., 2021; Nouping Fekoua et al., 2021). This section details the SEM, FTIR, XRD, TGA, and MIP experiments conducted for GC.

4.1. Scanning Electron Microscope (SEM) of geopolymer composite

SEM is an effective tool for examining organic and inorganic materials that range in size from nanometers to micrometers (μm) which produces exceptionally accurate pictures of a wide range of materials with a high magnification of up to 300,000x (Nohl et al., 2022; Liu et al., 2022b). In the case of NMs based GC, SEM was utilized to evaluate the impact of NMs on the microstructural improvement of the GC over time by obtaining high-resolution pictures.

4.1.1. Nano-silica (NS)

Gao et al. (2014) looked into how the curing period affected the morphology of a nano-silica mixed MK-based geopolymer with a 1.50 SiO_2/Na_2O ratio. They discovered that unreacted silica particles become activated over time, and the product's microstructure becomes compact and homogenous (Mustakim et al., 2020; Wang et al., 2019; Rodríguez et al., 2013; Khater, 2016a). Deb et al. (2015) looked at how the microstructure of a FA-based geopolymer changed when NS was added. NS particles worked as a filler material, compacting the hardened GPP and filling voids. Assaedi et al. (Behfarnia and Rostami, 2017) studied the microstructure of a FA geopolymer produced with the addition of NS in wet and dry mixing circumstances. Most of these FA particles were converted into geopolymer gel by adding 3.0% of NS. In comparison to wet mix conditions, the geopolymer matrix created in dry mix conditions had fewer microcracks. It was also discovered that in dry mixing conditions, as opposed to wet mixing conditions, NS performed better as a cavity filler. Khater (2016a) expanded his research to look at the microstructure of GGBFS-based geopolymer with NS added and discovered that the GGBFS geopolymer lacking NS has a very porous and heterogeneous morphological growth. Deb et al. (2015) made a similar observation that a higher degree of compact and a harder morphology was achieved by adding 2% NS to GGBFS-based FA geopolymer. Kang-Wei Lo et al. (2017) examined the impact of NS on a 5 percent MK-based geopolymer, identifying a molecule interaction site that is inert and causes gaps within the geopolymer composite.

GGBFS-based GPC with micro and NS were investigated micro structurally by Behfarnia and Rostami (2017). The formation of extra polymer gels caused the finding if NS was incorporated into the geopolymer mixture because of the pozzolanic activity of NS, which progressively occupies the Nano gaps. This gel adheres to particles, filling up gaps and linking them together. Similar to this, work was done by Ibrahim et al. (2018), which showed how incorporating NS affected the mechanical properties and morphology of GC. Chemical reactions between Si, Al, and alkali activators influenced the microstructure improvement of GC, the inclusion of NS will enhance the Si components and hasten the stimulation of the geopolymer in the GC mixture (Revathi et al., 2018; Behfarnia and Rostami, 2017).

4.1.2. Nano-alumina (NA)

Minimal publications have examined how incorporating NA influences the morphology of GC. Huang and Han (2011) looked into using highly crystalline α- Al_2O_3 as a resource of alumina used to make FA GC. According to the researchers, the aluminium component of Al_2O_3 participated in the Geopolymeric reaction, resulting in a more compact geopolymer microstructure. Thamer Alomayri (2019) has published some fascinating findings on the microstructure of a FA-based GPP containing NA. The geopolymer matrix without NA had non-reacted gaps and fly ash, but the geopolymer matrix with 2 percent of NA had greatly densified, indicating that the addition to serving as a gap filler, the NA assisted in the geopolymeric process. However, when the NA content is increased to 3 percent, the matrix created was found to be less dense, indicating that there is an excess of NA. He discovered that integrating up to 2% NA into the GPP specimens resulted in a significantly reduced porosity and a more homogenous and denser morphology than combinations without NA. When the percentage addition of NA exceeds 2%, the hardness of GPP declined, while porosity and micro cracking increased, as seen from the SEM micrographs.

4.1.3. Nano titanium dioxide (NT)

NT is likewise one among the NMs that is commonly employed in cement-based materials for a variety of purposes. The following are a few noteworthy research initiatives on the use of NT in geopolymer-based products. The microstructure of fluidized bed FA-based GPP was found to be densified with the addition of 5% NT, according to Duan et al. (2016). According to the authors, the nucleation and nanopore filling effects of NT influenced the rate of hydration. FA and MK-based geopolymer with NT have been found to have good mechanical bonding (SyamsidarNurfadilla, 2017). Similarly, Sastry et al. (2021) found that adding NT to FA-based GPC improved the microstructure by giving more reacted FA particles and a dense structure. The introduction of NT, it accelerates saturation and produces materials that are saturated through polymerization and nanoparticle stuffing, which was said to minimize the size and amount of unreacted FA particles (SyamsidarNurfadilla, 2017; Sahitya and Sastry, 2018).

4.1.4. Carbon nanotubes (CNT) and multi-walled Carbon Nano Tubes (MCNT)

MCNT is involved in bridging micro-cracks in GPP, indicating that MCNT and GPP have a good bonding (Gao et al., 2021a). Because of the consistent distribution of MCNT in the matrix, the GPM with 0.1 percent of MCNT was found to have a more compact and homogeneous matrix than those with 0 percent and 0.4 percent of MCNT. It has also been reported that agglomeration occurs at greater MCNT concentrations, such as 0.4%, resulting in a porous matrix. The inclusion of CNT in GPM improves polymerization and densifies the microstructure of the matrix (Jalali Mosallam et al., 2022; Siahkouhi et al., 2021; Gao et al., 2021b; Eisa et al., 2022).

According to FESEM micrographs reported by Abbasi et al. (2016), MCNT also serves as a networking process for the micro-cracks of MK-based GPP. As a result, it offers a strong link between both the GPP and the MCNTs' interface, enhancing the GPP's strength. After seven days of the curing period, they found a lot of unreacted particles inside the GPP specimens. They also stated that there were numerous gaps and voids within the GPP specimens, which they said were caused by water evaporation and trapped air within the GPP.

4.1.5. Nano clay (NC)

Assaedi et al. looked at how NC affected the thermal and hardened concrete characteristics of an FA based gropolmer (Assaedi et al.,

2016a). The amount of NC in the binder material ranged from 0 to 3%. According to SEM analysis, they discovered that the geopolymer structure comprises a significant amount of non-reacted and slightly processed FA components. With the addition of 1%, 2%, and 3% of NC, as density rises, it seems that the proportion of insoluble responsive molecules is reduced (Niu et al., 2021).

4.1.6. Nano Calcium Carbonate (NCC)

The micrographs reveal the interactions between Poly Vinyl Alcohol (PVA) fibers and the geopolymer matrix, which could aid in understanding the fracture mechanisms of PVA-GC reinforced with NCC. Heterogeneous structures may explain the poor mechanical properties of the sample with insufficient PVA fiber dispersion, micropores, and gaps enclosing the geopolymer substrate, as shown by the geopolymer micrographs. PVA fibers in the 2.0 percent NMs GC are evenly distributed throughout the matrix and quite well, resulting in a dense, uniform structure (Abdalla et al., 2022a; Assaedi, 2021).

4.1.7. Nano metakaolin (NMK)

Due to the presence of a higher number of unreacted and partially-reacted FA particles, SEM observations of the crushed surface of control GPM with 0 percent and 4 percent NMK results show that the microstructure of control GPM is less dense than GPM containing 4 percent NMK. It was discovered that after alkali activation of FA particles, the sodium (Na) component and the Si and Al components of FA had a larger content. The Si/Al ratios for the control GPM and the GPM with 4% NMK were 3.02 and 2.57, respectively (Kaur et al., 2018; Guzmán-Aponte et al., 2017).

4.1.8. Nano-zinc oxide (NZ)

The breakdown edges of the MK-geopolymer blend with and without 0.5 percent NZ were examined using a SEM (Zidi et al., 2020). SEM images showed that fresh geopolymer composite had a porous surface with non-reacted particulate that was evident. The geopolymer mixture uniformity, density, and compact were all improved by the incorporation of NZ. This could be because the geopolymer matrix and NZ filler have higher interfacial adhesion. This improvement could be attributed to the spaces being filled (Reshma et al., 2021).

4.1.9. Nano glass powder (NGP)

Huseien et al. (2020) and Samadi et al. (2020) employed energy dispersive SEM to examine the samples and their morphology (FESEM). It stated the addition of 5 and 10% NGP to a blended FA/GGBFS-based GPM improved the microstructure. As a result, fewer nano-gaps and residual particulates. As the NGP dosages were increased from 15 to 20 percent, the density of GPM dropped, and more non-reacted particulates were present. With NGP content of 5% and 10%, the samples performed remarkably well, with minimal porosity and unreacted particles. The FESEM pictures demonstrated the partial reactivity of FA particles, whereas a significant number of unreacted FA spheres remained in the alkali-activated Mortar matrix. An imperfect crystalline structure measuring 150–300 nm in diameter was discovered along with the amorphous reaction products. Around the FA particles, thread-like particles were also seen, some of which were almost completely encased in a thick layer of amorphous gel. Such crystals had previously been observed by Jang and colleagues (Jang and Lee, 2016). The alkali-activated mortar was found to be made up of a mixture of unreacted FA particles, a few crystals, and a reacted gel phase, according to FESEM imaging. Meanwhile, increasing the NGP level to 15% and 20% resulted in a higher number of unreacted particles with a poor density structure.

Fig. 7 shows the SEM images of GC with different Nanomaterials. These SEM images indicated that the incorporation of NMs densifies the GC system, improving the mechanical and durability properties of GC products.

Because the study on the effect of NFA and GO addition in geopolymer SEM micrographs are scarce. There is a scope for research on the effects of NFA and GO addition on the microstructural characteristics of SEM micrographs of GC.

4.2. FTIR of GC

The researchers revealed the best geopolymer mixtures' link data using the FTIR spectroscopic technique, which was also utilized to

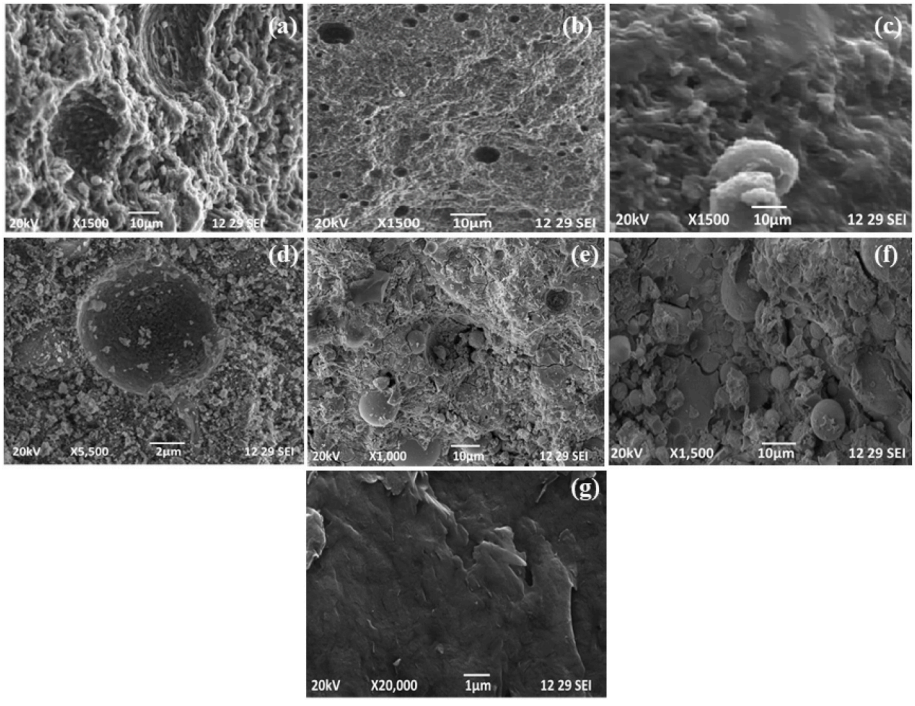

Fig. 7. SEM image of GC with NMs; (a) NC (Basiri et al., 2022); (b) NS (Huang et al., 2022); (c) NCC (Sastry et al., 2021); (d) MCNT (Maho et al., 2021); (e) NA (Zhang et al., 2020c); (f) NMK (Yip et al., 2005); (g) NT (Pardal et al., 2009).

identify reaction products and levels of polymerization in various geopolymer nanocomposite mixtures.

4.2.1. Nano silica

The researchers discovered that FTIR spectra of the geopolymer revealed a discrete intensity range around 1300 and 900 cm^{-1} linked with the Si–O-T asymmetric oscillation when NS MK-based geopolymer with different SiO_2/Na_2O ratios had been included (Mustakim et al., 2020; Revathi et al., 2018; Khater, 2016a). This bond is more responsible for determining the degree of polymerization than the Si–O–Si bonding peak (Gao et al., 2014). To ascertain the effects of incorporating NS on the mechanical hardness and morphology of natural pozzolan GPC, Ibrahim et al. (2018) conducted extensive research. They employed the ground-up GPP from the center of 25 square samples for their FTIR analysis. Their research showed that pure natural material and GPP without NS had nearly identical patterns in their FTIR absorbance spectrum. However, the problem diverged for GPP having NS, which was highlighted by alterations in the compound. For GPP with and without NS, an extending oscillation of the O–H connection in the interval of 3640 cm^{-1} to 2370 cm^{-1} and a bending vibration of HOH in the range of 1530 cm^{-1} to 1640 cm^{-1} were also found. The GPP's highest peaks, with corresponding NS contents of 1.0, 2.5, 5.0, and 7.5 percent. The apex in this location gradually migrated to the right as the NS content climbed from 0 to 7.5 percent. Sun et al. examined how NS influenced the efflorescence of MK GPM (Sun et al., 2020). The occurrence of poor H_2O links moisture consumed on the interface or retained in the structure was confirmed by the significant distinctive peaks around 3450 cm^{-1} and 1650 cm^{-1}, which were shown to connect to the stretching and curving of the O–H linkages. It was possible to gauge the level of polymerization using the Si–O-T bending peak with in geopolymer, which showed greater significant than the Si–O–Si bending twisting (Emad et al., 2018).

4.2.2. Nano alumina

FTIR research revealed that the integration of 5% NA had the highest polymerization phase among the different mixes, according to Huang and Han (2011). According to the authors, the major spectral band developed was at around 1000 cm^{-1}, which is attributable to Si–O-T; the peak amplitude of this range was reported for 5 percent NA's uneven lengthening oscillation.

4.2.3. Nano titanium dioxide

MK geopolymer with NT was compared with the reference specimen, and they concluded that the addition of NT had no significant effect on the FTIR spectra. Because of the MK process towards gelation, the peak at 463 cm^{-1} links to a decreased Si–O–Si intensity ratio. The band at about 703 cm^{-1} indicates Ti–O–Ti photosensitive species occur, which induces interaction with amorphous Al–O groups a reduction in intensity due to gel formation (Guzmán-Aponte et al., 2017). Because substantial literature on NT-added geopolymer is lacking, it may be deduced from the above-mentioned studies that the integration of NT alters the microstructure of alkali-activated materials. Furthermore, the filler effect, as well as the improvement of the polymerization reaction, the pore structure is modified, and the porosity is decreased when NT is added (Duan et al., 2016).

4.2.4. Carbon nanotubes (CNT)

Khater and Gawaad used 0.1, 0.2, 0.3, and 0.4% MCNT to perform FTIR on alkali-activated GPM. FTIR spectra of alkali-activated GPM cured at various ages without MCNT. The researchers noted a significant improvement in asymmetric stretching oscillation (T-O-Si) at around 975 cm^{-1} up to 3 months, which had been associated with a decline in asymmetric stretching oscillation (Si–O–Si) associated with non-solubilized particulates around 1100 cm^{-1}, indicating the increased dissolution of unreacted materials and increased amorphous character of geopolymer constituents. The decrease in symmetric stretching vibration of (Si–O–Si) attributed to a-quartz at around 797 cm^{-1} with increased hydration time was consistent with this. The inclusion of MCNT up to 0.1 percent boosted the nucleating efficiency and increased the dissolving of unreacted GGBFS components. The CO_3^{2-} vibration band was found to be reduced by up to 0.1 percent when MCNT was added, while the vibration band was increased by adding more MCNT. This was attributable to the fact that greater MCNT nucleation promoted the creation of a geopolymer structure and reduced the availability of free Na^+ species that would be carbonated (Khater and Abd El Gawaad, 2016). More study on CNT-included geopolymer is needed to determine CNT's impact on different AS-based geopolymer items.

4.2.5. Nano clay

Assaedi et al. studied the morphology of the GPP after adding 1%, 2%, and 3% NC. The FTIR analysis of every paste revealed the Si–O–Si uneven elongating oscillations at 1000 cm^{-1} in all specimens. The hydroxyl group exhibits a significant peak at about 3340 cm^{-1}, which indicates both physical and chemical-bound moisture via chemical bonds. In comparison to the control sample, the addition of NC boosted the amorphous phase and the polymerization process (Assaedi et al., 2016b). The authors obtained nearly identical outcomes in another study with the same percentage of NC for 4 and 32 weeks. Furthermore, the 32-week data show the two 1420 and 1480 cm^{-1} peaks shifting, demonstrating the presence of sodium carbonate. Throughout aging, the process proceeded slowly, utilizing additional Carbonyl groups and resulting in a tougher compound. Because of such, the moisture concentration decreased over this period to an optimal point, producing a shorter, wider peak at 3400 cm^{-1} (Assaedi et al., 2016a). The researchers noted that there is sufficient opportunity to examine the impact of NC utilization on the morphology of various kinds of geopolymer materials like GPP, GPM, and GPC by employing different AS providers at atmospheric and elevated temperature curing.

4.2.6. Nano calcium carbonate

Hasan Assaedi studied the compressive strength and flexural strength of GC-containing NCC particles at concentrations of 1, 2, and 3% (Assaedi, 2021). Broad intake spectra with maximum intensity that form between 3360 and 3380 cm^{-1} are the result of the lengthening of the hydroxyl groups in conjunction with the geopolymer system. O–H stretching is also linked to the next bands, which are positioned at the 1632–1645 cm^{-1} gap. At roughly 1393–1403 cm^{-1}, the carbonate groups are created when non-fixed Na particles react with atmospheric CO_2. Finally, the bands between the compounds are associated with the oscillation of Si–O–Al bonds, which correspond Na-polycialate geopolymer composite, which is essential for dependable cohesiveness among different composite elements (Assaedi et al., 2020; Supit and Shaikh, 2014). This evidence supports the effectiveness of the polymerization reaction.

4.2.7. Nano-zinc oxide

The interactions between the geopolymer and the filler were investigated using infrared analysis. The existence of sodium carbonate and the uneven strength of the T-O-Si band, as well as a bonding oscillation group attributable to the Si–O–Si group and two moisture particles, are responsible for the primary groups of a geopolymer that could be detected in the spectral of the reference specimen (Zidi et al., 2020). Due to the low concentration of NZ, the FTIR spectra show no significant difference between the NZ fillers (0.3 percent, 0.5 percent, and 0.7 percent integrated). The T-O-Si group's strength has also grown, indicating that the geopolymer and the synthetic Nanoparticles are in touch with one another. The spectrum reveals that no new functional groups developed after the insertion of NZ, implying that the NMs and the geopolymer matrix solely interacted physically (Khater, 2016a).

4.2.8. Nano Water Glass

The impact of NGP on the engineering qualities of GPM has been

investigated. Huseien et al. claimed that the FTIR recognized the action regions of Si–O and Al–O in GPM composites utilizing synthetic investigation to identify functional classes based on interaction oscillations. The frequency of the Si–O–Al group decreased, which pointed to an enhancement in the polymer gel product. When compared to specimens containing 0% NGP, When GPM included 5 and 10% NGP, this led to a more homogeneous morphology and more silicate alteration. An increase in the NGP concentration from 15% to 20% led to lower compressive strength and higher band frequency measurements. By raising the NGP level from 0% to 5%, Si–O–Si bending modes at 775.2 4 cm^{-1} were displaced to 754.2 4 cm^{-1}. With increased NGP concentration, the Si–O–Si bond frequency decreased, indicating an improvement in the production of polymer gel items. The vibration frequency dropped as the molecular molar mass of the connected atoms increased. The oscillation frequency dropped as a response to GGBFS freeing liquid Ca and shifting Si ions from Si–O links. The Si–O–Si oscillation frequency and SiO_2/Al_2O_3 ratio were increased when NGP was added (Zhang and Yue, 2018; Samadi et al., 2020; Huseien et al., 2020).

Fig. 8 shows the FTIR spectra of NMs added to different GC mixes. Since there hasn't been much research on the effects of NFA, NMK, and GO on the infrared spectra of GC, Investigation into the influence of NFA, NMK, and GO inclusion on the morphology characteristics of GC's infrared spectra has limited studies.

4.3. XRD of geopolymer composite

Investigators conducted XRD study to evaluate the chemical properties of different primary source cementitious compounds utilized for the manufacturing of GC, as well as the elemental compositions of geopolymer specimens following the polymerization process.

4.3.1. Nano silica

According to Phoongernkham et al. (Phoo-ngernkham et al., 2014), the density of quartz in NS-added FA-based GC was increased. Peaks at 29.5° and 32.05° 2-theta in XRD plots are indications that NS was used to synthesize polymer gel and geopolymer items. Adak et al. (2014) investigated the XRD patterns of FA-based GPM containing 6% NS. In the presence of NS, a few more peaks were identified, indicating the production of novel phases of $Na(AlSi_3O_8)$, SiO_2, $Na_2Si_2O_8$, $CaCO_3$, and Ca_3SiO_5. They discovered new crystalline chemicals in the geopolymer matrix, which were found in the 26–32° 2theta area in XRD. Another XRD study (Gao et al., 2015) was carried out on an alkali-activated GGBFS composite with NS added. GGBFS was replaced with NS in percentages ranging from 0% to 3% by mass. Through XRD examination, which revealed an improvement in peak intensity around 28.3° and 34.40° 2-theta, a greater proportion of hydrated calcium alumino-silicate and hydrated calcium silicate solutions were discovered. The hardened properties of FA GPC treated by adding 6% NS were examined by Adak et al. (2017). The concentration of quartz, hematite, and mullite has been stated to be greater in the nano-GPC samples than in the standard specimens because of the extra suppliers of SiO_2 that the NS added to the combination. In addition, they discovered that in nano-GPC specimens, novel phases of kaolinite, alite, albite, mullite, quartz, and amorphous products were formed, as opposed to the control GPC mixture.

Behfarnia and Rostami (2017) investigated the impact of micro silica and NS in the same environment upon overall penetration of GGBFS GPC. In control concrete specimens, three primary stages were generated, namely C-A-S-H gel, calcite ($CaCO_3$), and magnesium-aluminum-carbonate-hydroxide-hydrate ($Mg_6Al_2CO_3(OH)_{16}–4H_2O$), while adding NS resulted in the creation of additional phases, including calcium silicate carbonate (Tilleyite). A similar XRD investigation on the impact of NS incorporation on naturally occurring pozzolan- GPC was carried out by Ibrahim et al. (2018). The presence of NS in the mixture would have been critical in the formation of C–S–H gels with Al and Na in the binder structure, resulting in N-A-S-H gel and

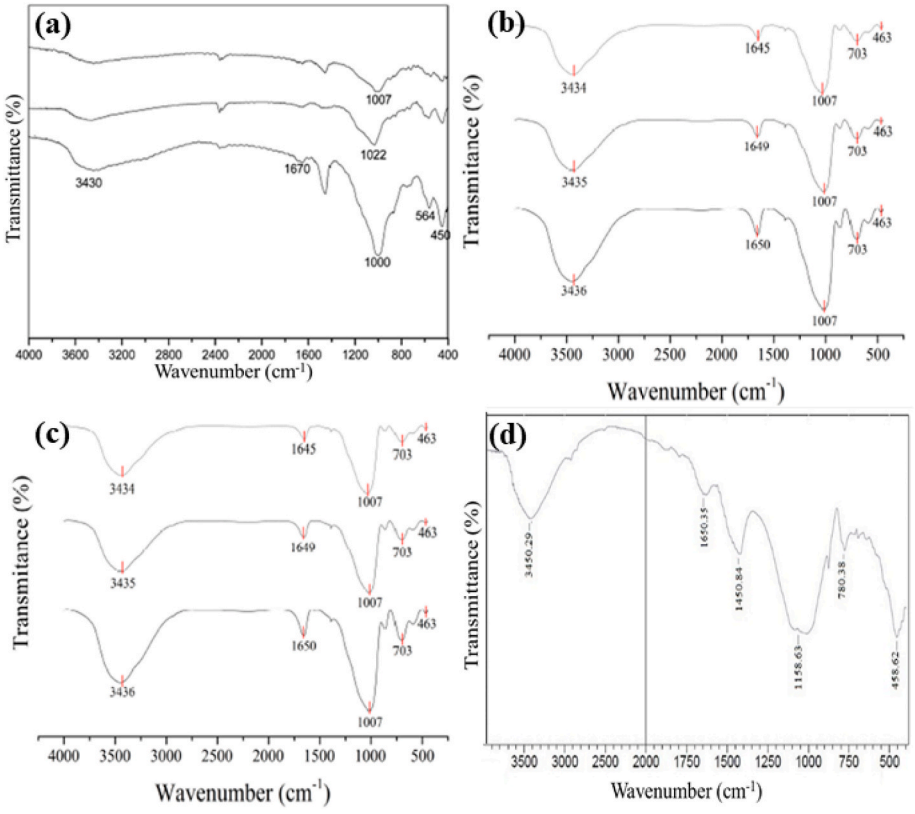

Fig. 8. FTIR spectra of GC with different NMs; (a) NA (Nazari and Sanjayan, 2015); (b) NC (Wei and Meyer, 2014); (c) NS (Adak et al., 2017); (d) NCC (Sastry et al., 2021).

C-A-S-H gel (Rodríguez et al., 2013).

4.3.2. Nano alumina

Phoo-ngernkham et al. (Phoo-ngernkham et al., 2014) discovered an XRD spectrum for NA admixed GPP that was comparable to those obtained in NS-added GPP. The creation of N-A-S-H gel is shown by the wider hump of geopolymer gel in the case of NA-added GPP. Thamer Alomayri (2019), on the other hand, recently published an experimental study examining the influence of different percentages of NA in FA-based GPP. Based on the XRD investigation, the author discovered that FA and geopolymer matrix with and without NA had a comparable XRD pattern. The production of an AS gel in geopolymer complexes was related to the presence of quartz and mullite particles in FA, which have an irregular crest among two levels of 16° and 27°. Furthermore, it has been stated that the XRD profiles of GPPs including NA and FA are equivalent, showing that these stages were not active throughout the polymerization reaction. Yet those filler components are included in the resulting GPP. As a result, it can be inferred that NA does not have a substantial impact on the polymerization reaction, but it will function as a nanocomposite that enhances the morphology by occupying the pores. As a result of its influence on pore filling capacity and geopolymerization reaction, it can be concluded that adding NA in modest amounts can improve the microstructure of the geopolymer matrix.

4.3.3. Nano titanium dioxide

The effect of adding NT to a fluidized bed FA-based GPP was examined by Duan et al. (2016). More hydrated structures are formed with the addition of NT, and Compared to standard geopolymer samples, it can be noticed that in the case of NT-incorporated GPP, a more crystalline component of albite was detected, with peaks exhibiting greater intensity showing more crystalline phase. Sastry et al. (2021) discovered that when different concentrations of NT were introduced to the GPC mix, which led to the development of a new mineral Anatase stage. They also discovered that adding NT to control FA-based GPC specimens changed the diffraction pattern from 20°-30° to 20°–38° (2θ). A more thorough investigation of the morphology of geopolymer complexes with different kinds of AS raw substances and the incorporation of NT is required to ascertain the impact of NT on polymerization.

4.3.4. Carbon nanotubes

When looking through the available literature from many conceivable sources, there is a significant gap in research showing an XRD investigation in analyzing the effect of adding CNT -based GC. In an investigation on alkali-activated GPM doped with MCNT, Khater et al. (Khater and El-Nagar, 2020) found that the system had a reasonable degree of distribution to the addition of 0.1 percent MCNT after 90 days. The inclusion of MCNT increased the efficiency of absorption, although no discernible alterations in the stages were seen. Khater and Abdel Gawaad (Khater and Abd El Gawaad, 2016) report that the synthesized MCNT, on the other hand, provides a variety of interaction locations for the crystallization of GPM's hydration results. The C–S–H stages were discovered to react with calcium ions in the porous liquid, causing them to attach to the carboxyl regions of the MCNT, which results in the network elongation of the C–S–H stages that develop can be influenced by the concentration of carboxyl groups on MCNT interfaces. The MCNTs in this mechanism, the authors proposed, serve as model structures during the hydration process.

4.3.5. Nano clay

Assaedi et al. (2016b) carried out an extensive examination of the use of NC platelets with FA GPP. In addition, Assaedi et al. (2016a) looked into the effects of adding NC to flax fabric-reinforced GPP. The NC platelets were introduced in varying quantities by weight, ranging from 1% to 3%. Two primary phases were identified based on their XRD analysis results: quartz and mullite. The crystalline phases of these new compounds were discovered to act as fillers in the mixture rather than engaging in polymerization activities. The emergence of an amorphous AS phase between $2\theta = 14°$ and 27° was indicated by the XRD pattern of NC-added GPP, which could be attributable to the activity of the polymerization reaction. The amorphous stage has an impact on the hardened performance of the geopolymer mix. The strength of the geopolymer increased as the amorphous phase increased (Elimbi et al., 2011). The structural qualities of the geopolymer nano-composites were enhanced by raising the matrix's physical qualities and the reinforcing flax fibers' adhesion to the substrate (Assaedi et al., 2016b). According to the authors, there isn't enough literature on incorporating NC in geopolymer. This area's field of study must be broadened to fully understand how NC incorporation affects the polymerization process.

4.3.6. Nano calcium carbonate

The morphology and hardened performance of FA GPP with varied NCC additions were studied by Assaedi et al. (2020). As per the standard X-ray sequence of FA-based geopolymer, including those are incorporating 1, 2, and 3 percent NCC, the broad hump shown on raw FA diffractograms among $2\theta = 15°$ and 35° changed to 18° and 40°, clearly showing the development of an amorphous geopolymer composite liable for structural strength improvement. Furthermore, certain mineral phases found in FA powder, such as magnetite, mullite, hematite, and quartz, were found on FA-based geopolymer with and without NCC; by strengthening the geopolymer substrate, these inorganic components may serve as micro-aggregates because they did not cause polymerization process (Kaze et al., 2018). Also, between 18 and 40 (2 h), the intensity of the hump increased, which might be associated with the probability of NCC particle decomposition, leading to the synthesis of C–S–H towards the major binding agent, including N-A-S-H, via the geopolymer system being increased (Assaedi et al., 2020).

4.3.7. Nano-zinc oxide

The XRD patterns of alkali-activated geopolymer with varying quantities of NZ added exhibited microstructure outcomes. In all of the samples, the spectra reveal prominent peaks at 28°, showing the development of an amorphous state (Zidi et al., 2020). Due to the agglomeration of NMs, the intense peak is shifted to the opposite side by an additional 0.7 percent NZ, which stymies the geopolymer synthesis. The XRD spectra revealed that the addition of 0.5 percent NZ improved the structural characteristics of MK-based geopolymer to the greatest degree. The influence of NZ on geopolymer characteristics was investigated by Rustan et al. (Rustan and Irhamsyah, 2017). When more than 2.5 percent of NZ was introduced, they discovered NZ peaks in the XRD spectra. These peaks were observed could be due to the low concentration of NZ utilized.

4.3.8. Nano Water Glass

Huseien et al. (2020), Samadi et al. (2020), and Hamzah et al. (2020) investigated the effects of NGP incorporation on the technical aspects of alkali-activated mortars. Following XRD patterns, as albite and gismondine concentrations were at their highest level, then the NGP operated in the alkali-activated mortars around 23.9° and 34.1°. The quartz (SiO_2) peak (36°) amplitude was reduced when NGP was added to the planned mortar. As a result, the higher quantities of gismondine and albite, as well as the lower levels of SiO_2, indicate the production of denser gels.

There is currently a scarcity of information on the effects of NFA, NMK, and GO on the XRD pattern of microstructural properties of GC in the literature. As a result, there is a large gap in the study on the impact of NFA, NMK and GO on the XRD pattern of microstructural properties of GC.

4.4. TGA of geopolymer composite

Researchers employed TGA to measure the thermal stability of GC. TGA is an effective method of assessing materials which are resistant to

temperature, especially geopolymers. This method is used to figure out how much a specimen's weight changes when its temperature rises. TGA can be used to figure out how much moisture and volatiles are in a specimen (Aguirre-Guerrero and Mejía de Gutiérrez, 2018; Patel et al., 2021).

4.4.1. Nano silica

Revathi et al. (2018) performed a practical investigation to show how the morphology and thermo-mechanical characteristics of blended FA and GGBFS-based GPM are influenced by the incorporation of NS. Loosely attached silanol groups cause weight loss at a temperature range below 250 °C, while linked silanol compound dissolution causes weight loss to last up to 450 °C (Adak et al., 2014; Khater, 2016b). Gao et al. (2013) also examined the impact of NS inclusion on the properties of alkali-activated MK-based GPP. TGA or DTA was conducted to study the loss of weight in the GPP specimen. The temperature variations from 50 to 350 °C were caused by free moisture drainage inside the capillaries. Evaporation of structural or mixed water resulted in a weight reduction from 350 °C to 550 °C in the same period. Further investigation into the impact of NS inclusion upon weight reduction showed that, at temperatures between 50 and 350 °C, weight reduction enhanced with raising the NS content. This might be connected to the NS's capability to uptake water molecules. Weight loss of the specimen was comparatively faster in rate around 50–350 °C with an optimum NS concentration of 1%.

4.4.2. Carbon nano tube

The hardened and morphological characteristics of MK GPP containing 0%, 0.50%, and 1.00% MCNT were investigated by Abbasi et al. (2016). Simultaneously with endothermic dehydroxylation in the DTA curve, weight loss begins in the TG graph between 535 and 650 °C.

4.4.3. Nano Clay

Assaedi et al., 2016a, 2016b looked into the impacts of adding NC to flax fabric-reinforced GPP microstructural, thermal, and mechanical properties. The weight loss of the GPP was reduced from 12.4 to 12.1, 11.5–11.8%, respectively, at the 1.0, 2.0, and 3.0 percent dosages of NC, indicating that, at a 2.0 percent dosage of NC, the geopolymer matrix's thermal stability significantly enhanced. This could be owing to NC's ability to fill holes, resulting in denser matrices. Furthermore, the thermograms of the pure geopolymer and nanocomposite samples demonstrate a weight loss from 25 to 225 °C due to the evaporation of absorbed water (Ravitheja and Kiran Kumar, 2019; Gadkar and Subramaniam, 2021; Zivica et al., 2014). At the same time, between 225 and 525 °C, the evaporation of physical free water caused most of the specimens to reduce their weight gradually. De-hydroxylation of the Si–OH bond produces a Si–O group and dissipated moisture content, which leads to gradual weight reduction (Li et al., 2012). Furthermore, between 500 and 700 °C, weight loss was moderate, which was attributed to the residual coal of FA (Ul Haq et al., 2014). A modest hump in DTG curves over 600 °C shows a marginal effect in weight reduction. As seen in the DTG plot, in which the nanocomposite peak relocated to elevated temperatures than the ordinary geopolymer line, the neat geopolymer slope displayed a significant decline as matched to the nanocomposite graphs in this region.

4.4.4. Nano calcium carbonate

Assaedi et al. (Assaedi, 2021) studied the engineering features of FA GPP using various dosages of NCC inclusion. In the TGA assessment, investigators stated that there is a significant loss in GPP after incorporating NCC. The weight losses were found to be 1, 2, 4, and 5% for GPP containing 0, 1, 2, and 3% NCC, respectively. Water loss that was directly connected to the geopolymer system was the cause of the weight loss in all geopolymer specimens. When NCC is incorporated into geopolymer production, the polymer gel is formed with the principal binder. Therefore, the considerable weight loss shown in TG curves could be a reflection of water released from these binders.

4.4.5. Nano-zinc oxide

The influence of NZ on the thermal properties of geopolymer was studied by Zidi et al. (2020). They conducted TG testing at temperatures between 25 and 450 °C to accurately control the starting of sample deterioration and gather exact thermal information. The authors divided the spectra into three main groups. The standard specimens lost approximately 2 percent of their starting mass between 25 and 70 °C. In contrast, the other sample remained invariant, suggesting that adding NZ to a geopolymer allows for water storage. The second range, from 70 to 200 °C, underwent considerable alterations, with the simple geopolymer line showing a moderate weight reduction and the NZ geopolymer curve showing a rapid reduction in its weight. Such alterations could be explained by NZ's uptake of free moisture content, whereas weight reduction in the third range between 200 and 450 °C maintained stable.

4.4.6. Nano Water Glass

Huseien et al. (2020), Samadi et al. (2020), and Hamzah et al. (2020) investigated the effects of NGP incorporation on the technical aspects of alkali-activated mortars. They used TGA testing to determine how much weight the GPM specimens lost with and without NGP. It was discovered that GPM specimens created with 5% NGP lost less weight of around 10.47% but samples tested with 15% NGP showed a 12.12% weight reduction. This was attributable to the excellent stability of mortars containing 5% NGP and a high polymer gel concentration, and a low Ca $(OH)_2$ percentage.

A few researchers looked at the TGA of NA, NT, NFA, NMK, and GO, including GC. However, there is currently limited information on the effects of these NMs on the TGA of GC in the literature. As a result, there is a large gap in the study on the impact of CNT, MWCNT, NCC, NFA, NMK, NZ, GO, and NGP.

4.5. MIP of geopolymer composite

Researchers applied MIP to examine the porous microstructure of GC. An effective approach to measuring pore size distribution, pore volume, and porosity in a variety of granular and powder substances are MIP. A porosimeter is a device that injects mercury into the pores of porous material using a pressurized chamber. Mercury enters the larger pores first when pressure is applied. As the pressure increases, the filling continues to smaller and smaller pores. The IUPAC pore radius categorization system divides pores into four types: micropores (1 nm), mesopores (1–25 nm), macropores (25–5000 nm), and air spaces or fractures (5000–50000 nm) (Li et al., 2017c; Tibbetts et al., 2020; Sidiq et al., 2020; Zeng et al., 2020).

4.5.1. Nano silica

The effects of NS additions on MK-based GPM efflorescence were examined by Sun et al. (2020). The big gaps appeared to close if NS was added to GPM samples, and additional pores with a smaller radius developed instead. This discovery showed that adding NS to a geopolymer framework resulted in a denser form. As the NS dose was raised, the most likely pore radius gradually reduced. The addition of 5% NS, further it was stated by Zidi et al. (2021) has two unique impacts on that MK-based GPP's pore size dispersion. When NS was added to the GPP, the number of microscopic pores appeared to decrease, and when 5 percent NS was added, the pore size increased. On the other hand, the ultimate porosity readings determined by the MIP revealed a substantial reduction in porosity readings of GPP, including 5% NS (22.8%) if compared with the comparable GPP samples (32.6%) with no NS concentrations.

4.5.2. Nano Titanium dioxide

The inclusion of NT is said to refine the pores of the geopolymer. The total porosity of the NT group was lower than that of the control group, which did not have any NT. It was also discovered that the inclusion of

additional NT resulted in the shrinking of the accumulative pore volume. NMs tend to function effectively as filler particles due to their compact nature. The much more expected pore dimension related to the greatest threshold number was 93 nm, 42 nm, 41 nm, and 36 nm, respectively, if 0%, 1%, 3%, and 5% NT were supplied to GPP mixes (Duan et al., 2016). The observation addressed that the NMs conglomerations' nuclei became greater and eventually occupied the pore volume surrounding them as the hydration mechanism advanced. When these "nuclei" are present, the hydration rate is greatly accelerated; hydrates quickly build up, expand toward the moisture environment and occupy any empty spaces to minimize the GPP's porosity (Chen et al., 2012). As per Yang et al. (2015), examined the impacts of NT incorporation on the morphological, early, and long-term hardened performance of alkali-activated GGBFS GPP. MIP investigation explained that NT minimizes overall porosity and alters the porous structure of alkali-activated GGBFS GPP. Added NT is also responsible for the paste's excessive shrinkage was substantially decreased.

4.5.3. Nano carbon nano tube

Luz et al. (da Luz et al., 2019) investigated the mechanical, rheological, and microstructural properties of MK-based GPP with pristine and functionalized CNT. When 0.1 percent CNT was introduced to the GPP, the enhanced hardened qualities might be attributed to a 19% decline in the number of macropores relative to the standard GPP. On the other hand, the drop in compressive strength and flexural strength with 0.2 percent CNT addition could be accounted for by a rise in overall porosity brought on by perhaps a rise in CNT group production.

4.5.4. Nano Alumina

The MIP data revealed the anticipated grain dimension dispersion graph of the geopolymer specimens with and without 2 percent NA (Zidi et al., 2019). This finding demonstrated that adding NMs to geopolymer alters the porosities and pore distribution of the geopolymer in distinct ways. NA, in reality, smaller holes were fewer, while larger holes were more numerous. Furthermore, with the addition of 2% NA, the percentage of geopolymer porosity reduces from 32.58 to 9.88. This could be owing to the NMs filling the pores (Rees et al., 2008).

4.5.5. Nano-zinc oxide

MIP analysis revealed the grain dimension dispersion graphs of the geopolymer specimens with and without 0.5 percent NZ (Zidi et al., 2020). This result indicates that the incorporation of NMs with geopolymer has various impacts on its porosity and pore dispersion. NZ preserved the larger holes but increased the size of the smaller holes. This can be explained by the NMs ability to absorb water (Nuaklong et al., 2018). With the addition of 0.5 percent additionally NZ, the percentage of geopolymer porosity is reduced from 32.58 to 31.35. This could be due to the quality of NMs filling the pores.

There are a few researchers who examined the MIP of NC, NCC, NFA, NMK, and GO, including GC. However, there is currently limited information on the effects of these NMs on the MIP of GC in the literature. As a result, there is a large gap in the study on the impact of NC, NCC, NFA, NMK, NGP, and GO. Table 2 consolidates the effect of NMs on different GC.

Table 2
Influence of different NMs on different GC.0.

Source material	NMs & Percentage	Composite type	Effects	Ref.
FA (Class C) and RA	NS (0.14, 0.18, and 0.25)	GPP	• Initial setting time – reduced by 67% • Final setting time – reduced by 60%	Chindaprasirt et al. (2012)
	NS (0.14, 0.18, 0.25, 0.5, and 0.8)	GPP	• Initial setting time – reduced by 83% • Final setting time – reduced by 80%	
	NA (0.2, 0.3, 0.33, 0.5, and 0.7)	GPP	• Initial setting time – reduced by 85% • Final setting time – reduced by 82%	
FA (Class F) + RA	NS (1, 2, and 3)	GPP	3% NS: • Compressive strength – increased by 42%	Riahi and Nazari (2012)
	NA (1 and 2)	GPP	• No influence on compressive strength (due to its crystalline nature)	
FA (Class F)	CNT (0.1, 0.5, and 1)	GPP	0.5% CNT: • Mechanical strength - increase	Saafi et al. (2013)
MK	NS (0, 1, 2, and 3) and SiO_2/Na_2O ratio = (1–2)	GPP	1% NS: • Initial setting time - reduced by 31% • Final setting time - reduced by 82% • Compressive strength – increased by 57% • Flexural strength - increased by 41% • Smallest cumulative pore volume – reduced by 18% • Highest mesopores volume – increase by 82% S/L ratio 1.03: • Compressive strength – maximum S/L ratio 1.5: • Microstructure – became denser	(Gao et al., 2013, 2014)
GGBFS	NC (0.5, 1, 1.5, 3, 5, and 7)	GPP	1% NS: • Compressive strength – increased by 15%	Hisham M Khater et al. (2013)
FA (Class C)	NS (4, 6, 8, and 10)	GPM	6% NS • compressive strength – increase	Adak et al. (2014)

(continued on next page)

5. Health and cost-effectiveness of nanomaterials

NMs are frequently utilized in the construction sector due to their capacity to enhance the properties of binders. Due to their nanoscale nature, these substances could seriously endanger public health (Ahmad et al., 2022). Nanomaterials can negatively impact cellular metabolism in the internal organs by impacting tissue surface, cell proliferation, and tissue wall because they can readily penetrate the cellular surface in the absence of endocytosis (Sumesh et al., 2017). According to certain studies thus far, asthma risk has increased on the effects of NMs on the bronchial and cardiovascular organs (Li et al., 2016). It has been

Table 2 (*continued*)

Source material	NMs & Percentage	Composite type	Effects	Ref.
			• Water absorption – decrease	
MK	NS (0, 1, 2, and 3)	GPP	1% NS: • Flexural strength - increased by 24% • Porosity – reduced by 8%	Kang Gao et al. (2014)
FA (Class F)	NS (0.5, 1, 1.5, 2, and 2.5)	GPP	1% NS: • Initial setting time - reduced by 150% • Final setting time - reduced by 123% • compressive strength – increased by 32% • Flexural strength - increased by 40% • Modulus of elasticity - increased by 26% 1.5% NS: • Compressive strength - increased by 15%	Guo et al. (2014)
	NA (0.5, 1, 1.5, 2, and 2.5)	GPP	2% NA: • Compressive strength - increased by 14%	
FA (Class F)	NA (1, 2, and 3)	GPP	1% NA: • Initial setting time - reduced by 8.5% • Final setting time - reduced by 8.2% • Compressive strength – increased by 32% • Modulus of elasticity - increased by 26% 2% NA: • Flexural strength - increased by 35%	Phoo-ngernkham et al. (2014)
	NS (1, 2, and 3)	GPP	1% NS: • Initial setting time - reduced by 150% • Final setting time - reduced by 123% • Compressive strength – increased by 32% • Modulus of elasticity - increased by 26%	

Table 2 (*continued*)

Source material	NMs & Percentage	Composite type	Effects	Ref.
			• Flexural strength – increased by 40% (due to the formation of geopolymer gel)	
FA (Class F)	NS (1, 2, and 3)	GPP	1% NS: • Compressive strength – increased by 27% • Flexural strength - increased by 29% 2% NS: • Compressive strength- increased by 21% (dry mix) • Flexural strength – increased by 22% (wet mix)	Assaedi et al. (2015)
FA (Class F)	NC (1,2 and 3)	GPP	2% NC: • Compressive strength – increased by 23% • Flexural strength - increased by 24% • Density – increased by 11% • Porosity – reduced by 7% • Water absorption – reduced by 17%	Assaedi et al. (2016b)
FA (Class F)	NS (5 and 10)	GPP	10% NS: • Compressive strength – reduced by 32%	Chindaprasirt and Somna (2015)
FA (Class F)	NS (0.5, 1, 1.5, 2, 2.5, and 3)	GPP	2% NS: • Compressive strength – increased by 151% • Microstructure - improved	Deb et al. (2015)
FA (Class F)	NS (1, 2, and 3)	GPP	2% NS: • Compressive strength – increased by 6% • Porosity – reduced by 11% • Slump get reduced	Gao et al. (2015)
GGBFS	NC (1, 1.5, 3, 5, and 7)	GPP	3% NC: • Compressive strength – increased by 65%	Hassaan et al. (2015)
FA (Class F)	NC (3 and 6)	GPP	• Early age strength - increase	Joshi et al. (2015)
FA (Class F)	NS (1, 2, and 3)	GPP	2% NS and 1% NA: • Water absorption – reduced by 17%	Nazari and Sanjayan (2015)
FA (Class F)	GO (0.1, 0.35, and 0.5)	GPP	0.35% GO: • Flexural strength -	Saafi et al. (2015)

(*continued on next page*)

Table 2 (*continued*)

Source material	NMs & Percentage	Composite type	Effects	Ref.
			increased by 134% • Modulus of elasticity – increased by 367%	
FA (Class F)	NC (6)	GPP	• Rheology - Enhances • Viscosity – Increase	Montes et al. (2015)
GGBFS	NS (0.5, 1, and 1.5)	GC	1.5% NS: • Compressive strength – increased by 7% • Loss of weight due to chloride – reduced by 6%	Patel et al. (2015)
FA (Class F)	NS (1 and 3)	GPP	1% NS: • Compressive strength – increased by 200% • Compressive strength – reduced under high pressure and temperature by 77.5%	Ridha and Yerikania (2015a)
FA (Class F)	GO (0.1, 0.5, and 1)	GPP	1% GO: • Compressive strength – increased by 144% • Flexural strength - increased by 216%	Ranjbar et al. (2015)
GGBFS	NT (0.5)	GPP	0.5% NT: • Compressive strength – increased by 9% • Flexural strength - increased by 38% • Cumulative Porosity – reduced by 31% • Shrinkage – reduced by 21%	Yang et al. (2015)
MK	CNT (0.5 and 1)	GPP	0.5% CNT: • Compressive strength – increased by 32% • Flexural strength - increased by 28% >0.5% MCNT: • Compressive strength – decrease • Flexural strength – decrease (due to agglomeration)	Abbasi et al. (2016)
FA (Class F)	NT (1, 3, and 5)	GPP	5% NT: • Early and later age strength – increase • Compressive strength –	Duan et al. (2016)

Table 2 (*continued*)

Source material	NMs & Percentage	Composite type	Effects	Ref.
			increased by 27% • Shrinkage – reduced by 50% • Carbonation depth – reduced by 57% (180 days) • Porosity – decrease • Microstructure - improved	
GGBFS	CNT (0.1, 0.2, 0.3, and 0.4)	GPM	0.1% MCNT: • Increases Nucleation sites for geopolymer gel formation • Compressive strength – increase • Shrinkage – reduce • Microstructure – improved >1% MCNT: • Porosity – increase	Khater and Abd El Gawaad (2016)
FA (Class F)	NS (1 and 3)	GPP	3% NS: • Density – reduced by 7% 1% NS: • Compressive strength – increased by 117%	Ridha and Yerikania (2015b)
FA (Class F)	CNT (0.05, 0.01, 0.15, and 0.2)	GPM	0.15% CNT: • Maximum mechanical property	Rovnaník et al. (2016)
MK	GO (0.05, 0.1, 0.35, and 0.5)	GPP	0.35% GO: • Flexural strength – increase by 61.5% (due to bridging effect)	Yan et al. (2016)
GGBFS	NS (1–3)	GPP	3% NS: • Promotes hydration process • Enhances microstructure • Reduces porosity	Wang et al. (2019)
FA	NA (1–3)	GPP	3% NA: • Compressive strength – increase • FLexural strength – increase • Modulus of elasticity – increase • Impact strength – increase • Microstructure – improved	Alomayri (2019)
Volcanic ash	NS 5	GPC	5% NS: • Compressive strength – increase at a higher curing temperature	Ibrahim et al. (2018)
GGBFS	NS, NA, NC (1–3)	GPC	• The addition of NS shows	Shahrajabian and Behfarnia (2018)

(*continued on next page*)

Table 2 (*continued*)

Source material	NMs & Percentage	Composite type	Effects	Ref.
			maximum mechanical and durability properties than other two NMs	
MK	NS (1–2)	GPP	2% NS: • Compressive strength – increase • Setting time – increase	Lo et al. (2017)
FA	Colloidal NS (6)	GPC	6% NS: • Enhances polymerization process • Better Mechanical strength at ambient curing temperature	Adak et al. (2017)
FA	NS (1–3)	GPM	2% NS: • Enhances the early-age strength of mortar	Deb et al. (2016)
FA (Class F)	NC (1–3)	GPP	2% NC: • Ccompressive strength – increase • Flexural strength – increase Further addition of NC shows agglomeration and poor dispersion	Assaedi et al. (2016a)
FA	NA (5)	GPP	5% NA: • Compressive strength – increased • Microstructure - improved	Huang and Han (2011)

[Note: NMs = Nano Materials; GC = Geopolymer Composite; FA = Fly ash; NS = Nano Silica; GPP = Geopolymer Paste; RA = Rice husk ash; NA = Nano Alumina; CNT = Carbon Nano Tube; MK = Metakaolin; GGBFS = Ground Granulated Blast Furnace Slag; NC = Nano Clay; GPM = Geopolymer Mortar; GPC = Geopolymer Concrete; GO = Graphene Oxide; NT = Nano TiO_2; MCNT = Multiwall Carbon Nano Tube.].

discovered that NS particulates with a size of 70 nm may enter the skin and travel all through the body through the lymphatic network, leading to serious skin disorders. The respiratory system is also at risk from CNT (Pacurari et al., 2016). NMs toxicity is unquestionably dependent on several characteristics, including the crystallinity of nanoparticles, surface area, shape, particle size, and concentration of NMs inhaled. NT and NA are the most hazardous NMs compared to their micro-sized forms. Therefore, medical concerns could be minimized, and its utilization in the constructing field can really be increased if NMs are appropriately handled during processing or transportation. Additionally, the proper protective measures should be implemented when working with the utilization of NMs in the constructing market or the research lab for categorization (Monteiro et al., 2022; Uskoković, 2021).

5.1. Cost efficiency

The strength-to-cost ratio was established in order to classify the NMs blended GC in terms of its cost-effectiveness. The material cost was determined according to the cost information provided by the material distributors. Since the sources of raw goods are closer to the study location, the price of resource shipping is minimal and thus insignificant. The integrated Nanomaterials GC's cost-effectiveness was calculated and depicted in Table 3. The greater performance of the GC mix is indicated by the larger cost efficiency. Table .3 shows that the cost-efficiency of the NS (Bagheri and Moukannaa, 2021) embedded mix was better than that of other Nano materials embedded GC mix. GC made using NS is more affordable price than GC made with other NMs embedded GC mixtures. The use of NS, which results in a compact microstructure, could be the cause of better cost-effectiveness (Bagheri and Moukannaa, 2021). The mix with NS (Du et al., 2022) has a similar cost-efficiency to the GC produced with NS, as reported by Mustakim et al. (Bagheri and Moukannaa, 2021). It should be highlighted that the cost of NMs and the use of alkaline activators such as sodium hydroxide and sodium silicate contribute significantly to the high manufacturing costs of GC.

There is a significant gap regarding direct cost-effectiveness in the available literature, which may answer the construction industry's legitimate worry about using NMs in construction applications. NMs may provide numerous advantages in the design and construction process. Despite this, the huge amount of start-up expenditure of NMs seems to be limiting the market for NMs in the building industry. Nanotechnology extends the service life of construction materials while lowering maintenance expenses (Uskoković, 2021; Abulmagd and Etman, 2018; Tewari et al., 2022). As a result, the constructions' strength, lifespan, and lesser service expenditures can be used to determine whether utilizing NMs in cement-based products is cost-effective. The inclusion of NMs in cement-based materials properties can increase a structure's lifespan and hence save service costs. Furthermore, studies must be done to assess the cost-effectiveness of using NMs in the civil engineering field.

5.2. Limitations, challenges, and future scope

A substantial amount of research has been done on the effects of substituting or including different NMs on the properties of GC, based on a review of the literature. The number of research works carried out in the field of NMs in GC is shown in Fig. 2. As shown in Fig. 3, GPP incorporating different kinds of NMs has been the subject of extensive investigation, making up roughly 45.31 percent of all studies. An average of 40.63 percent and 14.06 percent of all investigation has been made on GPC and GPP separately. As a result, it is recommended that more research can be done on the properties of GPC treated with NMs. A few academics recommended various changes to the current typical concrete mix design techniques when it related to GPC mix design. Moreover, extensive study is required to determine the ideal proportioning and designing concrete matrix for nano-GC. As a result, it is crucial to make further efforts to standardize assessment protocols, scientific criteria, and behavior criteria that are effectively relevant to nano-geopolymer technologies.

Therefore, additional investigation on nano-GC is needed to comprehend the polymerization process. Furthermore, NMs dispersion in GC is one of the key problems in ensuring the degree of Nano modification; consequently, more study is needed to analyze, visualize and describe NMs dispersion in GC to obtain improved NMs dispersion. According to a few reports based on experimental investigation, admixed NMs diffuse easily in GC without clustering (Jittabut and Horpibulsuk, 2019; Parveen et al., 2013; Ahmed et al., 2022b; Hamed et al., 2019; Heister et al., 2010). Investigations should focus on various sustainable development considerations, including sociological, economic, and ecological aspects. As a result, experiments have to conduct to analyze the strengths and weaknesses of nano-GC conclusively, and a life phase assessment approach is suggested. This approach may take into account the screening mechanism for natural resources, the manufacturing technique, the curing process, the construction operation, the servicing technique, and a model for estimating the item's life span.

Nonetheless, one of the most significant restrictions on the

Table 3
Cost efficiency comparison of GC with different NMs addition.

Sl. No.	Materials	Rate ($/MT)	NA (Huang and Han, 2011)		NS (Sun et al., 2022)		NS (Du et al., 2022)		NS (Bagheri and Moukannaa, 2021)	
			QTY (1 m^3)	Cost ($/$m^3$)	QTY (1 m^3)	Cost ($/$m^3$)	QTY (1 m^3)	Cost ($/$m^3$)	QTY (1 m^3)	Cost ($/$m^3$)
1	Fly Ash	13.49	-	-	220.5	2.97	-	-	343	4.63
2	GGBFS	80	362.8	29.02	220.5	17.64	500	40	144.79	11.58
3	Fine aggregate	7.55	990	7.47	864.83	6.53	825	6.23	490	3.7
4	Coarse aggregate	9.44	810	7.65	742.21	7.01	825	7.79	1470	13.88
5	Sodium hydroxide	512.64	122.4	62.75	64.3	32.96	28.55	14.64	73	37.42
6	Sodium silicate	121.41	40.8	4.95	160.7	19.51	160.75	19.52	154	18.7
7	Super plasticizer	2383.10	-	-	22.5	53.62	6	14.3	19.6	46.71
8	Viscosity Modifying Agent	2822.06	-	-	-	-	4	11.3	-	-
9	Nano Silica	15051.18	-	-	10	150.51	10	150.51	2.205	33.19
10	Nano Alumina	50170.61	7.256	364.04	-	-	-	-	-	-
11	Total cost ($/$m^3$)			475.88		290.75		264.29		169.81
12	28 days compressive strength (MPa)			44		65		78		63
13	Cost Efficiency (MPa/$/$m^3$)			0.09		0.22		0.30		0.37

[Note: GGBFS-Ground granulated blast furnace slag; $-US dollar; MPa-Mega Pascal; MT-Metric ton; QTY- Quantity; NA- Nano Alumina; NS- Nano Silica.].

incorporation of NMs into GC is its cost. Despite the long-term benefits of employing these materials, the price is significantly influenced by the first capital invested amount. The cost of equipment and technologies is relatively high due to the sophisticated machinery needed to synthesize and classify NMs. Over time, expenses are projected to decline as consumption increases and manufacturing technique advances. Another stumbling block to the widespread use of NMs in the building industry is health and environmental problems. Penetration to the underground water table, emission into the atmosphere via dusty production, and exposure to extremely harmful substances are just a few of the challenges that might arise. As a result, the construction sector may focus more on the large-scale manufacture of NS for use in GC. Because NS is produced at a lower cost and with less energy, it has better pozzolanic reactivity and nano-filling effects, resulting in more durable GC. Therefore, NMs be embedded into many GC with lesser structural and serviceability characteristics, such as GPC which includes reprocessed plastic particles and GPC containing grain rubber particles, to favorably customize its composite. Furthermore, the efficiency of NMs exposed to fire and high temperatures necessitated additional research.

It is evident from this study that the majority of the focus is on investigating the compressive strength and microstructure of geopolymer products with NMs. The influence of different NMs in various types of AS sources on other mechanical properties, such as compressive strength, flexural strength, tensile strength, and durability has to be investigated. The impacts of various NMs on the characteristics of GC with various AS sources and their effects have been investigated extensively in the literature over the last decade, as shown in Table 2. The shrinkage and behaviour at high temperatures need further investigation, as researchers have reported contradicting results. Due to conflicting results, more research is needed to determine the effects of GC with NMs at elevated temperatures. Also, a research gap is observed concerning shrinkage and corrosion of GC with NMs. So in the future, there is scope for the area on GC with NMs.

6. Conclusions

In this extensive survey, the process connecting to the impact of different Nanomaterials on the key features of various geopolymer composites, including fresh, mechanical, durability, and microstructural properties, was described and explored in detail.The following conclusions can be drawn after performing a thorough assessment of the literature.

1. Nano materials used in geopolymer composite mixes include nano-Al_2O_3, Carbon Nano Tubes, Multiwall Carbon Nano Tubes, nano-SiO_2, nano-$CaCO_3$, nano-TiO_2, nano-ZnO, Graphene Oxide, Nano-metakaolin, Nano-fly ash, Nano Water Glass and Nano-clay. At the little proportion replacement of less than 10%, all these Nano materials were generally utilized for binder substitute ingredients in the development of different geopolymer composites.
2. Nano silica was the most commonly utilized Nano material in the production of Nano geopolymer composite because of its capacity to fill Nanoscale pores and the formation of additional gels. But the high initial cost of nanomaterials hinders their practical usage, and hence cheaper Nano materials should be developed in the future to help the construction industry.
3. In geopolymer concrete mixtures, the average amount of nano silica utilized is 3% of the total binder used. The optimal dosage of the same Nano materials can differ based on the types of binders used.
4. Although distinct Nanomaterials have diverse chemical and physical characteristics, as evident from XRD and TEM, their effect on the properties of GC is identical. The particle diameter and ratio between specific surface and volume appear to have an impact on the fresh, mechanical, and durability properties of geopolymer mixes.
5. The effects of Nano materials inside geopolymer composite include nanoscale filling of gaps and spaces, accelerating chemical interactions between the elements of the geopolymer composite, engaging in chemical reactions, and improving transition zones between surfaces.
6. Incorporating Nano materials into the geopolymer concrete reduces mortar and paste composites and fresh properties such as flow table test and slump cone value. The workability was lowered because the Nano materials could react quickly with the sodium silicate, sodium hydroxide, and water due to their huge specific surface region, resulting in a viscous and adhesive concrete composite mix. However, several studies have found that increasing Nano materials dosages increased the workability of geopolymer composite resulting from the ball-bearing action caused by the Nano material's spherical shape. As a result, more research is needed to determine whether Nano materials improve the workability of geopolymer composite or not.
7. When a few types of nanomaterials and their dosages were introduced in geopolymer composite, the initial and final setting times were increased. In contrast, some other types of nanomaterials cause a considerable reduction in the same. Similarly, the hardened properties of geopolymer composite get increase with the addition of nanomaterials until it reaches an optimal

percentage. Beyond this, it tends to decrease due to agglomeration and poor dispersion of nanomaterial within the geopolymer composite.

8. The durability of GC increases when various nanomaterials are added, both in terms of kind and quantity. These benefits were primarily brought about by the nanomaterials' particle extraction phase, which stops hostile components from penetrating the saturated gel phase's inner structure and results in a harder composition that resists destruction by adverse circumstances. However, adding Nano Silica will produce a polymer film, and its higher proportion in GPC will minimize the level of degradation of the aluminosilicate composition. In comparison, other studies stated that the addition of Nano materials to geopolymer concrete products results in the formation of a new phase, calcium silicate carbonate. The layered and laminate structures of this new product have a negative impact on the durability of the geopolymer composite.
9. The introduction of Nano materials has a considerable impact on the microstructure characteristics of GC. According to SEM analysis, the microstructure property of GC is upgraded due to the formation of geopolymer gels that covers the nano-void gaps. Further, some Nano materials, such as Nano silica, give more Si elements, resulting in an increased polymerization and polycondensation reaction causing the morphology and hardness of GPC to enhance.
10. According to the XRD analysis, new mineral humps, peaks, and phases were generated due to the inclusion of nanomaterials in the composites. The generation of additional crystalline peaks with higher intensity in the graph indicates the formation of new compounds in the geopolymer composite with the addition of nanomaterials.
11. According to TGA findings, adding Nano materials to GC enhances the temperature resistance and mass reduction at various temperature levels. This was attributed to the filling ability of Nano materials, which made the composites harder than control geopolymer mixes, resulting in more C-A-S-H, C–S–H, and N-A-S-H gels formation.
12. From MIP analysis, enhanced micro profiles in geopolymer composite due to the closing of large pores were observed with the addition of nanomaterials. Further additional gaps with a lesser dimension were formed, which led to the development of additional C-A-S-H, C–S–H, and N-A-S-H gels.
13. The complex formation and interaction of nanomaterials with geopolymer composite were analyzed using the FTIR analysis. All the bending vibration, stretching vibration, and asymmetric stretching vibrations, together with their shifting observed from the graph, indicates the interaction of nanomaterials with the geopolymer composite. In the geopolymer mix composites with Nano materials, the Si–O–Si, CO_2, O–H, Al–O–Si, and H–O–H bonding were found to be good.

Credit author statement

Mr. Samuvel Raj R: Investigation, Writing - Original Draft, Review & Editing, Dr. G. Prince Arulraj: Conceptualization, Methodology, Supervision, Validation, Review & Editing, Mr. Balamurali Kanagaraj: Investigation, Dr. M.Z. Naser: Investigation & Review & Editing, Dr. Eva Lubloy; Investigation.

Declaration of competing interest

The authors declare that they have no known competing financial interests or personal relationships that could have appeared to influence the work reported in this paper.

Data availability

No data was used for the research described in the article.

Acknowledgments

The research reported in this paper is a part of project no. BME-NVA-02, implemented with the support provided by the Ministry of Innovation and Technology of Hungary from the National Research Development and Innovation Fund, financed under the TKP2021 funding scheme.

List of abbreviation

AS	Alumina silicate
C-A-S-H	Calcium alumino silicate hydrate
CNT	Carbon nanotube
C–S–H	Calcium-silicate-hydrate
DSC	Differential Scanning Calorimeter
DTG	Derivative Thermo grams
EDX	Dispersive energy X-ray
FA	Fly ash
FESEM	Field Emission Scan Electron Microscopy
FR-GPP	Fibre reinforced geopolymer paste
FTIR	Fourier transform infrared
GC	Geopolymer composite
GGBFS	Ground granular blast furnace slag
GO	Graphene oxide
GPC	Geopolymer concrete
GPM	Geopolymer mortar
GPP	Geopolymer paste
MIP	Mercury intrusion porosimetry
MK	Metakaolin
MCNT	Multiwall carbon nanotube
mm	Millimeter
μm	Micrometer
NC	Nano clay
N-A-S-H	Sodium alumino silicate hydrate
NCC	Nano calcium carbonate
NFA	Nano fly ash
nm	Nanometer
NMK	Nano-metakaolin
NA	Nano-Al_2O_3
NMs	Nanomaterials
NS	Nano-SiO_2
NT	Nano-TiO_2
NGP	Nano glass powder
NZ	Nano zinc oxide
PFA	Palm oil fuel ash
PVA	Polyvinyl alcohol
RCPT	Rapid chloride permeability test
RA	Rice husk ash
SC-GPC	Self-compacting geopolymer concrete
SEM	Scanning electron microscope
SH	Sodium hydroxide
SS	Sodium silicate
TEM	Transmission Electron Microscope
TGA	Thermogravimetric analyzer
XRD	X-ray diffraction
XRF	X-ray fluorescence

References

Abbasi, S.M., Ahmadi, H., Khalaj, G., Ghasemi, B., 2016. Microstructure and mechanical properties of a metakaolinite-based geopolymer nanocomposite reinforced with carbon nanotubes. Ceram. Int. 42, 15171–15176. https://doi.org/10.1016/j.ceramint.2016.06.080.

Abdalla, J.A., Skariah, B., Hawileh, R.A., Yang, J., Bhushan, B., 2022a. Influence of nano-TiO2, nano-Fe2O3, nanoclay and nano-CaCO3 on the properties of cement/geopolymer concrete. Clean. Mater. 4 https://doi.org/10.1016/j.clema.2022.100061.

Abdalla, J.A., Thomas, B.S., Hawileh, R.A., Yang, J., Jindal, B.B., Ariyachandra, E., 2022b. Influence of nano-TiO2, nano-Fe2O3, nanoclay and nano-CaCO3 on the properties of cement/geopolymer concrete. Clean. Mater. 4 https://doi.org/10.1016/j.clema.2022.100061.

Abdel-Gawwad, H.A., Abo-El-Enein, S.A., 2016. A novel method to produce dry geopolymer cement powder. HBRC J 12, 13–24. https://doi.org/10.1016/j.hbrcj.2014.06.008.

Abhilash, P.P., Nayak, D.K., Sangoju, B., Kumar, R., Kumar, V., 2021. Effect of nano-silica in concrete; a review. Construct. Build. Mater. 278, 122347 https://doi.org/10.1016/j.conbuildmat.2021.122347.

Abulmagd, S., Etman, Z.A., 2018. Nanotechnology in repair and protection of structures state-of-the-art. J. Civ. Environ. Eng. https://doi.org/10.4172/2165-784x.1000306, 08.

Adak, D., Sarkar, M., Mandal, S., 2014. Effect of nano-silica on strength and durability of fly ash based geopolymer mortar. Construct. Build. Mater. 70, 453–459. https://doi.org/10.1016/j.conbuildmat.2014.07.093.

Adak, D., Sarkar, M., Mandal, S., 2017. Structural performance of nano-silica modified fly-ash based geopolymer concrete. Construct. Build. Mater. 135, 430–439. https://doi.org/10.1016/j.conbuildmat.2016.12.111.

Aggarwal, P., Singh, R.P., Aggarwal, Y., 2015. Use of nano-silica in cement based materials — a review. Cogent Eng 2 (1). https://doi.org/10.1080/23311916.2015.1078018.

Aguirre-Guerrero, A.M., Mejía de Gutiérrez, R., 2018. Efficiency of electrochemical realkalisation treatment on reinforced blended concrete using FTIR and TGA. Construct. Build. Mater. 193, 518–528. https://doi.org/10.1016/j.conbuildmat.2018.10.195.

Ahmad, A., Gulraiz, Y., Ilyas, S., Bashir, S., 2022. Polysaccharide based nano materials: health implications. Food Hydrocoll. Heal. 2, 100075 https://doi.org/10.1016/j.fhfh.2022.100075.

Ahmed, M.M., El-Naggar, K.A.M., Tarek, D., Ragab, A., Sameh, H., Zeyad, A.M., Tayeh, B.A., Maafa, I.M., Yousef, A., 2021. Fabrication of thermal insulation geopolymer bricks using ferrosilicon slag and alumina waste. Case Stud. Constr. Mater. 15, e00737 https://doi.org/10.1016/j.cscm.2021.e00737.

Ahmed, H.U., Mohammed, A.S., Faraj, R.H., Qaidi, S.M.A., Mohammed, A.A., 2022a. Compressive strength of geopolymer concrete modified with nano-silica: experimental and modeling investigations. Case Stud. Constr. Mater. 16, e01036 https://doi.org/10.1016/j.cscm.2022.e01036.

Ahmed, H.U., Mohammed, A.A., Mohammed, A.S., 2022b. The role of nanomaterials in geopolymer concrete composites: a state-of-the-art review. J. Build. Eng. 49, 104062 https://doi.org/10.1016/j.jobe.2022.104062.

Akarsh, P.K., Marathe, S., Bhat, A.K., 2021. Influence of graphene oxide on properties of concrete in the presence of silica fumes and M-sand. Construct. Build. Mater. 268, 121093 https://doi.org/10.1016/j.conbuildmat.2020.121093.

Akbari, M., Tahamtan, M.H.N., Fallah-Valukolaee, S., Herozi, M.R.Z., Shirvani, M.A., 2022. Investigating fracture characteristics and ductility of lightweight concrete containing crumb rubber by means of WFM and SEM methods. Theor. Appl. Fract. Mech. 117, 103148 https://doi.org/10.1016/j.tafmec.2021.103148.

Al-Azzawi, M., Yu, T., Hadi, M.N.S., 2018. Factors affecting the bond strength between the fly ash-based geopolymer concrete and steel reinforcement. Structures 14, 262–272. https://doi.org/10.1016/j.istruc.2018.03.010.

Al-Shether, B., Al-Attar, T., Hassan, Z.A., 2016. Effect of curing system on metakaolin based geopolymer concrete. J. Univ. Babylon - Eng. Sci. 24, 569–576.

Ali, L., El Ouni, M.H., Raza, A., Janjua, S., Ahmad, Z., Ali, B., Ben Kahla, N., Bai, Y., 2021. Experimental investigation on the mechanical and fracture evaluation of carbon Fiber-Reinforced cementitious composites with Nano-Calcium carbonate. Construct. Build. Mater. 308, 125095 https://doi.org/10.1016/j.conbuildmat.2021.125095.

Aliabdo, A.A., Abd Elmoaty, A.E.M., Salem, H.A., 2016. Effect of water addition, plasticizer and alkaline solution constitution on fly ash based geopolymer concrete performance. Construct. Build. Mater. 121, 694–703. https://doi.org/10.1016/j.conbuildmat.2016.06.062.

Alomayri, T., 2019. Experimental study of the microstructural and mechanical properties of geopolymer paste with nano material (Al2O3). J. Build. Eng. 25, 100788 https://doi.org/10.1016/j.jobe.2019.100788.

Alsalman, A., Assi, L.N., Kareem, R.S., Carter, K., Ziehl, P., 2021. Energy and CO2 emission assessments of alkali-activated concrete and Ordinary Portland Cement concrete: a comparative analysis of different grades of concrete. Clean. Environ. Syst. 3, 100047 https://doi.org/10.1016/j.cesys.2021.100047.

Alvee, A.R., Malinda, R., Akbar, A.M., Ashar, R.D., Rahmawati, C., Alomayri, T., Raza, A., Shaikh, F.U.A., 2022. Experimental study of the mechanical properties and microstructure of geopolymer paste containing nano-silica from agricultural waste and crystalline admixtures. Case Stud. Constr. Mater. 16, e00792 https://doi.org/10.1016/j.cscm.2021.e00792.

Ambikakumari Sanalkumar, K.U., Yang, E.H., 2021. Self-cleaning performance of nano-TiO2 modified metakaolin-based geopolymers. Cem. Concr. Compos. 115, 103847 https://doi.org/10.1016/j.cemconcomp.2020.103847.

Amiri, Y., Hassaninasab, S., Chehri, K., Zahedi, M., 2022. Investigating the effect of adding bacillus bacteria and nano-clay on cement mortar properties. Case Stud. Constr. Mater. 17, e01167 https://doi.org/10.1016/j.cscm.2022.e01167.

An, Q., Pan, H., Zhao, Q., Du, S., Wang, D., 2022. Strength development and microstructure of recycled gypsum-soda residue-GGBS based geopolymer. Construct. Build. Mater. 331, 127312 https://doi.org/10.1016/j.conbuildmat.2022.127312.

Anil Kumar Reddy, K.R.N., 2022. Comparative study on mechanical properties of fly ash & GGBFS based geopolymer concrete and OPC concrete using nano-alumina. Mater. Today Proc. 60, 399–404. https://doi.org/10.1016/j.matpr.2022.01.260.

Arafa, S., Milad, A., Yusoff, N.I.M., Al-Ansari, N., Yaseen, Z.M., 2021. Investigation into the permeability and strength of pervious geopolymer concrete containing coated biomass aggregate material. J. Mater. Res. Technol. 15, 2075–2087. https://doi.org/10.1016/j.jmrt.2021.09.045.

Arefi, M.R., Rezaei-Zarchi, S., 2012. Synthesis of zinc oxide nanoparticles and their effect on the compressive strength and setting time of self-compacted concrete paste as cementitious composites. Int. J. Mol. Sci. 13, 4340–4350. https://doi.org/10.3390/ijms13044340.

Arivumangai, A., Narayanan, R.M., Felixkala, T., 2020. Study on sulfate resistance behaviour of granite sand as fine aggregate in concrete through material testing and XRD analysis. Mater. Today Proc. 43, 1724–1729. https://doi.org/10.1016/j.matpr.2020.10.354.

Asadi, I., Baghban, M.H., Hashemi, M., Izadyar, N., Sajadi, B., 2022. Phase change materials incorporated into geopolymer concrete for enhancing energy efficiency and sustainability of buildings: a review. Case Stud. Constr. Mater. 17, e01162 https://doi.org/10.1016/j.cscm.2022.e01162.

Ashby, M., Ferreira, P., Schodek, D., 2009. Preface, Nanomater. Nanotechnologies Des. https://doi.org/10.1016/b978-0-7506-8149-0.00002-7 xiii–xviii.

Assaedi, H., 2021. The role of nano-CaCO3 in the mechanical performance of polyvinyl alcohol fibre-reinforced geopolymer composites. Compos. Interfac. 28, 527–542. https://doi.org/10.1080/09276440.2020.1793096.

Assaedi, H., Shaikh, F.U.A., Low, I.M., 2015. Characteristics of Nanosilica-Geopolymer Nanocomposites and Mixing Effect 9, 1471–1478.

Assaedi, H., Shaikh, F.U.A., Low, I.M., 2016a. Effect of nano-clay on mechanical and thermal properties of geopolymer. J. Asian Ceram. Soc. 4, 19–28. https://doi.org/10.1016/j.jascer.2015.10.004.

Assaedi, H., Shaikh, F.U.A., Low, I.M., 2016b. Characterizations of flax fabric reinforced nanoclay-geopolymer composites. Compos. B Eng. 95, 412–422. https://doi.org/10.1016/j.compositesb.2016.04.007.

Assaedi, H., Alomayri, T., Kaze, C.R., Jindal, B.B., Subaer, S., Shaikh, F., Alraddadi, S., 2020. Characterization and properties of geopolymer nanocomposites with different contents of nano-CaCO3. Construct. Build. Mater. 252, 119137 https://doi.org/10.1016/j.conbuildmat.2020.119137.

Atis, C.D., Karahan, O., Avs, E.B.G., 2017. Influence of duration of heat curing and extra rest period after heat curing on the strength and transport characteristic of alkali activated class. F fly ash geopolymer mortar 151, 363–369. https://doi.org/10.1016/j.conbuildmat.2017.06.041.

Azeem, M., Junaid, M.T., Azhar, M., 2021. Correlated strength enhancement mechanisms in carbon nanotube based geopolymer and OPC binders. Construct. Build. Mater. 305, 124748 https://doi.org/10.1016/j.conbuildmat.2021.124748.

Aziz, A., Benzaouak, A., Bellil, A., Alomayri, T., Ni el Hassani, I.E.E., Achab, M., El Azhari, H., Et-Tayea, Y., Shaikh, F.U.A., 2021. Effect of acidic volcanic perlite rock on physio-mechanical properties and microstructure of natural pozzolan based geopolymers. Case Stud. Constr. Mater. 15, e00712 https://doi.org/10.1016/j.cscm.2021.e00712.

Baghabra Al-Amoudi, O.S., Al-Kutti, W.A., Ahmad, S., Maslehuddin, M., 2009. Correlation between compressive strength and certain durability indices of plain and blended cement concretes. Cem. Concr. Compos. 31, 672–676. https://doi.org/10.1016/j.cemconcomp.2009.05.005.

Bagheri, A., Moukannaa, S., 2021. A new approach to the reuse of waste glass in the production of alkali-activated materials. Clean. Eng. Technol. 4, 100212 https://doi.org/10.1016/j.clet.2021.100212.

Bahoria, B.V., Parbat, D.K., Nagarnaik, P.B., 2018. XRD Analysis of Natural sand, Quarry dust, waste plastic (ldpe) to be used as a fine aggregate in concrete. Mater. Today Proc. 5, 1432–1438. https://doi.org/10.1016/j.matpr.2017.11.230.

Bai, S., Yu, L., Guan, X., Li, H., Ou, J., 2022. Study on the long-term chloride permeability of nano-silica modified cement pastes cured at negative temperature. J. Build. Eng. 57, 104854 https://doi.org/10.1016/j.jobe.2022.104854.

Basiri, A., Zaïri, F., Azadi, M., Ghasemi-Ghalebahman, A., 2022. Micromechanical constitutive modeling of tensile and cyclic behaviors of nano-clay reinforced metal matrix nanocomposites. Mech. Mater. 168, 104280 https://doi.org/10.1016/j.mechmat.2022.104280.

Basquiroto de Souza, F., Shamsaei, E., Sagoe-Crentsil, K., Duan, W., 2022. Proposed mechanism for the enhanced microstructure of graphene oxide–Portland cement composites. J. Build. Eng. 54, 104604 https://doi.org/10.1016/j.jobe.2022.104604.

Bayiha, B.N., Billong, N., Yamb, E., Kaze, R.C., Nzengwa, R., 2019. Effect of limestone dosages on some properties of geopolymer from thermally activated halloysite. Construct. Build. Mater. 217, 28–35. https://doi.org/10.1016/j.conbuildmat.2019.05.058.

Bazán, A.M., Gálvez, J.C., Reyes, E., Galé-Lamuela, D., 2018. Study of the rust penetration and circumferential stresses in reinforced concrete at early stages of an accelerated corrosion test by means of combined SEM, EDS and strain gauges. Construct. Build. Mater. 184, 655–667. https://doi.org/10.1016/j.conbuildmat.2018.06.195.

Behfarnia, K., Rostami, M., 2017. Effects of micro and nanoparticles of SiO2 on the permeability of alkali activated slag concrete. Construct. Build. Mater. 131, 205–213. https://doi.org/10.1016/j.conbuildmat.2016.11.070.

Behfarnia, K., Salemi, N., 2013. The effects of nano-silica and nano-alumina on frost resistance of normal concrete. Construct. Build. Mater. 48, 580–584. https://doi.org/10.1016/j.conbuildmat.2013.07.088.

Belaïd, F., 2022. How does concrete and cement industry transformation contribute to mitigating climate change challenges? Resour. Conserv. Recycl. Adv. 15, 200084 https://doi.org/10.1016/j.rcradv.2022.200084.

Bellum, R.R., Muniraj, K., Indukuri, C.S.R., Madduru, S.R.C., 2020. Investigation on performance enhancement of fly ash-GGBFS based graphene geopolymer concrete. J. Build. Eng. 32, 101659 https://doi.org/10.1016/j.jobe.2020.101659.
Bhushan, B., Sharma, R., 2020. The effect of nanomaterials on properties of geopolymers derived from industrial by-products : a state-of-the-art review. Construct. Build. Mater. 252, 119028 https://doi.org/10.1016/j.conbuildmat.2020.119028.
Bohn, B.P., Von Mühlen, C., Pedrotti, M.F., Zimmer, A., 2021. A novel method to produce a ceramic paver recycling waste glass. Clean. Eng. Technol. 2 https://doi.org/10.1016/j.clet.2021.100043.
Camiletti, J., Soliman, A.M., Nehdi, M.L., 2013. Effect of nano-calcium carbonate on early-age properties of ultrahigh-performance concrete. Mag. Concr. Res. 65, 297–307. https://doi.org/10.1680/macr.12.00015.
Cao, M., Ming, X., He, K., Li, L., Shen, S., 2019. Effect of macro-, micro- and nano-calcium carbonate on properties of cementitious composites-A review. Materials 12. https://doi.org/10.3390/ma12050781.
Carolina, A., Trindade, C., De Andrade, F., Ahmed, H., 2017. On the mechanical behavior of metakaolin based geopolymers under elevated temperatures 2 . Materials and processing. Mater. Res. 20, 265–272. https://doi.org/10.1590/1980-5373-MR-2017-0101.
Carriço, A., Bogas, J.A., Hawreen, A., Guedes, M., 2018. Durability of multi-walled carbon nanotube reinforced concrete. Construct. Build. Mater. 164, 121–133. https://doi.org/10.1016/j.conbuildmat.2017.12.221.
Çevik, A., Alzeebaree, R., Humur, G., Niş, A., Gülşan, M.E., 2018. Effect of nano-silica on the chemical durability and mechanical performance of fly ash based geopolymer concrete. Ceram. Int. 44, 12253–12264. https://doi.org/10.1016/j.ceramint.2018.04.009.
Charitha, V., Athira, V.S., Jittin, V., Bahurudeen, A., Nanthagopalan, P., 2021. Use of different agro-waste ashes in concrete for effective upcycling of locally available resources. Construct. Build. Mater. 285, 122851 https://doi.org/10.1016/j.conbuildmat.2021.122851.
Charpentier, C., Paredes, R., Ceccherini-silberstein, F., 2022. Journal of Global Antimicrobial Resistance Virological efficacy of switch to DTG plus 3TC in a retrospective observational cohort of suppressed HIV-1 patients with or without past M184V – the LAMRES Study. J. Glob. Antimicrob. Resist. https://doi.org/10.1016/j.jgar.2022.07.022, 0–35.
Chen, S.J., Collins, F.G., Macleod, A.J.N., Pan, Z., Duan, W.H., Wang, C.M., 2011. Carbon nanotube-cement composites: a retrospect. IES J. Part A Civ. Struct. Eng. 4, 254–265. https://doi.org/10.1080/19373260.2011.615474.
Chen, J., Kou, S.C., Poon, C.S., 2012. Hydration and properties of nano-TiO 2 blended cement composites. Cem. Concr. Compos. 34, 642–649. https://doi.org/10.1016/j.cemconcomp.2012.02.009.
Chen, J., Wu, J., Ge, H., Zhao, D., Liu, C., Hong, X., 2016. Reduced graphene oxide deposited carbon fiber reinforced polymer composites for electromagnetic interference shielding. Composer Part A Appl. Sci. Manuf. 82, 141–150. https://doi.org/10.1016/j.compositesa.2015.12.008.
Chen, Y., Al-Neshawy, F., Punkki, J., 2021. Investigation on the effect of entrained air on pore structure in hardened concrete using MIP. Construct. Build. Mater. 292, 123441 https://doi.org/10.1016/j.conbuildmat.2021.123441.
Chen, S., Ruan, S., Zeng, Q., Liu, Y., Zhang, M., Tian, Y., Yan, D., 2022. Pore structure of geopolymer materials and its correlations to engineering properties: a review. Construct. Build. Mater. 328, 127064 https://doi.org/10.1016/j.conbuildmat.2022.127064.
Chindaprasirt, P., 2007. Workability and strength of coarse high calcium fly ash geopolymer 29, 224–229. https://doi.org/10.1016/j.cemconcomp.2006.11.002.
Chindaprasirt, P., Somna, K., 2015. Effect of addition of microsilica and nanoalumina on compressive strength and products of high calcium fly ash geopolymer with low concentration NaOH. Adv. Mater. Res. 1103, 29–36. 10.4028/www.scientific.net/amr.1103.29.
Chindaprasirt, P., De Silva, P., Sagoe-Crentsil, K., Hanjitsuwan, S., 2012. Effect of SiO 2 and Al 2O 3on the setting and hardening of high calcium fly ash-based geopolymer systems. J. Mater. Sci. 47, 4876–4883. https://doi.org/10.1007/s10853-012-6353-y.
Chinnu, S.N., Minnu, S.N., Bahurudeen, A., Senthilkumar, R., 2021. Reuse of industrial and agricultural by-products as pozzolan and aggregates in lightweight concrete. Construct. Build. Mater. 302, 124172 https://doi.org/10.1016/j.conbuildmat.2021.124172.
Chintalapudi, K., Pannem, R.M.R., 2020. The effects of Graphene Oxide addition on hydration process, crystal shapes, and microstructural transformation of Ordinary Portland Cement. J. Build. Eng. 32, 101551 https://doi.org/10.1016/j.jobe.2020.101551.
Chu, S.H., Li, L.G., Kwan, A.K.H., 2021. Development of extrudable high strength fiber reinforced concrete incorporating nano calcium carbonate. Addit. Manuf. 37 https://doi.org/10.1016/j.addma.2020.101617.
Cong, P., Cheng, Y., 2021. ScienceDirect Advances in geopolymer materials : a comprehensive review. J. Traffic Transp. Eng. (English Ed. 8, 283–314. https://doi.org/10.1016/j.jtte.2021.03.004.
da Luz, G., Gleize, P.J.P., Batiston, E.R., Pelisser, F., 2019. Effect of pristine and functionalized carbon nanotubes on microstructural, rheological, and mechanical behaviors of metakaolin-based geopolymer. Cem. Concr. Compos. 104, 103332 https://doi.org/10.1016/j.cemconcomp.2019.05.015.
de Azevedo, A.R.G., Amin, M., Hadzima-Nyarko, M., Saad Agwa, I., Zeyad, A.M., Tayeh, B.A., Adesina, A., 2022. Possibilities for the application of agro-industrial wastes in cementitious materials: a brief review of the Brazilian perspective. Clean. Mater. 3, 100040 https://doi.org/10.1016/j.clema.2021.100040.
Deb, P.S., Sarker, P.K., Barbhuiya, S., 2015. Effects of nano-silica on the strength development of geopolymer cured at room temperature. Construct. Build. Mater. 101, 675–683. https://doi.org/10.1016/j.conbuildmat.2015.10.044.
Deb, P.S., Sarker, P.K., Barbhuiya, S., 2016. Sorptivity and acid resistance of ambient-cured geopolymer mortars containing nano-silica. Cem. Concr. Compos. 72, 235–245. https://doi.org/10.1016/j.cemconcomp.2016.06.017.
Dehkordi, E.R., Ramezanianpour, A.A., Moodi, F., 2022. Application of pre-fabricated geopolymer permanent formworks (PGPFs): a novel approach to provide durability and mechanical strength of reinforced concrete. J. Build. Eng. 45 https://doi.org/10.1016/j.jobe.2021.103517.
Derinpinar, A.N., Karakoç, M.B., Özcan, A., 2022. Performance of glass powder substituted slag based geopolymer concretes under high temperature. Construct. Build. Mater. 331 https://doi.org/10.1016/j.conbuildmat.2022.127318.
Devi, S.C., Khan, R.A., 2020a. Compressive strength and durability behavior of graphene oxide reinforced concrete composites containing recycled concrete aggregate. J. Build. Eng. 32, 101800 https://doi.org/10.1016/j.jobe.2020.101800.
Devi, S.C., Khan, R.A., 2020b. Effect of graphene oxide on mechanical and durability performance of concrete. J. Build. Eng. 27, 101007 https://doi.org/10.1016/j.jobe.2019.101007.
Diaz, E.I., Allouche, E.N., Eklund, S., 2010. Factors affecting the suitability of fly ash as source material for geopolymers. Fuel 89, 992–996. https://doi.org/10.1016/j.fuel.2009.09.012.
Ding, S., Xiang, Y., Ni, Y.Q., Thakur, V.K., Wang, X., Han, B., Ou, J., 2022. In-situ synthesizing carbon nanotubes on cement to develop self-sensing cementitious composites for smart high-speed rail infrastructures. Nano Today 43, 101438. https://doi.org/10.1016/j.nantod.2022.101438.
Du, D.F., Wang, J.H., Wang, X., Su, C., 2022. Compressive behavior and stress-strain model of square confined ambient-cured fly ash and slag-based geopolymer concrete. Case Stud. Constr. Mater. 17, e01203 https://doi.org/10.1016/j.cscm.2022.e01203.
Duan, P., Yan, C., Luo, W., Zhou, W., 2016. Effects of adding nano-TiO2 on compressive strength, drying shrinkage, carbonation and microstructure of fluidized bed fly ash based geopolymer paste. Construct. Build. Mater. 106, 115–125. https://doi.org/10.1016/j.conbuildmat.2015.12.095.
Dutta Joydev Assessment of Soil and Water Quality in and Around the Small Tea Gardens of Gohpur and Biswanath Chariali Sub Division of Sonitpur District assam india, No TitleывМывМыв, Ятыатат. вы12у (2007) 245. http://www.digilib.unila.ac.id/4949/15/BAB II.pdf.
Duxson, P., Provis, J.L., Lukey, G.C., Mallicoat, S.W., Kriven, W.M., Van Deventer, J.S.J., 2005. Understanding the relationship between geopolymer composition, microstructure and mechanical properties. Colloids Surfaces A Physicochem. Eng. Asp. 269, 47–58. https://doi.org/10.1016/j.colsurfa.2005.06.060.
Duxson, P., Fernández-Jiménez, A., Provis, J.L., Lukey, G.C., Palomo, A., Van Deventer, J.S.J., 2007. Geopolymer technology: the current state of the art. J. Mater. Sci. 42, 2917–2933. https://doi.org/10.1007/s10853-006-0637-z.
Edser, C., 2005. Reducing the environmental impact of laundry. Focus Surfactants 1–2. https://doi.org/10.1016/s1351-4210(05)70693-4, 2005.
Eisa, M.S., Mohamady, A., Basiouny, M.E., Abdulhamid, A., Kim, J.R., 2022. Mechanical properties of asphalt concrete modified with carbon nanotubes (CNTs). Case Stud. Constr. Mater. 16, e00930 https://doi.org/10.1016/j.cscm.2022.e00930.
Ekinci, E., Türkmen, İ., Kantarci, F., Karakoç, M.B., 2019. The improvement of mechanical, physical and durability characteristics of volcanic tuff based geopolymer concrete by using nano silica, micro silica and Styrene-Butadiene Latex additives at different ratios. Construct. Build. Mater. 201, 257–267. https://doi.org/10.1016/j.conbuildmat.2018.12.204.
El-Feky, M.S., Mohsen, A., Maher El-Tair, A., Kohail, M., 2022. Microstructural investigation for micro- nano-silica engineered magnesium oxychloride cement. Construct. Build. Mater. 342, 127976 https://doi.org/10.1016/j.conbuildmat.2022.127976.
Elia, H., 2018. Using nano- and micro-titanium dioxide (TiO2) in concrete to reduce air pollution. J. Nanomed. Nanotechnol. 3–7. https://doi.org/10.4172/2157-7439.1000505, 09.
Elimbi, A., Tchakoute, H.K., Njopwouo, D., 2011. Effects of calcination temperature of kaolinite clays on the properties of geopolymer cements. Construct. Build. Mater. 25, 2805–2812. https://doi.org/10.1016/j.conbuildmat.2010.12.055.
Emad, H., Soufi, W., Elmannaey, A., Abd-El-Aziz, M., et al., 2018. Effect of Nano-Silica on the Mechanical Properties of Slag Geopolymer Concrete. Researchgate.Net.. https://www.researchgate.net/profile/Ahmed_Elmannaey/publication/322626157_Effect_of_Nano_silica_on_the_mechanical_properties_of_slag_geopolymer_concrete/links/5a81feb8a6fdcc6f3ead6eb7/Effect-of-Nano-silica-on-the-mechanical-properties-of-slag-geopolymer-
Falikman, V., Gusev, B., 2015. Nanotechologies in new structural concretes: practice and outlook. Concr. - Innov. Des. Fib Symp. Proc. 232–234.
Fang, G., Ho, W.K., Tu, W., Zhang, M., 2018. Workability and mechanical properties of alkali-activated fly ash-slag concrete cured at ambient temperature. Construct. Build. Mater. 172, 476–487. https://doi.org/10.1016/j.conbuildmat.2018.04.008.
Feng, J., Yang, F., Qian, S., 2021. Improving the bond between polypropylene fiber and cement matrix by nano calcium carbonate modification. Construct. Build. Mater. 269, 121249 https://doi.org/10.1016/j.conbuildmat.2020.121249.
Ferro, G., Tulliani, J.M., Musso, S., 2011. Carbon nanotubes cement composites. Frat. Ed. Integrità Strutt. 5, 34–44. https://doi.org/10.3221/IGF-ESIS.18.04.
Fu, Q., Xu, W., Zhao, X., Bu, M.X., Yuan, Q., Niu, D., 2021. The microstructure and durability of fly ash-based geopolymer concrete: a review. Ceram. Int. 47, 29550–29566. https://doi.org/10.1016/j.ceramint.2021.07.190.
Fu, Q., Zhang, Z., Zhao, X., Xu, W., Niu, D., 2022. Effect of nano calcium carbonate on hydration characteristics and microstructure of cement-based materials: a review. J. Build. Eng. 50, 104220 https://doi.org/10.1016/j.jobe.2022.104220.
Gadkar, A., Subramaniam, K.V.L., 2021. Rheology control of alkali-activated fly ash with nano clay for cellular geopolymer application. Construct. Build. Mater. 283, 122687 https://doi.org/10.1016/j.conbuildmat.2021.122687.

Gao, K., Lin, K.L., Wang, D., Hwang, C.L., Le Anh Tuan, B., Shiu, H.S., Cheng, T.W., 2013. Effect of nano-SiO2 on the alkali-activated characteristics of metakaolin-based geopolymers. Construct. Build. Mater. 48, 441–447. https://doi.org/10.1016/j.conbuildmat.2013.07.027.

Gao, K., Lin, K.L., Wang, D., Hwang, C.L., Shiu, H.S., Chang, Y.M., Cheng, T.W., 2014. Effects SiO2/Na2O molar ratio on mechanical properties and the microstructure of nano-SiO2 metakaolin-based geopolymers. Construct. Build. Mater. 53, 503–510. https://doi.org/10.1016/j.conbuildmat.2013.12.003.

Gao, X., Yu, Q.L., Brouwers, H.J.H., 2015. Characterization of alkali activated slag – fly ash blends containing nano-Silica. Construct. Build. Mater. 98, 397–406. https://doi.org/10.1016/j.conbuildmat.2015.08.086.

Gao, F., Tian, W., Cheng, X., 2021a. Investigation of moisture migration of MWCNTs concrete after different heating-cooling process by LF-NMR. Construct. Build. Mater. 288, 123146 https://doi.org/10.1016/j.conbuildmat.2021.123146.

Gao, Y., Jing, H., Zhao, Z., Shi, X., Li, L., 2021b. Influence of ultrasonication energy on reinforcing-roles of CNTs to strengthen ITZ and corresponding anti-permeability properties of concrete. Construct. Build. Mater. 303, 124451 https://doi.org/10.1016/j.conbuildmat.2021.124451.

Garcia-Lodeiro, I., Palomo, A., Fernández-Jiménez, A., MacPhee, D.E., 2011. Compatibility studies between N-A-S-H and C-A-S-H gels. Study in the ternary diagram Na2O-CaO-Al2O3-SiO 2-H2O. Cement Concr. Res. 41, 923–931. https://doi.org/10.1016/j.cemconres.2011.05.006.

Gartner, E., 2004. Industrially interesting approaches to “low-CO2” cements. Cement Concr. Res. 34, 1489–1498. https://doi.org/10.1016/j.cemconres.2004.01.021.

Ge, X., Hu, X., Shi, C., 2022. The effect of different types of class F fly ashes on the mechanical properties of geopolymers cured at ambient environment. Cem. Concr. Compos. 130, 104528 https://doi.org/10.1016/j.cemconcomp.2022.104528.

Ghafoor, M.T., Khan, Q.S., Qazi, A.U., Sheikh, M.N., Hadi, M.N.S., 2021. Influence of alkaline activators on the mechanical properties of fly ash based geopolymer concrete cured at ambient temperature. Construct. Build. Mater. 273 https://doi.org/10.1016/j.conbuildmat.2020.121752.

Ghods, P., Isgor, O.B., Carpenter, G.J.C., Li, J., McRae, G.A., Gu, G.P., 2013. Nano-scale study of passive films and chloride-induced depassivation of carbon steel rebar in simulated concrete pore solutions using FIB/TEM. Cement Concr. Res. 47, 55–68. https://doi.org/10.1016/j.cemconres.2013.01.009.

Görür, E.B., Karahan, O., Bilim, C., Ilkentapar, S., Luga, E., 2015. Very high strength (120 MPa) class F fly ash geopolymer mortar activated at different NaOH amount , heat curing temperature and heat curing duration. Construct. Build. Mater. 96, 673–678. https://doi.org/10.1016/j.conbuildmat.2015.08.089.

Gülşan, M.E., Alzeebaree, R., Rasheed, A.A., Niş, A., Kurtoğlu, A.E., 2019. Development of fly ash/slag based self-compacting geopolymer concrete using nano-silica and steel fiber. Construct. Build. Mater. 211, 271–283. https://doi.org/10.1016/j.conbuildmat.2019.03.228.

Gunasekera, C., Setunge, S., Law, D.W., 2014. Correlations between Mechanical Properties of Low-Calcium Fly Ash Geopolymer Concretes, pp. 1–9. https://doi.org/10.1061/(ASCE)MT.1943-5533.0001916.

Guo, X., Shi, H., Dick, W.A., 2010. Compressive strength and microstructural characteristics of class C fly ash geopolymer. Cem. Concr. Compos. 32, 142–147. https://doi.org/10.1016/j.cemconcomp.2009.11.003.

Guo, X., Hu, W., Shi, H., 2014. Microstructure and self-solidification/stabilization (S/S) of heavy metals of nano-modified CFA-MSWIFA composite geopolymers. Construct. Build. Mater. 56, 81–86. https://doi.org/10.1016/j.conbuildmat.2014.01.062.

Guzmán-Aponte, L.A., de Gutiérrez, R.M., Maury-Ramírez, A., 2017. Metakaolin-based geopolymer with added TiO 2 particles: physicomechanical characteristics. Coatings 7, 1–12. https://doi.org/10.3390/coatings7120233.

Habibnejad Korayem, A., Ghoddousi, P., Shirzadi Javid, A.A., Oraie, M.A., Ashegh, H., 2020. Graphene oxide for surface treatment of concrete: a novel method to protect concrete. Construct. Build. Mater. 243, 118229 https://doi.org/10.1016/j.conbuildmat.2020.118229.

Hakamy, A., Shaikh, F.U.A., Low, I.M., 2015. Characteristics of nanoclay and calcined nanoclay-cement nanocomposites. Compos. B Eng. 78, 174–184. https://doi.org/10.1016/j.compositesb.2015.03.074.

Hamada, H., Alattar, A., Tayeh, B., Yahaya, F., Thomas, B., 2022. Effect of recycled waste glass on the properties of high-performance concrete: a critical review. Case Stud. Constr. Mater. 17, e01149 https://doi.org/10.1016/j.cscm.2022.e01149.

Hamed, N., El-Feky, M.S., Kohail, M., Nasr, E.S.A.R., 2019. Effect of nano-clay de-agglomeration on mechanical properties of concrete. Construct. Build. Mater. 205, 245–256. https://doi.org/10.1016/j.conbuildmat.2019.02.018.

Hamidi, F., Valizadeh, A., Aslani, F., 2022. The effect of scoria, perlite and crumb rubber aggregates on the fresh and mechanical properties of geopolymer concrete. Structures 38, 895–909. https://doi.org/10.1016/j.istruc.2022.02.031.

Hamzah, H.K., Joudah, Z.H., Georgescu, D.P., Khalid, N.H.A., Huseien, G.F., 2020. Laboratory evaluation of alkali-activated mortars modified with nanosilica from glass bottle wastes. Mater. Today Proc. 46, 2098–2104. https://doi.org/10.1016/j.matpr.2021.04.471.

Han, B., Yu, X., Ou, J., 2011. Multifunctional and smart carbon nanotube reinforced cement-based materials. Nanotechnol. Civ. Infrastruct. 1–47. https://doi.org/10.1007/978-3-642-16657-0_1.

Han, B., Zhang, L., Zeng, S., Dong, S., Yu, X., Yang, R., Ou, J., 2017. Nano-core effect in nano-engineered cementitious composites. Composer Part A Appl. Sci. Manuf. 95, 100–109. https://doi.org/10.1016/j.compositesa.2017.01.008.

Han, X., Wang, B., Feng, J., 2022. Relationship between fractal feature and compressive strength of concrete based on MIP. Construct. Build. Mater. 322, 126504 https://doi.org/10.1016/j.conbuildmat.2022.126504.

Hardjito, B.V.R.D., Wallah, S.E., Sumajouw, D.M., 2004. On the development of fly ash-based geopolymer concrete. ACI Mater. J. 101, 467–472. https://doi.org/10.14359/13485.

Harrison, E., Berenjian, A., Seifan, M., 2020. Recycling of waste glass as aggregate in cement-based materials. Environ. Sci. Ecotechnol. 4, 100064 https://doi.org/10.1016/j.ese.2020.100064.

Hassaan, M.M., Khater, H.M., El-Mahllawy, M.S., El Nagar, A.M., 2015. Production of geopolymer composites enhanced by nano-kaolin material. J. Adv. Ceram. 4, 245–252. https://doi.org/10.1007/s40145-015-0156-y.

Hassan, A., Arif, M., Shariq, M., 2019. Effect of curing condition on the mechanical properties of fly ash-based geopolymer concrete. SN Appl. Sci. 1 https://doi.org/10.1007/s42452-019-1774-8.

Hassan, A., Arif, M., Shariq, M., 2020. A review of properties and behaviour of reinforced geopolymer concrete structural elements- A clean technology option for sustainable development. J. Clean. Prod. 245 https://doi.org/10.1016/j.jclepro.2019.118762.

He, Z., Zhu, X., Wang, J., Mu, M., Wang, Y., 2019. Comparison of CO 2 emissions from OPC and recycled cement production. Construct. Build. Mater. 211, 965–973. https://doi.org/10.1016/j.conbuildmat.2019.03.289.

Heister, E., Lamprecht, C., Neves, V., Tîlmaciu, C., Datas, L., Flahaut, E., Soula, B., Hinterdorfer, P., Coley, H.M., Silva, S.R.P., McFadden, J., 2010. Higher dispersion efficacy of functionalized carbon nanotubes in chemical and biological environments. ACS Nano 4, 2615–2626. https://doi.org/10.1021/nn100069k.

Hisham M Khater, M.L., El-Sabbagh, B.A., Fanny, Mona, Mohamed, Ezzat, 2013. Effect of nano-clay on alkali activated water-cooled slag geopolymer. Curr. J. Appl. Sci. Technol. 3, 764–776. https://doi.org/10.9734/BJAST/2013/2690.

Hosseini, P., Afshar, A., Vafaei, B., Booshehrian, A., Molaei Raisi, E., Esrafili, A., 2017. Effects of nano-clay particles on the short-term properties of self-compacting concrete. Eur. J. Environ. Civ. Eng. 21, 127–147. https://doi.org/10.1080/19648189.2015.1096308.

Huang, Y., Han, M., 2011. The influence of α-Al2O3 addition on microstructure, mechanical and formaldehyde adsorption properties of fly ash-based geopolymer products. J. Hazard Mater. 193, 90–94. https://doi.org/10.1016/j.jhazmat.2011.07.029.

Huang, J., Zhou, Y., Yang, X., Dong, Y., Jin, M., Liu, J., 2022. A multi-scale study of enhancing mechanical property in ultra-high performance concrete by steel-fiber@Nano-silica. Construct. Build. Mater. 342, 128069 https://doi.org/10.1016/j.conbuildmat.2022.128069.

Huo, W., Zhu, Z., Zhang, J., Kang, Z., Pu, S., Wan, Y., 2021. Utilization of OPC and FA to enhance reclaimed lime-fly ash macadam based geopolymers cured at ambient temperature. Construct. Build. Mater. 303, 124378 https://doi.org/10.1016/j.conbuildmat.2021.124378.

Huseien, G.F., Hamzah, H.K., Mohd Sam, A.R., Khalid, N.H.A., Shah, K.W., Deogrescu, D.P., Mirza, J., 2020. Alkali-activated mortars blended with glass bottle waste nano powder: environmental benefit and sustainability. J. Clean. Prod. 243 https://doi.org/10.1016/j.jclepro.2019.118636.

Hussin, M.W., Bhutta, M.A.R., Azreen, M., Ramadhansyah, P.J., Mirza, J., 2014. Performance of blended ash geopolymer concrete at elevated temperatures. Mater. Struct. https://doi.org/10.1617/s11527-014-0251-5.

Ibrahim, M., Johari, M.A.M., Maslehuddin, M., Rahman, M.K., 2018. Influence of nano-SiO2 on the strength and microstructure of natural pozzolan based alkali activated concrete. Construct. Build. Mater. 173, 573–585. https://doi.org/10.1016/j.conbuildmat.2018.04.051.

Isfahani, F.T., Redaelli, E., Lollini, F., Li, W., Bertolini, L., 2016. Effects of nanosilica on compressive strength and durability properties of concrete with different water to binder ratios. Adv. Mater. Sci. Eng. https://doi.org/10.1155/2016/8453567, 2016.

Isil Ozer, S.S.-U., 2015. Relations between the structural characteristics and compressive strength in metakaolin based geopolymers with different molar Si/Al ratios. Ceram. Int. https://doi.org/10.1016/j.ceramint.2015.04.125.

Jalali Mosallam, S., Pesaran Behbahani, H., Shahpari, M., Abaeian, R., 2022. The effect of carbon nanotubes on mechanical properties of structural lightweight concrete using LECA aggregates. Structures 35, 1204–1218. https://doi.org/10.1016/j.istruc.2021.09.003.

Jamnam, S., Maho, B., Techaphatthanakon, A., Ruttanapun, C., Aemlaor, P., Zhang, H., Sukontasukkul, P., 2022. Effect of graphene oxide nanoparticles on blast load resistance of steel fiber reinforced concrete. Construct. Build. Mater. 343, 128139 https://doi.org/10.1016/j.conbuildmat.2022.128139.

Jang, J.G., Lee, H.K., 2016. Effect of fly ash characteristics on delayed high-strength development of geopolymers. Construct. Build. Mater. 102, 260–269. https://doi.org/10.1016/j.conbuildmat.2015.10.172.

Jiang, S., Zhou, D., Zhang, L., Ouyang, J., Yu, X., Cui, X., Han, B., 2018. Comparison of compressive strength and electrical resistivity of cementitious composites with different nano- and micro-fillers. Arch. Civ. Mech. Eng. 18, 60–68. https://doi.org/10.1016/j.acme.2017.05.010.

Jittabut, P., Horpibulsuk, S., 2019. Physical and microstructure properties of geopolymer nanocomposite reinforced with carbon nanotubes. Mater. Today Proc. 17, 1682–1692. https://doi.org/10.1016/j.matpr.2019.06.199.

Joseph, B., Mathew, G., 2012. Influence of aggregate content on the behavior of fly ash based geopolymer concrete. Sci. Iran. 19, 1188–1194. https://doi.org/10.1016/j.scient.2012.07.006.

Joshi, A., Montes, C., Salehi, S., Allouche, E., Lvov, Y., 2015. Optimization of geopolymer properties by coating of fly-ash microparticles with nanoclays. J. Inorg. Organomet. Polym. Mater. 25, 282–292. https://doi.org/10.1007/s10904-014-0105-1.

Junaid, M.F., ur Rehman, Z., Kuruc, M., Medveď, I., Bačinskas, D., Čurpek, J., Čekon, M., Ijaz, N., Ansari, W.S., 2022. Lightweight concrete from a perspective of sustainable reuse of waste byproducts. Construct. Build. Mater. 319 https://doi.org/10.1016/j.conbuildmat.2021.126061.

Kambham, B.S., Ram, V.V., Raju, S., 2019. Investigation of laboratory and field aging of bituminous concrete with and without anti-aging additives using FESEM and FTIR. Construct. Build. Mater. 222, 193–202. https://doi.org/10.1016/j.conbuildmat.2019.06.153.

Kamseu, E., Akono, A.T., Nana, A., Kaze, R.C., Leonelli, C., 2021. Performance of geopolymer composites made with feldspathic solid solutions: micromechanics and microstructure. Cem. Concr. Compos. 124, 104241 https://doi.org/10.1016/j.cemconcomp.2021.104241.

Kanagaraj, B., Anand, N., Raj R, S., Lubloy, E., 2022a. Performance evaluation of sodium silicate waste as a replacement for conventional sand in geopolymer concrete. J. Clean. Prod. 375, 134172 https://doi.org/10.1016/j.jclepro.2022.134172.

Kanagaraj, B., Anand, N., Samuvel Raj, R., Lubloy, E., 2022b. Performance evaluation on engineering properties of sodium silicate binder as a precursor material for the development of cement-free concrete. Dev. Built Environ. 12, 100092 https://doi.org/10.1016/j.dibe.2022.100092.

Kanagaraj, B., Anand, N., Johnson Alengaram, U., Samuvel Raj, R., Kiran, T., 2022c. Exemplification of sustainable sodium silicate waste sediments as coarse aggregates in the performance evaluation of geopolymer concrete. Construct. Build. Mater. 330, 127135 https://doi.org/10.1016/j.conbuildmat.2022.127135.

Kang Gao, C.-L.H., Lin, Kae-Long, Wang, DeYing, Shiu, Hau-Shing, Bui Le Anh Tuan, T.-W.C., 2014. Thin-film-Transistor liquid-crystal display waste glass and nano-SiO2 as substitute sources for metakaolin-based geopolymer. Environ. Prog. Sustain. Energy 33, 947–955. https://doi.org/10.1002/ep.11868.

Kaur, M., Singh, J., Kaur, M., 2018. Microstructure and strength development of fly ash-based geopolymer mortar: role of nano-metakaolin. Construct. Build. Mater. 190, 672–679. https://doi.org/10.1016/j.conbuildmat.2018.09.157.

Kaze, C.R., Tchakoute, H.K., Mbakop, T.T., Mache, J.R., Kamseu, E., Melo, U.C., Leonelli, C., Rahier, H., 2018. Synthesis and properties of inorganic polymers (geopolymers) derived from Cameroon-meta-halloysite. Ceram. Int. 44, 18499–18508. https://doi.org/10.1016/j.ceramint.2018.07.070.

Khalaf, M.A., Cheah, C.B., Ramli, M., Ahmed, N.M., Al-Asady, A.M.A., Ali, A.M.A., Al-Shwaiter, A., Tangchirapat, W., 2021. Engineering and gamma-ray attenuation properties of steel furnace slag heavyweight concrete with nano calcium carbonate and silica. Construct. Build. Mater. 267, 120878 https://doi.org/10.1016/j.conbuildmat.2020.120878.

Khale, D., Chaudhary, R., 2007. Mechanism of geopolymerization and factors influencing its development: a review. J. Mater. Sci. 42, 729–746. https://doi.org/10.1007/s10853-006-0401-4.

Khater, H.M., 2016a. Effect of nano-silica on microstructure formation of low-cost geopolymer binder. Nanocomposites 2, 84–97. https://doi.org/10.1080/20550324.2016.1203515.

Khater, H.M.M., 2016b. Physicomechanical properties of nano-silica effect on geopolymer composites. J. Build. Mater. Struct. 3, 1–14. https://doi.org/10.34118/jbms.v3i1.20.

Khater, H.M., Abd El Gawaad, H.A., 2016. Characterization of alkali activated geopolymer mortar doped with MWCNT. Construct. Build. Mater. 102, 329–337. https://doi.org/10.1016/j.conbuildmat.2015.10.121.

Khater, H.M., El-Nagar, A.M., 2020. Preparation of sustainable of eco-friendly MWCNT-geopolymer composites with superior sulfate resistance. Adv. Compos. Hybrid Mater. 3, 375–389. https://doi.org/10.1007/s42114-020-00170-4.

Kim, G.M., Nam, I.W., Yang, B., Yoon, H.N., Lee, H.K., Park, S., 2019. Carbon nanotube (CNT) incorporated cementitious composites for functional construction materials: the state of the art. Compos. Struct. 227, 111244 https://doi.org/10.1016/j.compstruct.2019.111244.

Kiran Kumar, N.L.N., Gopala Krishna Sastry, K.V.S., 2017. Effects of nano silica on the strengths of geopolymer concrete cured at ambient temperature. Int. J. Civ. Eng. Technol. 8, 437–444.

Konios, D., Stylianakis, M.M., Stratakis, E., Kymakis, E., 2014. Dispersion behaviour of graphene oxide and reduced graphene oxide. J. Colloid Interface Sci. 430, 108–112. https://doi.org/10.1016/j.jcis.2014.05.033.

Korczak, K., Kochański, M., Skoczkowski, T., 2022. Mitigation options for decarbonization of the non-metallic minerals industry and their impacts on costs, energy consumption and GHG emissions in the EU - systematic literature review. J. Clean. Prod. 358 https://doi.org/10.1016/j.jclepro.2022.132006.

Kotop, M.A., Alharbi, Y.R., Abadel, A.A., Binyahya, A.S., 2021. Engineering properties of geopolymer concrete incorporating hybrid. Ain Shams Eng. J. 12, 3641–3647. https://doi.org/10.1016/j.asej.2021.04.022.

Krishna, R.S., Mishra, J., Nanda, B., Patro, S.K., Adetayo, A., Qureshi, T.S., 2021. The role of graphene and its derivatives in modifying different phases of geopolymer composites: a review. Construct. Build. Mater. 306, 124774 https://doi.org/10.1016/j.conbuildmat.2021.124774.

Kumar, G.V.K.N., 2022. Effect on mechanical, durability and micro structural properties of high strength self compacting concrete with inclusion of micro and nano silica. Mater. Today Proc. 60, 569–575. https://doi.org/10.1016/j.matpr.2022.02.064.

Li, Z., Wang, H., He, S., Lu, Y., Wang, M., 2006. Investigations on the preparation and mechanical properties of the nano-alumina reinforced cement composite. Mater. Lett. 60, 356–359. https://doi.org/10.1016/j.matlet.2005.08.061.

Li, Q., Xu, H., Li, F., Li, P., Shen, L., Zhai, J., 2012. Synthesis of geopolymer composites from blends of CFBC fly and bottom ashes. Fuel 97, 366–372. https://doi.org/10.1016/j.fuel.2012.02.059.

Li, N., Georas, S., Alexis, N., Fritz, P., Xia, T., Williams, M.A., Horner, E., Nel, A., 2016. A work group report on ultrafine particles (American Academy of Allergy, Asthma & Immunology): why ambient ultrafine and engineered nanoparticles should receive special attention for possible adverse health outcomes in human subjects. J. Allergy Clin. Immunol. 138, 386–396. https://doi.org/10.1016/j.jaci.2016.02.023.

Li, W., Li, X., Chen, S.J., Long, G., Liu, Y.M., Duan, W.H., 2017a. Effects of nanoalumina and graphene oxide on early-age hydration and mechanical properties of cement paste. J. Mater. Civ. Eng. 29, 1–9. https://doi.org/10.1061/(asce)mt.1943-5533.0001926.

Li, Z., Han, B., Yu, X., Dong, S., Zhang, L., Dong, X., Ou, J., 2017b. Effect of nano-titanium dioxide on mechanical and electrical properties and microstructure of reactive powder concrete. Mater. Res. Express 4. https://doi.org/10.1088/2053-1591/aa87db.

Li, B., Mao, J., Nawa, T., Han, T., 2017c. Mesoscopic damage model of concrete subjected to freeze-thaw cycles using mercury intrusion porosimetry and differential scanning calorimetry (MIP-DSC). Construct. Build. Mater. 147, 79–90. https://doi.org/10.1016/j.conbuildmat.2017.04.136.

Li, F., Liu, L., Yang, Z., Li, S., 2021. Physical and mechanical properties and micro characteristics of fly ash-based geopolymer paste incorporated with waste Granulated Blast Furnace Slag (GBFS) and functionalized Multi-Walled Carbon Nanotubes (MWCNTs). J. Hazard Mater. 401, 123339 https://doi.org/10.1016/j.jhazmat.2020.123339.

Li, M., Luo, R., Qin, L., Liu, H., Duan, P., Jing, W., Zhang, Z., Liu, X., 2022a. High temperature properties of graphene oxide modified metakaolin based geopolymer paste. Cem. Concr. Compos. 125, 104318 https://doi.org/10.1016/j.cemconcomp.2021.104318.

Li, W., Shumuye, E.D., Shiying, T., Wang, Z., Zerfu, K., 2022b. Eco-friendly fibre reinforced geopolymer concrete: a critical review on the microstructure and long-term durability properties. Case Stud. Constr. Mater. 16, e00894 https://doi.org/10.1016/j.cscm.2022.e00894.

Lin, K.L., Shiu, H.S., Shie, J.L., Cheng, T.W., Hwang, C.L., 2012. Effect of composition on characteristics of thin film transistor liquid crystal display (TFT-LCD) waste glass-metakaolin-based geopolymers. Construct. Build. Mater. 36, 501–507. https://doi.org/10.1016/j.conbuildmat.2012.05.018.

Lin, C., Wei, W., Hu, Y.H., 2016. Catalytic behavior of graphene oxide for cement hydration process. J. Phys. Chem. Solid. 89, 128–133. https://doi.org/10.1016/j.jpcs.2015.11.002.

Liu, C., Hunag, X., Wu, Y.Y., Deng, X., Zheng, Z., Yang, B., 2022a. Studies on mechanical properties and durability of steel fiber reinforced concrete incorporating graphene oxide. Cem. Concr. Compos. 130, 104508 https://doi.org/10.1016/j.cemconcomp.2022.104508.

Liu, B., Mastalerz, M., Schieber, J., 2022b. SEM petrography of dispersed organic matter in black shales: a review. Earth Sci. Rev. 224, 103874 https://doi.org/10.1016/j.earscirev.2021.103874.

Lo, K.W., Lin, K.L., Cheng, T.W., Chang, Y.M., Lan, J.Y., 2017. Effect of nano-SiO2 on the alkali-activated characteristics of spent catalyst metakaolin-based geopolymers. Construct. Build. Mater. 143, 455–463. https://doi.org/10.1016/j.conbuildmat.2017.03.152.

Lv, S., Ma, Y., Qiu, C., Sun, T., Liu, J., Zhou, Q., 2013. Effect of graphene oxide nanosheets of microstructure and mechanical properties of cement composites. Construct. Build. Mater. 49, 121–127. https://doi.org/10.1016/j.conbuildmat.2013.08.022.

M, R., Bharathi, S.M.L., 2022. Sustainable utilization of pre-treated and nano fly ash powder for the development of durable geopolymer mortars. Adv. Powder Technol. 33, 103696 https://doi.org/10.1016/j.apt.2022.103696.

Maho, B., Sukontasukkul, P., Sua-Iam, G., Sappakittipakorn, M., Intarabut, D., Suksiripattanapong, C., Chindaprasirt, P., Limkatanyu, S., 2021. Mechanical properties and electrical resistivity of multiwall carbon nanotubes incorporated into high calcium fly ash geopolymer. Case Stud. Constr. Mater. 15, e00785 https://doi.org/10.1016/j.cscm.2021.e00785.

Manzur, T., Yazdani, N., Emon, M.A.B., 2016. Potential of carbon nanotube reinforced cement composites as concrete repair material. J. Nanomater. 2016 https://doi.org/10.1155/2016/1421959.

Matalkah, F., Ababneh, A., Aqel, R., 2022. Effects of nanomaterials on mechanical properties, durability characteristics and microstructural features of alkali-activated binders: a comprehensive review. Construct. Build. Mater. 336, 127545 https://doi.org/10.1016/j.conbuildmat.2022.127545.

Mathews, M.E., Anand, N., Kodur, V.K., Arulraj, P., 2021. The bond strength of self-compacting concrete exposed to elevated temperature. Proceedings of the Institution of Civil Engineers-Structures and Buildings 174 (9), 804–821.

Mathews, M.E., Kiran, T., Hasa Naidu, V.C., Jeyakumar, G., Anand, N., 2020. Effect of high-temperature on the mechanical and durability behaviour of concrete. Mater. Today Proc. 42, 718–725. https://doi.org/10.1016/j.matpr.2020.11.153.

Maury-Ramirez, A., Demeestere, K., De Belie, N., 2012. Photocatalytic activity of titanium dioxide nanoparticle coatings applied on autoclaved aerated concrete: effect of weathering on coating physical characteristics and gaseous toluene removal. J. Hazard Mater. 211–212, 218–225. https://doi.org/10.1016/j.jhazmat.2011.12.037.

McDonald, L.J., Afzal, W., Glasser, F.P., 2022. Evidence of scawtite and tilleyite formation at ambient conditions in hydrated Portland cement blended with freshly-precipitated nano-size calcium carbonate to reduce greenhouse gas emissions. J. Build. Eng. 48, 103906 https://doi.org/10.1016/j.jobe.2021.103906.

Mermerdaş, K., Manguri, S., Nassani, D.E., Oleiwi, S.M., 2017. Effect of aggregate properties on the mechanical and absorption characteristics of geopolymer mortar. Eng. Sci. Technol. an Int. J. 20, 1642–1652. https://doi.org/10.1016/j.jestch.2017.11.009.

Mijarsh, M.J.A., Megat Johari, M.A., Ahmad, Z.A., 2015. Effect of delay time and Na2SiO3 concentrations on compressive strength development of geopolymer mortar synthesized from TPOFA. Construct. Build. Mater. 86, 64–74. https://doi.org/10.1016/j.conbuildmat.2015.03.078.

min Zhan, P., hai He, Z., ming Ma, Z., feng Liang, C., xiang Zhang, X., Abreham, A.A., yan Shi, J., 2020. Utilization of nano-metakaolin in concrete: a review. J. Build. Eng. 30, 101259 https://doi.org/10.1016/j.jobe.2020.101259.

Mohamed, E.A., Harbi, H.F.A.L., Aref, N., 2019. Radioprotective efficacy of zinc oxide nanoparticles on γ-ray-induced nuclear DNA damage in Vicia faba L. as evaluated by DNA bioassays. J. Radiat. Res. Appl. Sci. 12, 423–436. https://doi.org/10.1080/16878507.2019.1690798.

Mohammed, A.A., Ahmed, H.U., Mosavi, A., 2021. Survey of mechanical properties of geopolymer concrete: a comprehensive review and data analysis. Materials 14. https://doi.org/10.3390/ma14164690.

Mohseni, E., Kazemi, M.J., Koushkbaghi, M., Zehtab, B., Behforouz, B., 2019. Evaluation of mechanical and durability properties of fiber-reinforced lightweight geopolymer composites based on rice husk ash and nano-alumina. Construct. Build. Mater. 209, 532–540. https://doi.org/10.1016/j.conbuildmat.2019.03.067.

Monteiro, H., Moura, B., Soares, N., 2022. Advancements in nano-enabled cement and concrete: innovative properties and environmental implications. J. Build. Eng. 56, 104736 https://doi.org/10.1016/j.jobe.2022.104736.

Montes, C., Joshi, A., Salehi, S., Lvov, Y., Allouche, E., 2015. Study of the interaction between nanoclay and fly ash and its impact on the enhancement of the rheological properties of geopolymer binders. Nanotechnol. Constr. https://doi.org/10.1007/978-3-319-17088-6.

Moukannaa, S., Aboulayt, A., Hakkou, R., Benzaazoua, M., Ohenoja, K., Palomo, A., Fernández-Jimenez, A., 2022. Fusion of phosphate by-products and glass waste for preparation of alkali-activated binders. Compos. B Eng. 242, 110044 https://doi.org/10.1016/j.compositesb.2022.110044.

Mowlaei, R., Lin, J., Basquiroto de Souza, F., Fouladi, A., Habibnejad Korayem, A., Shamsaei, E., Duan, W., 2021. The effects of graphene oxide-silica nanohybrids on the workability, hydration, and mechanical properties of Portland cement paste. Construct. Build. Mater. 266, 121016 https://doi.org/10.1016/j.conbuildmat.2020.121016.

Mudgal, M., Chouhan, R.K., Kushwah, S., Srivastava, A.K., 2020. Enhancing reactivity and properties of fly-ash-based solid-form geopolymer via ball-milling. Emerg. Mater. Res. 9, 2–9. https://doi.org/10.1680/jemmr.19.00065.

Muhd Norhasri, M.S., Hamidah, M.S., Mohd Fadzil, A., Megawati, O., 2016. Inclusion of nano metakaolin as additive in ultra high performance concrete (UHPC). Construct. Build. Mater. 127, 167–175. https://doi.org/10.1016/j.conbuildmat.2016.09.127.

Mustakim, S.M., Das, S.K., Mishra, J., Aftab, A., Alomayri, T.S., 2020. Microsilis-2020.Pdf.

Nana, A., Epey, N., Rodrique, K.C., Deutou, J.G.N., Djobo, J.N.Y., Tomé, S., Alomayri, T. S., Ngouné, J., Kamseu, E., Leonelli, C., 2021. Mechanical strength and microstructure of metakaolin/volcanic ash-based geopolymer composites reinforced with reactive silica from rice husk ash (RHA). Materialia 16, 101083. https://doi.org/10.1016/j.mtla.2021.101083.

Naskar, S., Kumar, A., 2016. Effect of nano materials in geopolymer concrete ☪. Perspect. Sci. 8, 273–275. https://doi.org/10.1016/j.pisc.2016.04.049.

Nath, P., Sarker, P.K., Rangan, V.B., 2015. Early age properties of low-calcium fly ash geopolymer concrete suitable for ambient curing. Procedia Eng. 125, 601–607. https://doi.org/10.1016/j.proeng.2015.11.077.

Nazari, A., Riahi, S., 2013. Predicting the effects of nanoparticles on compressive strength of ash-based geopolymers by gene expression programming, Neural Comput. Appl 23, 1677–1685. https://doi.org/10.1007/s00521-012-1127-7.

Nazari, A., Sanjayan, J.G., 2015. Hybrid effects of alumina and silica nanoparticles on water absorption of geopolymers: application of Taguchi approach. Meas. J. Int. Meas. Confed. 60, 240–246. https://doi.org/10.1016/j.measurement.2014.10.004.

Nazir, M.S., Mohamad Kassim, M.H., Mohapatra, L., Gilani, M.A., Raza, M.R., Majeed, K., 2016. Characteristic properties of nanoclays and characterization of nanoparticulates and nanocomposites. Eng. Mater. 35–55. https://doi.org/10.1007/978-981-10-1953-1_2.

Ng, C., Alengaram, U.J., Wong, L.S., Mo, K.H., Jumaat, M.Z., Ramesh, S., 2018. A review on microstructural study and compressive strength of geopolymer mortar, paste and concrete. Construct. Build. Mater. 186, 550–576. https://doi.org/10.1016/j.conbuildmat.2018.07.075.

Niu, X.J., Bin Li, Q., Hu, Y., Tan, Y.S., Liu, C.F., 2021. Properties of cement-based materials incorporating nano-clay and calcined nano-clay: a review. Construct. Build. Mater. 284 https://doi.org/10.1016/j.conbuildmat.2021.122820.

Nohl, J.F., Farr, N.T.H., Sun, Y., Hughes, G.M., Cussen, S.A., Rodenburg, C., 2022. Low-voltage SEM of air-sensitive powders: from sample preparation to micro/nano analysis with secondary electron hyperspectral imaging. Micron 156, 103234. https://doi.org/10.1016/j.micron.2022.103234.

Noorvand, H., Abang Ali, A.A., Demirboga, R., Farzadnia, N., Noorvand, H., 2013. Incorporation of nano TiO2 in black rice husk ash mortars. Construct. Build. Mater. 47, 1350–1361. https://doi.org/10.1016/j.conbuildmat.2013.06.066.

Nouping Fekoua, J.N., Kaze, C.R., Duna, L.L., Ghazouni, A., Ndassa, I.M., Kamseu, E., Rossignol, S., Leonelli, C., 2021. Effects of curing cycles on developing strength and microstructure of goethite-rich aluminosilicate (corroded laterite) based geopolymer composites. Mater. Chem. Phys. 270, 124864 https://doi.org/10.1016/j.matchemphys.2021.124864.

Noushini, A., Castel, A., 2018. Performance-based criteria to assess the suitability of geopolymer concrete in marine environments using modified ASTM C1202 and ASTM C1556 methods. Mater. Struct. Constr. 51 https://doi.org/10.1617/s11527-018-1267-z.

Noushini, A., Aslani, F., Castel, A., Ian, R., Uy, B., Foster, S., 2016. Compressive stress-strain model for low-calcium fl y ash-based geopolymer and heat-cured Portland cement concrete. Cem. Concr. Compos. 73, 136–146. https://doi.org/10.1016/j.cemconcomp.2016.07.004.

Nuaklong, P., Sata, V., Wongsa, A., Srinavin, K., Chindaprasirt, P., 2018. Recycled aggregate high calcium fly ash geopolymer concrete with inclusion of OPC and nano-SiO2. Construct. Build. Mater. 174, 244–252. https://doi.org/10.1016/j.conbuildmat.2018.04.123.

Nuaklong, P., Jongvivatsakul, P., Pothisiri, T., Sata, V., Chindaprasirt, P., 2020. Influence of rice husk ash on mechanical properties and fire resistance of recycled aggregate high-calcium fly ash geopolymer concrete. J. Clean. Prod. 252, 119797 https://doi.org/10.1016/j.jclepro.2019.119797.

Okoye, F.N., Prakash, S., Singh, N.B., 2017. Durability of fly ash based geopolymer concrete in the presence of silica fume. J. Clean. Prod. 149, 1062–1067. https://doi.org/10.1016/j.jclepro.2017.02.176.

Omer, S.A., Demirboga, R., Khushefati, W.H., 2015. Relationship between compressive strength and UPV of GGBFS based geopolymer mortars exposed to elevated temperatures. Construct. Build. Mater. 94, 189–195. https://doi.org/10.1016/j.conbuildmat.2015.07.006.

Pacurari, M., Lowe, K., Tchounwou, P.B., Kafoury, R., 2016. A review on the respiratory system toxicity of carbon nanoparticles. Int. J. Environ. Res. Publ. Health 13. https://doi.org/10.3390/ijerph13030325.

Panda, M.J.T.B., Paul, S.C., Hui, L.J., Tay, Y.W.D., 2017. Additive manufacturing of geopolymer for sustainable built environment. J. Clean. Prod. 167, 281–288. https://doi.org/10.1016/j.jclepro.2017.08.165.

Pardal, X., Pochard, I., Nonat, A., 2009. Experimental study of Si-Al substitution in calcium-silicate-hydrate (C-S-H) prepared under equilibrium conditions. Cement Concr. Res. 39, 637–643. https://doi.org/10.1016/j.cemconres.2009.05.001.

Parveen, S., Rana, S., Fangueiro, R., 2013. A review on nanomaterial dispersion, microstructure, and mechanical properties of carbon nanotube and nanofiber reinforced cementitious composites. J. Nanomater. 2013 https://doi.org/10.1155/2013/710175.

Parveen, D. Singhal, Junaid, M.T., Jindal, B.B., Mehta, A., 2018. Mechanical and microstructural properties of fly ash based geopolymer concrete incorporating alccofine at ambient curing. Construct. Build. Mater. 180, 298–307. https://doi.org/10.1016/j.conbuildmat.2018.05.286.

Patankar, S.V., Jamkar, S.S., Ghugal, Y.M., 2012. Effect of water-to-geopolymer binder ratio on the production of fly ash based geopolymer concrete. Int. J. Adv. Technol. Civ. Eng. 1, 296–300. https://doi.org/10.47893/ijatce.2012.1048.

Patankar, S.V., Ghugal, Y.M., Jamkar, S.S., 2014. Effect of concentration of sodium hydroxide and degree of heat curing on fly ash-based geopolymer mortar. Indian J. Mater. Sci. 1–6. https://doi.org/10.1155/2014/938789, 2014.

Patel, Y., Patel, I.N., Shah, M.J., 2015. Experimental investigation on compressive strength and durability properties of geopolymer concrete incorporating with nano silica. Int. J. Civ. Eng. Technol. 6, 135–143.

Patel, S., Orlov, A., Ariyachandra, E., Peethamparan, S., 2021. Effect of flue gas temperature on NO2 adsorption by aged recycled concrete Waste: DRIFTS, TGA and BET study. Chem. Eng. J. 420, 130413 https://doi.org/10.1016/j.cej.2021.130413.

Pavithra, P., Srinivasula Reddy, M., Dinakar, P., Hanumantha Rao, B., Satpathy, B.K., Mohanty, A.N., 2016a. Effect of the Na 2 SiO 3/NaOH Ratio and NaOH Molarity on the Synthesis of Fly Ash-Based Geopolymer Mortar, pp. 336–344. https://doi.org/10.1061/9780784480151.034.

Pavithra, P., Srinivasula Reddy, M., Dinakar, P., Hanumantha Rao, B., Satpathy, B.K., Mohanty, A.N., 2016b. A mix design procedure for geopolymer concrete with fly ash. J. Clean. Prod. 133, 117–125. https://doi.org/10.1016/j.jclepro.2016.05.041.

Pawluczuk, E., Kalinowska-Wichrowska, K., Jiménez, J.R., Fernández-Rodríguez, J.M., Suescum-Morales, D., 2021. Geopolymer concrete with treated recycled aggregates: macro and microstructural behavior. J. Build. Eng. 44 https://doi.org/10.1016/j.jobe.2021.103317.

Phoo-ngernkham, T., Chindaprasirt, P., Sata, V., Hanjitsuwan, S., Hatanaka, S., 2014. The effect of adding nano-SiO2 and nano-Al2O3 on properties of high calcium fly ash geopolymer cured at ambient temperature. Mater. Des. 55, 58–65. https://doi.org/10.1016/j.matdes.2013.09.049.

Poloju, K.K., Srinivasu, K., 2020. Impact of GGBS and strength ratio on mechanical properties of geopolymer concrete under ambient curing and oven curing. Mater. Today Proc. 42, 962–968. https://doi.org/10.1016/j.matpr.2020.11.934.

Prakasam, G., Murthy, A.R., Saffiq Reheman, M., 2020. Mechanical, durability and fracture properties of nano-modified FA/GGBS geopolymer mortar. Mag. Concr. Res. 72, 207–216. https://doi.org/10.1680/jmacr.18.00059.

Qian, X., Wang, J., Wang, L., Fang, Y., 2019. Enhancing the performance of metakaolin blended cement mortar through in-situ production of nano to sub-micro calcium carbonate particles. Construct. Build. Mater. 196, 681–691. https://doi.org/10.1016/j.conbuildmat.2018.11.134.

Quackatz, L., Griesche, A., Kannengiesser, T., 2022. Spatially resolved EDS, XRF and LIBS measurements of the chemical composition of duplex stainless steel welds: a comparison of methods. Spectrochim. Acta Part B At. Spectrosc. 193, 106439 https://doi.org/10.1016/j.sab.2022.106439.

Rajendran, M., Akasi, M., 2020. Performance of crumb rubber and nano fly ash based ferro-geopolymer panels under impact load. KSCE J. Civ. Eng. 24, 1810–1820. https://doi.org/10.1007/s12205-020-0854-z.

Ranjbar, N., Mehrali, M., Mehrali, M., Alengaram, U.J., Jumaat, M.Z., 2015. Graphene nanoplatelet-fly ash based geopolymer composites. Cement Concr. Res. 76, 222–231. https://doi.org/10.1016/j.cemconres.2015.06.003.

Rashad, A.M., 2014. Recycled waste glass as fine aggregate replacement in cementitious materials based on Portland cement. Construct. Build. Mater. 72, 340–357. https://doi.org/10.1016/j.conbuildmat.2014.08.092.

Ravitheja, A., Kiran Kumar, N.L.N., 2019. A study on the effect of nano clay and GGBS on the strength properties of fly ash based geopolymers. Mater. Today Proc. 19, 273–276. https://doi.org/10.1016/j.matpr.2019.06.761.

Razi, A., Malinda, R., Muna, A., Dwi, R., Rahmawati, C., Alomayri, T., Raza, A., Uddin, F., Shaikh, A., 2022. Case Studies in Construction Materials Experimental study of the mechanical properties and microstructure of geopolymer paste containing nano-silica from agricultural waste and crystalline admixtures. Case Stud. Constr. Mater. 16, e00792 https://doi.org/10.1016/j.cscm.2021.e00792.

Rees, C.A., Provis, J.L., Lukey, G.C., van Deventer, J.S.J., 2008. The mechanism of geopolymer gel formation investigated through seeded nucleation. Colloids Surfaces A Physicochem. Eng. Asp. 318, 97–105. https://doi.org/10.1016/j.colsurfa.2007.12.019.

Reshma, T.V., Manjunatha, M., Bharath, A., Tangadagi, R.B., Vengala, J., Manjunatha, L. R., 2021. Influence of ZnO and TiO2 on mechanical and durability properties of concrete prepared with and without polypropylene fibers. Materialia 18, 101138. https://doi.org/10.1016/j.mtla.2021.101138.

Revathi, T., Jeyalakshmi, R., Rajamane, N.P., 2018. Study on the Role of N-SiO 2 Incorporation in Thermo-Mechanical and Microstructural Properties of Ambient Cured FA-GGBS Geopolymer Matrix. Elsevier B.V. https://doi.org/10.1016/j.apsusc.2018.01.281

Riahi, S., Nazari, A., 2012. The effects of nanoparticles on early age compressive strength of ash-based geopolymers. Ceram. Int. 38, 4467–4476. https://doi.org/10.1016/j.ceramint.2012.02.021.

Ridha, S., Yerikania, U., 2015a. The strength compatibility of nano-SiO 2 geopolymer cement for oil well under HPHT conditions. J. Civ. Eng. Res. 6–10. https://doi.org/10.5923/c.jce.201501.02, 2015.

Ridha, S., Yerikania, U., 2015b. New nano-geopolymer cement system improves wellbore integrity upon acidizing job: experimental findings. Soc. Pet. Eng. - SPE/IATMI Asia Pacific Oil Gas Conf. Exhib. APOGCE 1–7. https://doi.org/10.2118/176419-ms, 2015.

Rodríguez, E.D., Bernal, S.A., Provis, J.L., Paya, J., Monzo, J.M., Borrachero, M.V., 2013. Effect of nanosilica-based activators on the performance of an alkali-activated fly ash binder. Cem. Concr. Compos. 35, 1–11. https://doi.org/10.1016/j.cemconcomp.2012.08.025.

Rovnaník, P., Šimonová, H., Topolář, L., Schmid, P., Keršner, Z., 2016. Effect of carbon nanotubes on the mechanical fracture properties of fly ash geopolymer. Procedia Eng. 151, 321–328. https://doi.org/10.1016/j.proeng.2016.07.360.

Rustan, M., Irhamsyah, S., 2017. Studi tentang pengaruh nanopartikel ZnO (seng oksida) terhadap kuat tekan geopolimer berbahan dasar metakaolin. J. Sains Dan Pendidik. Fis. 11, 286–291.

Saafi, M., Andrew, K., Tang, P.L., McGhon, D., Taylor, S., Rahman, M., Yang, S., Zhou, X., 2013. Multifunctional properties of carbon nanotube/fly ash geopolymeric nanocomposites. Construct. Build. Mater. 49, 46–55. https://doi.org/10.1016/j.conbuildmat.2013.08.007.

Saafi, M., Tang, L., Fung, J., Rahman, M., Liggat, J., 2015. Enhanced properties of graphene/fly ash geopolymeric composite cement. Cement Concr. Res. 67, 292–299. https://doi.org/10.1016/j.cemconres.2014.08.011.

Sahitya, P., Sastry, K.V.S.G.K., 2018. Influence Of Nano Tio 2 On Geopolymer Concrete 5, 760–763.

Saini, G., Vattipalli, U., 2020. Assessing properties of alkali activated GGBS based self-compacting geopolymer concrete using nano-silica. Case Stud. Constr. Mater. 12, e00352 https://doi.org/10.1016/j.cscm.2020.e00352.

Sajjad, U., Sheikh, M.N., Hadi, M.N.S., 2021. Experimental study of the effect of graphene on properties of ambient-cured slag and fly ash-based geopolymer paste and mortar. Construct. Build. Mater. 313, 125403 https://doi.org/10.1016/j.conbuildmat.2021.125403.

Saloni, Parveen, Lim, Y.Y., Pham, T.M., 2021a. Effective utilisation of ultrafine slag to improve mechanical and durability properties of recycled aggregates geopolymer concrete. Clean. Eng. Technol. 5, 100330 https://doi.org/10.1016/j.clet.2021.100330.

Saloni, Parveen, Lim, Y. Yan, Pham, T.M., 2021b. Influence of Portland cement on performance of fine rice husk ash geopolymer concrete: strength and permeability properties. Construct. Build. Mater. 300, 124321 https://doi.org/10.1016/j.conbuildmat.2021.124321.

Saloni, Parveen, Pham, T.M., Lim, Y.Y., Malekzadeh, M., 2021c. Effect of pre-treatment methods of crumb rubber on strength, permeability and acid attack resistance of rubberised geopolymer concrete. J. Build. Eng. 41, 1–12. https://doi.org/10.1016/j.jobe.2021.102448.

Samadi, M., Shah, K.W., Huseien, G.F., 2020. Influence of Glass Silica Waste Nano Powder on the Mechanical and Microstructure Properties of Alkali-Activated Mortars.

Sarkar, M., Maiti, M., Maiti, S., Xu, S., Li, Q., 2018. ZnO-SiO2 nanohybrid decorated sustainable geopolymer retaining anti-biodeterioration activity with improved durability. Mater. Sci. Eng. C 92, 663–672. https://doi.org/10.1016/j.msec.2018.07.005.

Sastry, K.V.S.G.K., Sahitya, P., Ravitheja, A., 2021. Influence of nano TiO2 on strength and durability properties of geopolymer concrete. Mater. Today Proc. 45, 1017–1025. https://doi.org/10.1016/j.matpr.2020.03.139.

Satheesh Raja, R., Manisekar, K., 2016. Experimental and statistical analysis on mechanical properties of nano flyash impregnated GFRP composites using central composite design method. Mater. Des. 89, 884–892. https://doi.org/10.1016/j.matdes.2015.10.043.

Saxena, S.K., Kumar, M., Singh, N.B., 2018. Effect of Alccofine powder on the properties of Pond fly ash based Geopolymer mortar under different conditions. Environ. Technol. Innovat. https://doi.org/10.1016/j.eti.2017.12.010.

Sekkal, W., Zaoui, A., 2022. High strength metakaolin-based geopolymer reinforced by pristine and covalent functionalized carbon nanotubes. Construct. Build. Mater. 327, 126910 https://doi.org/10.1016/j.conbuildmat.2022.126910.

Shahrajabian, F., Behfarnia, K., 2018. The effects of nano particles on freeze and thaw resistance of alkali-activated slag concrete. Construct. Build. Mater. 176, 172–178. https://doi.org/10.1016/j.conbuildmat.2018.05.033.

Shaikh, F.U.A., Supit, S.W.M., 2015. Compressive Strength and Durability of High-Volume Fly Ash Concrete Reinforced with Calcium Carbonate Nanoparticles. Elsevier Ltd. https://doi.org/10.1016/B978-0-08-100079-3.00011-9.

Shalini, S.S.A., Gurunarayanan, G., 2016. Performance of rice husk ash in geopolymer concrete. Int. J. Innov. Res. Sci. Tech. 2, 73–77.

Shekari, A.H., Razzaghi, M.S., 2011. Influence of nano particles on durability and mechanical properties of high performance concrete. Procedia Eng. 14, 3036–3041. https://doi.org/10.1016/j.proeng.2011.07.382.

Sheng, K., Li, D., Yuan, X., 2021. Methyl orange assisted dispersion of graphene oxide in the alkaline environment for improving mechanical properties and fluidity of ordinary portland cement composites. J. Build. Eng. 43, 103166 https://doi.org/10.1016/j.jobe.2021.103166.

Shi, C., 2004. Effect of mixing proportions of concrete on its electrical conductivity and the rapid chloride permeability test (ASTM C1202 or ASSHTO T277) results. Cement Concr. Res. 34, 537–545. https://doi.org/10.1016/j.cemconres.2003.09.007.

Shi, X., Zhang, C., Wang, X., Zhang, T., Wang, Q., 2022a. Response surface methodology for multi-objective optimization of fly ash-GGBS based geopolymer mortar. Construct. Build. Mater. 315, 125644 https://doi.org/10.1016/j.conbuildmat.2021.125644.

Shi, D., Geng, Y., Li, S., Gao, J., Hou, D., Jin, Z., Liu, A., 2022b. Efficacy and mechanism of graphene oxide modified silane emulsions on waterproof performance of foamed concrete. Case Stud. Constr. Mater. 16, e00908 https://doi.org/10.1016/j.cscm.2022.e00908.

Shilar, F.A., Ganachari, S.V., Patil, V.B., Khan, T.M.Y., Dawood Abdul Khadar, S., 2022. Molarity activity effect on mechanical and microstructure properties of geopolymer concrete: a review. Case Stud. Constr. Mater. 16, e01014 https://doi.org/10.1016/j.cscm.2022.e01014.

Siahkouhi, M., Razaqpur, G., Hoult, N.A., Hajmohammadian Baghban, M., Jing, G., 2021. Utilization of carbon nanotubes (CNTs) in concrete for structural health monitoring (SHM) purposes: a review. Construct. Build. Mater. 309, 125137 https://doi.org/10.1016/j.conbuildmat.2021.125137.

Sidiq, A., Gravina, R.J., Setunge, S., Giustozzi, F., 2020. High-efficiency techniques and micro-structural parameters to evaluate concrete self-healing using X-ray tomography and Mercury Intrusion Porosimetry: a review. Construct. Build. Mater. 252, 119030 https://doi.org/10.1016/j.conbuildmat.2020.119030.

Sonal, T., Urmil, D., Darshan, B., 2022. Case Studies in Construction Materials Behaviour of ambient cured prestressed and non-prestressed geopolymer concrete beams. Case Stud. Constr. Mater. 16, e00798 https://doi.org/10.1016/j.cscm.2021.e00798.

C. Sreenivasulu, J.G. Jawahar, M.V.S. Reddy, D.P. Kumar, c r v i h o e f, (n.d.).

Su, Z., Hou, W., Sun, Z., 2020. Recent advances in carbon nanotube-geopolymer composite. Construct. Build. Mater. 252, 118940 https://doi.org/10.1016/j.conbuildmat.2020.118940.

Sui, Y., Liu, S., Ou, C., Liu, Q., Meng, G., 2021. Experimental investigation for the influence of graphene oxide on properties of the cement-waste concrete powder composite. Construct. Build. Mater. 276, 122229 https://doi.org/10.1016/j.conbuildmat.2020.122229.

Sumesh, M., Alengaram, U.J., Jumaat, M.Z., Mo, K.H., Alnahhal, M.F., 2017. Incorporation of nano-materials in cement composite and geopolymer based paste and mortar – a review. Construct. Build. Mater. 148, 62–84. https://doi.org/10.1016/j.conbuildmat.2017.04.206.

Sun, K., Peng, X., Wang, S., Zeng, L., Ran, P., Ji, G., 2020. Effect of nano-SiO2 on the efflorescence of an alkali-activated metakaolin mortar. Construct. Build. Mater. 253, 118952 https://doi.org/10.1016/j.conbuildmat.2020.118952.

Sun, J., Tang, Y., Wang, J., Wang, X., Wang, J., Yu, Z., Cheng, Q., Wang, Y., 2022. A multi-objective optimisation approach for activity excitation of waste glass mortar. J. Mater. Res. Technol. 17, 2280–2304. https://doi.org/10.1016/j.jmrt.2022.01.066.

Supit, S.W.M., Shaikh, F.U.A., 2014. Effect of Nano-CaCO3 on compressive strength development of high volume fly ash mortars and concretes. J. Adv. Concr. Technol. 12, 178–186. https://doi.org/10.3151/jact.12.178.

Suwan, T., Fan, M., 2014. Influence of OPC replacement and manufacturing procedures on the properties of self-cured geopolymer. Construct. Build. Mater. 73, 551–561. https://doi.org/10.1016/j.conbuildmat.2014.09.065.

Syamsidar, D., Nurfadilla, Subaer, 2017. The properties of nano TiO2-geopolymer composite as a material for functional surface application. MATEC Web Conf 97. https://doi.org/10.1051/matecconf/20179701013.

Tayeh, B.A., Zeyad, A.M., Agwa, I.S., Amin, M., 2021. Effect of elevated temperatures on mechanical properties of lightweight geopolymer concrete. Case Stud. Constr. Mater. 15, e00673 https://doi.org/10.1016/j.cscm.2021.e00673.

Taylor, P., Gonzalez, M., Cao, J., Tighe, S.L., 2014. State-of-the-art report on use of nano-materials in concrete. Int. J. Pavement Eng. 37–41. https://doi.org/10.1080/10298436.2014.893327.

Tewari, C., Tatrari, G., Kumar, S., Pandey, S., Rana, A., Pal, M., Sahoo, N.G., 2022. Green and cost-effective synthesis of 2D and 3D graphene-based nanomaterials from Drepanostachyum falcatum for bio-imaging and water purification applications. Chem. Eng. J. Adv. 10, 100265 https://doi.org/10.1016/j.ceja.2022.100265.

Thanaraj, D.P., Anand, N., Arulraj, P., Al-Jabri, K., 2020. Investigation on structural and thermal performance of reinforced concrete beams exposed to standard fire. Journal of Building Engineering 32, 101764.

Thokchom, S., Mandal, K.K., Ghosh, S., 2012. Effect of Si/Al ratio on performance of fly ash geopolymers at elevated temperature. Arabian J. Sci. Eng. 37, 977–989. https://doi.org/10.1007/s13369-012-0230-5.

Tibbetts, C.M., Tao, C., Paris, J.M., Ferraro, C.C., 2020. Mercury intrusion porosimetry parameters for use in concrete penetrability qualification using the Katz-Thompson relationship. Construct. Build. Mater. 263, 119834 https://doi.org/10.1016/j.conbuildmat.2020.119834.

Triwulan, M., Ekaputri, J.J., Priyanka, N.F., 2017. The effect of temperature curing on geopolymer concrete. MATEC Web Conf 97. https://doi.org/10.1051/matecconf/20179701005, 0–5.

Ugheoke, B.I., Onche, E.O., Namessan, O.N., Asikpo, G.A., 2006. Property optimization of kaolin-rice husk insulating fire-bricks, leonardo electron. J. Pract. Technol. 9, 167–178. http://lejpt.academicdirect.org/A09/167_178.pdf.

Ul Haq, E., Kunjalukkal Padmanabhan, S., Licciulli, A., 2014. Synthesis and characteristics of fly ash and bottom ash based geopolymers-A comparative study. Ceram. Int. 40, 2965–2971. https://doi.org/10.1016/j.ceramint.2013.10.012.

Unis, H., Mohammed, A.S., Faraj, R.H., Qaidi, S.M.A., Mohammed, A.A., 2022. Case Studies in Construction Materials Compressive strength of geopolymer concrete modified with nano-silica : experimental and modeling investigations. Case Stud. Constr. Mater. 16, e01036 https://doi.org/10.1016/j.cscm.2022.e01036.

Uskoković, V., 2021. Health economics matters in the nanomaterial world: cost-effectiveness of utilizing an inhalable antibacterial nanomaterial for the treatment of multidrug-resistant pneumonia. Technol. Soc. 66 https://doi.org/10.1016/j.techsoc.2021.101641.

Vijai, K., Kumutha, R., Vishnuram, B.G., 2010. Effect of types of curing on strength of geopolymer concrete. Int. J. Phys. Sci. 5, 1419–1423.

Wang, J., Du, P., Zhou, Z., Xu, D., Xie, N., Cheng, X., 2019. Effect of nano-silica on hydration, microstructure of alkali-activated slag. Construct. Build. Mater. 220, 110–118. https://doi.org/10.1016/j.conbuildmat.2019.05.158.

Wang, Z., Yu, Q., Feng, P., Brouwers, H.J.H., 2022a. Variation of self-cleaning performance of nano-TiO2 modified mortar caused by carbonation: from hydrates to carbonates. Cement Concr. Res. 158, 106852 https://doi.org/10.1016/j.cemconres.2022.106852.

Wang, H., Treble, P., Baker, A., Rich, A.M., Bhattacharyya, S., Oriani, F., Akter, R., Chinu, K., Wainwright, I., Marjo, C.E., 2022b. Sulphur variations in annually layered stalagmites using benchtop micro-XRF, Spectrochim. Acta - Part B at. Spectroscopy (Ott.) 189, 106366. https://doi.org/10.1016/j.sab.2022.106366.

Wei, J., Meyer, C., 2014. Sisal fiber-reinforced cement composite with Portland cement substitution by a combination of metakaolin and nanoclay. J. Mater. Sci. 49, 7604–7619. https://doi.org/10.1007/s10853-014-8469-8.

Wei, K., Jin, P., Hui, M., Heng, S., Toh, G., Joo, J., Lee, C., Yun, X., Soo, D., Mao, Z., Ji, R., Xu, J., Zhu, Q., 2022. Energy & Buildings Application of phase change materials in building components and the use of nanotechnology for its improvement. Energy Build. 262, 112018 https://doi.org/10.1016/j.enbuild.2022.112018.

Weil, M., Dombrowski, K., Buchwald, A., 2009. Life-cycle analysis of geopolymers. Geopolymers Struct. Process. Prop. Ind. Appl. 194–210. https://doi.org/10.1533/9781845696382.2.194.

Weir, A., Westerhoff, P., Fabricius, L., Hristovski, K., Von Goetz, N., 2012. Titanium dioxide nanoparticles in food and personal care products. Environ. Sci. Technol. 46, 2242–2250. https://doi.org/10.1021/es204168d.

Wiesner, J.-Y.B.Mark R. (Ed.), 2007. Environmental Nanotechnology - Applications and Impacts of Nanomaterials. McGraw-Hill Professional, New York. https://doi.org/10.1036/0071477500.

Wilson, W., Rivera-Torres, J.M., Sorelli, L., Durán-Herrera, A., Tagnit-Hamou, A., 2017. The micromechanical signature of high-volume natural pozzolan concrete by combined statistical nanoindentation and SEM-EDS analyses, Cem. Concr. Res. 91, 1–12. https://doi.org/10.1016/j.cemconres.2016.10.004.

Witkowski, H., Koniorczyk, M., 2018. New sampling method to improve the reliability of FTIR analysis for Self-Compacting Concrete. Construct. Build. Mater. 172, 196–203. https://doi.org/10.1016/j.conbuildmat.2018.03.216.

Xiao, R., Huang, B., Zhou, H., Ma, Y., Jiang, X., 2022. A state-of-the-art review of crushed urban waste glass used in OPC and AAMs (geopolymer): progress and challenges. Clean. Mater. 4, 100083 https://doi.org/10.1016/j.clema.2022.100083.

Xie, T., Ozbakkaloglu, T., 2015. Behavior of low-calcium fly and bottom ash-based geopolymer concrete cured at ambient temperature. Ceram. Int. 41, 5945–5958. https://doi.org/10.1016/j.ceramint.2015.01.031.

Xie, J., Zhang, H., Duan, L., Yang, Y., Yan, J., Shan, D., Liu, X., Pang, J., Chen, Y., Li, X., Zhang, Y., 2020. Effect of nano metakaolin on compressive strength of recycled concrete. Construct. Build. Mater. 256 https://doi.org/10.1016/j.conbuildmat.2020.119393.

Yahya, Z., Abdullah, M.M.A.B., Hussin, K., Ismail, K.N., Razak, R.A., Sandu, A.V., 2015. Effect of solids-to-liquids, Na2SiO3-to-NaOH and curing temperature on the palm oil boiler ash (Si + Ca) geopolymerisation system. Materials 8, 2227–2242. https://doi.org/10.3390/ma8052227.

Yan, S., He, P., Jia, D., Yang, Z., Duan, X., Wang, S., Zhou, Y., 2016. Effect of reduced graphene oxide content on the microstructure and mechanical properties of graphene–geopolymer nanocomposites. Ceram. Int. 42, 752–758. https://doi.org/10.1016/j.ceramint.2015.08.176.

Yang, L.Y., Jia, Z.J., Zhang, Y.M., Dai, J.G., 2015. Effects of nano-TiO2 on strength, shrinkage and microstructure of alkali activated slag pastes. Cem. Concr. Compos. 57, 1–7. https://doi.org/10.1016/j.cemconcomp.2014.11.009.

Yang, H., Yan, Y., Hu, Z., 2020. The preparation of nano calcium carbonate and calcium silicate hardening accelerator from marble waste by nitric acid treatment and study of early strength effect of calcium silicate on C30 concrete. J. Build. Eng. 32, 101507 https://doi.org/10.1016/j.jobe.2020.101507.

Yang, H., Monasterio, M., Zheng, D., Cui, H., Tang, W., Bao, X., Chen, X., 2021. Effects of nano silica on the properties of cement-based materials: a comprehensive review. Construct. Build. Mater. 282, 122715 https://doi.org/10.1016/j.conbuildmat.2021.122715.

Yaswanth, K.K., Revathy, J., Gajalakshmi, P., 2022. Influence of copper slag on Mechanical , durability and microstructural properties of GGBS and RHA blended strain hardening geopolymer composites. Construct. Build. Mater. 342, 128042 https://doi.org/10.1016/j.conbuildmat.2022.128042.

Yildirim, G., Sahmaran, M., Ahmed, H.U., 2015. Influence of hydrated lime addition on the self-healing capability of high-volume fly ash incorporated cementitious composites. J. Mater. Civ. Eng. 27, 04014187 https://doi.org/10.1061/(asce)mt.1943-5533.0001145.

Yip, C.K., Lukey, G.C., Van Deventer, J.S.J., 2005. The coexistence of geopolymeric gel and calcium silicate hydrate at the early stage of alkaline activation. Cement Concr. Res. 35, 1688–1697. https://doi.org/10.1016/j.cemconres.2004.10.042.

Yip, C.K., Lukey, G.C., Provis, J.L., van Deventer, J.S.J., 2008. Effect of calcium silicate sources on geopolymerisation. Cement Concr. Res. 38, 554–564. https://doi.org/10.1016/j.cemconres.2007.11.001.

Youssf, O., Elchalakani, M., Hassanli, R., Roychand, R., Zhuge, Y., Gravina, R.J., Mills, J. E., 2022. Mechanical performance and durability of geopolymer lightweight rubber concrete. J. Build. Eng. 45, 103608 https://doi.org/10.1016/j.jobe.2021.103608.

Yu, L., Wu, R., 2020. Using graphene oxide to improve the properties of ultra-high-performance concrete with fine recycled aggregate. Construct. Build. Mater. 259, 120657 https://doi.org/10.1016/j.conbuildmat.2020.120657.

Zaid, O., Hashmi, S.R.Z., Aslam, F., Abedin, Z.U., Ullah, A., 2022. Experimental study on the properties improvement of hybrid graphene oxide fiber-reinforced composite concrete. Diam. Relat. Mater. 124, 108883 https://doi.org/10.1016/j.diamond.2022.108883.

Zeng, Q., Chen, S., Yang, P., Peng, Y., Wang, J., Zhou, C., Wang, Z., Yan, D., 2020. Reassessment of mercury intrusion porosimetry for characterizing the pore structure of cement-based porous materials by monitoring the mercury entrapments with X-ray computed tomography. Cem. Concr. Compos. 113, 103726 https://doi.org/10.1016/j.cemconcomp.2020.103726.

Zhang, L., Yue, Y., 2018. Influence of waste glass powder usage on the properties of alkali-activated slag mortars based on response surface methodology. Construct. Build. Mater. 181, 527–534. https://doi.org/10.1016/j.conbuildmat.2018.06.040.

Zhang, S.P., Zong, L., 2014. Evaluation of Relationship between Water Absorption and Durability of Concrete Materials, p. 2014.

Zhang, M.H., Islam, J., Peethamparan, S., 2012. Use of nano-silica to increase early strength and reduce setting time of concretes with high volumes of slag. Cem. Concr. Compos. 34, 650–662. https://doi.org/10.1016/j.cemconcomp.2012.02.005.

Zhang, P., Wang, K., Wang, J., Guo, J., Hu, S., Ling, Y., 2020a. Mechanical properties and prediction of fracture parameters of geopolymer/alkali-activated mortar modified with PVA fiber and nano-SiO2. Ceram. Int. 46, 20027–20037. https://doi.org/10.1016/j.ceramint.2020.05.074.

Zhang, H.Y., Qiu, G.H., Kodur, V., Yuan, Z.S., 2020b. Spalling behavior of metakaolin-fly ash based geopolymer concrete under elevated temperature exposure. Cem. Concr. Compos. 106, 103483 https://doi.org/10.1016/j.cemconcomp.2019.103483.

Zhang, H., Li, L., Yuan, C., Wang, Q., Sarker, P.K., Shi, X., 2020c. Deterioration of ambient-cured and heat-cured fly ash geopolymer concrete by high temperature exposure and prediction of its residual compressive strength. Construct. Build. Mater. 262, 120924 https://doi.org/10.1016/j.conbuildmat.2020.120924.

Zhu, Y., Zhang, Z., 2021. Investigation of the anticorrosion layer of reinforced steel based on graphene oxide in simulated concrete pore solution with 3 wt.% NaCl. J. Build. Eng. 44, 103302 https://doi.org/10.1016/j.jobe.2021.103302.

Zhu, Y., Qian, Y., Zhang, L., Bai, B., Wang, X., Li, J., Bi, S., Kong, L., Liu, W., Zhang, L., 2021. Enhanced thermal conductivity of geopolymer nanocomposites by incorporating interface engineered carbon nanotubes. Compos. Commun. 24 https://doi.org/10.1016/j.coco.2021.100691.

Zidi, Z., Ltifi, M., Ben Ayadi, Z., El Mir, L., 2019. Synthesis of nano-alumina and their effect on structure, mechanical and thermal properties of geopolymer. J. Asian Ceram. Soc. 7, 524–535. https://doi.org/10.1080/21870764.2019.1676498.

Zidi, Z., Ltifi, M., Ben Ayadi, Z., Mir, L.E.L., Nóvoa, X.R., 2020. Effect of nano-ZnO on mechanical and thermal properties of geopolymer. J. Asian Ceram. Soc. 8, 1–9. https://doi.org/10.1080/21870764.2019.1693682.

Zidi, Z., Ltifi, M., Zafar, I., 2021. Synthesis and attributes of nano-SiO2 local metakaolin based-geopolymer. J. Build. Eng. 33, 101586 https://doi.org/10.1016/j.jobe.2020.101586.

Zivica, V., Palou, M.T., Bágeľ, T.I.Ľ., 2014. High strength metahalloysite based geopolymer. Compos. B Eng. 57, 155–165. https://doi.org/10.1016/j.compositesb.2013.09.034.